การผลิตแอลฟีนิลอะลานีนโดย *Escherichia coli* รีคอมบิแนนท์ภายใต้การควบคุมการแสดงออกของโปรโมเตอร์ T7 และ ara

นางสาวภคินี รัชนีลัดดาจิต

วิทยานิพนธ์นี้เป็นส่วนหนึ่งของการศึกษาตามหลักสูตรปริญญาวิทยาศาสตรมหาบัณฑิต
สาขาวิชาชีวเคมีและชีววิทยาโมเลกุล ภาควิชาชีวเคมี
คณะวิทยาศาสตร์ จุฬาลงกรณ์มหาวิทยาลัย
ปีการศึกษา 2557

L- PHENYLALANINE PRODUCTION BY RECOMBINANT *Escherichia coli* UNDER REGULATION OF T7 AND ara PROMOTERS

Miss Pakinee Ratchaneeladdajit

A Thesis Submitted in Partial Fulfillment of the Requirements
for the Degree of Master of Science Program in Biochemistry and Molecular Biology
Department of Biochemistry
Faculty of Science
Chulalongkorn University
Academic Year 2014

Thesis Title	L- PHENYLALANINE PRODUCTION BY RECOMBINANT *Escherichia coli* UNDER REGULATION OF T7 AND ara PROMOTERS
By	Miss Pakinee Ratchaneeladdajit
Field of Study	Biochemistry and Molecular Biology
Thesis Advisor	Assistant Professor Kanoktip Packdibamrung, Ph.D.

Accepted by the Faculty of Science, Chulalongkorn University in Partial Fulfillment of the Requirements for the Master's Degree

.....Dean of the Faculty of Science
(Professor Supot Hannongbua, Ph.D.)

THESIS COMMITTEE

.....Chairman
(Professor Aran Incharoensakdi)

.....Thesis Advisor
(Assistant Professor Kanoktip Packdibamrung, Ph.D.)

.....Examiner
(Assistant Professor Kunlaya Somboonwiwat)

.....External Examiner
(Assistant Professor Kiattawee Choowongkomon, Ph.D.)

ภคินี รัชนีลัดดาจิต : การผลิตแอลฟีนิลอะลานีนโดย *Escherichia coli* รีคอมบิแนนท์ภายใต้การควบคุมการแสดงออกของโปรโมเตอร์ T7 และ ara (L-PHENYLALANINE PRODUCTION BY RECOMBINANT *Escherichia coli* UNDER REGULATION OF T7 AND ara PROMOTERS) อ.ที่ปรึกษาวิทยานิพนธ์หลัก: ผศ. ดร.กนกทิพย์ ภักดีบำรุง, หน้า.

แอล-ฟีนิลอะลานีน (L-Phe) เป็นสารตั้งต้นในการผลิตสารสำคัญในทางการแพทย์และอุตสาหกรรมอาหาร เช่น แอสปาร์แตม จากความต้องการในการใช้แอสปาร์แตมที่เพิ่มมากขึ้น นำไปสู่การปรับปรุงผลิต L-Phe ในจุลินทรีย์โดยเฉพาะใน *Escherichia coli* โดยกระบวนการวิศวกรรมเมแทบอลิซึม งานวิจัยนี้ได้ทำการเพิ่มการผลิตแอล-ฟีนิลอะลานีนโดยโคลนยีนที่สำคัญในวิถีการสังเคราะห์ L-Phe จำนวน 4 ยีน (*aroB, aroL, phedh* และ *tktA*) เข้าสู่เวคเตอร์ pRSFDuet-1 จากนั้นทรานส์ฟอร์มเข้าสู่ *E. coli* BL21(DE3) ร่วมกับยีนที่เข้ารหัสโปรตีนที่นำกลีเซอรอลเข้าสู่เซลล์ (*glpF*) และยีนที่เข้ารหัสโปรตีนที่นำกรดอะมิโนชนิดอะโรมาติกออกนอกเซลล์ (*yddG*) ที่อยู่ในเวคเตอร์ pBAD33 การหาความเข้มข้นที่เหมาะสมของกลีเซอรอล แอมโมเนียมซัลเฟต โดยใช้ response surface methodology (RSM) พบว่า โคลนดังกล่าวสามารถผลิต L-Phe ได้สูงสุด คือ 746 มิลลิกรัมต่อลิตร เมื่อเลี้ยงในสูตรอาหารที่มีส่วนประกอบดังนี้ (กรัมต่อลิตร): กลีเซอรอล 31; แอมโมเนียมซัลเฟต 63; $MgSO_4 \cdot 7H_2O$ 0.3; $CaCl_2 \cdot 2H_2O$ 0.015; KH_2PO_4 3.0; K_2HPO_4 12; NaCl 1; $FeSO_4 \cdot 7H_2O$/Na-citrate 0.075/1.0; thiamine·HCl 0.0075 และสารละลาย trace element (ประกอบด้วย (กรัมต่อลิตร): $Al_2(SO_4)_3 \cdot 18H_2O$ 2.0; $CoSO_4 \cdot 7H_2O$ 0.75; $CuSO_4 \cdot 5\ H_2O$ 2.5; H_3BO_3 0.5; $MnSO_4 \cdot H_2O$ 24; $Na_2MoO_4 \cdot 2H_2O$ 3.0; $NiSO_4 \cdot 6H_2O$ 2.5 and $ZnSO_4 \cdot 7H_2O$ 15) 1.5 มิลลิลิตรต่อลิตร pH 7.0 ที่อุณหภูมิ 37 องศาเซลเซียส หลังการเหนี่ยวนำโดยอะราบิโนส 0.02 เปอร์เซ็นต์ เป็นเวลา 240 ชั่วโมง

ภาควิชา ชีวเคมี ลายมือชื่อนิสิต .....

สาขาวิชา ชีวเคมีและชีววิทยาโมเลกุล ลายมือชื่อ อ.ที่ปรึกษาหลัก .....

ปีการศึกษา 2557

5472218123 : MAJOR BIOCHEMISTRY AND MOLECULAR BIOLOGY
KEYWORDS: L-PHENYLALANINE, DUAL PLASMID SYSTEM

PAKINEE RATCHANEELADDAJIT: L- PHENYLALANINE PRODUCTION BY RECOMBINANT *Escherichia coli* UNDER REGULATION OF T7 AND ara PROMOTERS. ADVISOR: ASST. PROF. KANOKTIP PACKDIBAMRUNG, Ph.D., pp.

L-Phenylalanine (L-Phe) is mainly used as a reactant for production of important substances in medical and food industry such as aspartame. An increase in demand for aspartame leads to the improvement of L-Phe production in microorganisms, especially *Escherichia coli* by metabolic engineering. In this research, L-Phe production was increased by cloning four important genes in L-Phe biosynthesis pathway (*aroB, aroL, phedh* and *tktA*) into pRSFDuet-1 vector. After that the recombinant plasmid was co-transformed with pBAD33 vector containing a glycerol uptake gene (*glpF*) and an aromatic amino acid exporter gene (*yddG*) into *E. coli* BL21(DE3). Response surface methodology (RSM) was applied to optimize concentration of glycerol and ammonium sulfate. The highest production of L-Phe at 746 mg/L was obtained when the recombinant clone was cultured in minimum medium containing (g/L): glycerol 31; $(NH_4)_2SO_4$ 63; $MgSO_4 \cdot 7H_2O$ 0.3; $CaCl_2 \cdot 2H_2O$ 0.015; KH_2PO_4 3.0; K_2HPO_4 12; NaCl 1; $FeSO_4 \cdot 7H_2O$/Na-citrate 0.075 /1.0; thiamine·HCl 0.0075 and trace element solution (containing (g/L): $Al_2(SO_4)_3 \cdot 18H_2O$ 2.0; $CoSO_4 \cdot 7H_2O$ 0.75; $CuSO_4 \cdot 5\ H_2O$ 2.5; H_3BO_3 0.5; $MnSO_4 \cdot H_2O$ 24; $Na_2MoO_4 \cdot 2H_2O$ 3.0; $NiSO_4 \cdot 6H_2O$ 2.5 and $ZnSO_4 \cdot 7\ H_2O$ 15) 1.5 ml/L pH 7.0 at 37 ^oC after induction by 0.02% arabinose for 240 hours.

Department:	Biochemistry	Student's Signature	.....
Field of Study:	Biochemistry and Molecular Biology	Advisor's Signature	.....
Academic Year:	2014		

ACKNOWLEDGEMENTS

Although I am responsible for the thesis in its entirety, the completion of this thesis would not have been possible without any helps from my thesis advisor, Assistant Professor Dr. Kanoktip Packdibamrung. All compositions of this thesis, including its content, approach, possible shortcomings and effective guidance throughout the project, were brought a completion under her kindness and effective encouragement. My heart-felt thanks go to my thesis advisor with the greatest attitude for her kind assistance and careful attention to every single detail in this thesis.

I wish, therefore, to express my deep appreciation to the Department of Biochemistry, Faculty of Science, Chulalongkorn University and particularly to those of my colleagues, 707 lab members and other alliances of the department who have tried out earlier experimental suggestions and given meaningful advices to improve and develop my knowledge, skills and background in Biochemistry and other related fields.

I would also like to give my grateful thank to members serving as a thesis committee – Professor Dr. Aran Incharoensakdi, Assistant Professor Dr. Kunlaya Somboonwiwat and Assistant Professor Kiattawee Choowongkomon – for their contributions on comments for providing beneficial recommendations to this thesis.

Finally, my last deepest gratitude was dedicated to my family which their hopes have given me inspirations for my chosen path of life. My thanks always go to their understanding, helping and supporting everything since the day I was born till the day of my graduation.

CONTENTS

Page

Page

CHAPTER I

INTRODUCTION

1.1 Amino acids

Amino acids are organic compounds which consist of an alpha carbon atom linked to a carboxyl group (-COOH), amino group ($-NH_2$), hydrogen atom and side chain. There are about 500 known amino acids that can be classified in many ways (Wendisch, 2007). One of these classifications is considered on their involvement in protein structure: proteinogenic or non-proteinigenic amino acids. Proteinogenic amino acids are amino acids that are precursors to protein, and are incorporated into proteins during translation. There are 23 proteinogenic amino acids but only 21 of them (alanine, arginine, asparagine, aspartic acid, cysteine, glutamine, glutamic acid, glycine, histidine, isoleucine, leucine, lysine, methionine, phenylalanine, proline, serine, threonine, tryptophan, tyrosine, valine and *N*-formylmethionine) are encoded directly by triplet codon in the genetic code and are known as "standard" amino acids. The remaining 2, selenocysteine and pyrrolysine, are incorporated into proteins by unique synthetic mechanisms. Nine proteinogenic amino acids (histidine, isoleucine, leucine, lysine, methionine, phenylalanine, threonine, tryptophan and valine) are called “essential amino acids” because they cannot be synthesized from cellular metabolites in the human or animal body; therefore they must be intake from food (Sprenger, 2007).

Many important proteinogenic and non-proteinogenic amino acids play critical non-protein roles within the body. For example, glutamic acid and gamma-amino-butyric acid (GABA) are the main excitatory and inhibitory neurotransmitters in the human brain, respectively; hydroxyproline is a major component of the connective tissue collagen; glycine is used to synthesise porphyrins used in red blood cells; and carnitine is used in lipid transport (Ganguly, 2001; London et al., 1949 and Sprenger, 2007).

Because of their biological importance, amino acids are significant in nutrition and are commonly used in nutritional supplements, fertilizers, drugs and food technology. Nowadays, amino acid market is over $6 billion with production amounts of 3 million tons per year. World production of amino acids are shown in Table 1.1 (Demain, 2007).

There are four general processes to produce amino acids: chemical synthesis, fermentation, extraction and enzymatic reaction (Leuchtenberger et al., 2005). The main reason to choose between those processes are: available technology, costs of raw material, market prices and sizes, cost of running fermentation and the environmental impact of the process itself. This thesis focuses on the production of L-phenylalanine which is the forth market value of all amino acids by fermentation of *Escherichia coli*.

1.2 L-Phenylalanine

Phenylalanine (L-Phe, $C_9H_{11}NO_2$; MW. 165.19; 2-amino-3-phenylpropanoic acid) has benzyl side chain so it is classified as nonpolar and hydrophobic amino acid. There are two forms of phenylalanine made in the laboratory: D-phenylalanine and L-phenylalanine. L-Phe is an essential proteinogenic amino acid. Sources of L-Phe are meat, fish, eggs, cheese, and milk. L-Phe is a precursor in the biosynthesis of other amino acids including L-tyrosine, the monoamine signaling molecules L-dopa, dopamine, norepinephrine (noradrenaline), and epinephrine (adrenaline) as shown in Figure 1.1 (Van de Rest et al., 2015). L-Phe is important to maintain of monoamine neurotransmitters in the brain. These neurotransmitters are control of movement which were stimulated heart, the rate of metabolism, and mobilize many of the body's energy reserves. It has adjusted activity of brain, control cooperation and motion, and regulates the flow of information to different areas of the brain. (Daniel et al., 1976; Fernstrom and Fernstrom, 2007).

Table 1.1 Worldwide production of amino acids (Demain, 2007)

Amino acid	**Process**	**Tons / Year**	**Market ($)**
L-Alanine	Enzymatic	500	-
L-Arginine	Fermentation	1,200	150 million
L-Aspartic acid	Enzymatic	10,000	43 million
L-Cysteine	Enzymatic	3,000	4.6 million
L-Glutamic acid	Fermentation	1,600,000	1.5 billion
L-Glutamine	Fermentation	1,300	-
Glycine	Chemical	22,000	-
L-Histidine	Fermentation	400	-
L-Isoleucine	Fermentation	400	-
L-Leucine	Fermentation	500	-
L-Lysine-HCl	Fermentation	850,000	1.5 billion
DL-Methionine	Chemical	400,000	2.3 billion
L-Phenylalanine	Fermentation	12,650	198 million
L-Proline	Fermentation	350	-
L-Serine	Fermentation	300	-
L-Threonine	Fermentation	70,000	270 million
L-Trytophan	Enzymatic	3,000	150 million
L-Tyrosine	Fermentation	165	50 million
L-Valine	Fermentation	500	-

1.3 Application of L-phenylalanine

L-Phe is the most important commercially produced aromatic amino acids and is an important building block in pharmaceutical and food additive industries (Bongaerts et al., 2001). L-Phe is produced predominantly for the production of the low-calorie sweetened aspartame. Other applications of L-Phe are using in infusion fluids, in food additives as an intermediate for the synthesis of active compound and as a flavor enhancer.

1.3.1 Medical use of L-phenylalanine

Effects of L-phenylalanine in the brain include antagonize of glycine and glutamate at specific receptors in the cortex and hippocampus that repress neurotransmitters can also contribute to the antidepressant (Glushakov et al., 2003). Phenylalanine is used in the therapeutically products as for analgesic and antidepressant effects (Mitchell, 2008). Birkmayer and coworkers (1984) studied the power of combination of L-Phe and selegiline, antidepressant drug. Selegiline is a monoamine oxidase inhibitor for treatment of depression and Parkinson's disease. The 5 – 10 mg/day of selegiline combined with L-Phe 250 mg/day were treated to 155 depressed patients. The results showed that this combination was effective for 90% of outpatients and 81% of inpatients suffering from depression. In that study, the combination of selegiline and L-Phe significantly improved mood in 9 out of the 10 patients. The improvement in mood occurred within hours of taking the combination and 6 of the patients were complete relief after 3 weeks. Other drugs containing phenylalanine are shown in Appendix A.

1.3.2 Industrial use of L-phenylalanine

L-Phe is mainly used as a nutritional supplement and as a precursor for the synthesis of food additives. Considering the size of its market, aspartame (L-aspartyl-L-phenylalanine methyl ester) is the most important compound having L-Phe as a precursor. Aspartame is the most widely used low-calorie sweetener with an estimated world market of USD $1.5 billion by over 200 million people around the world

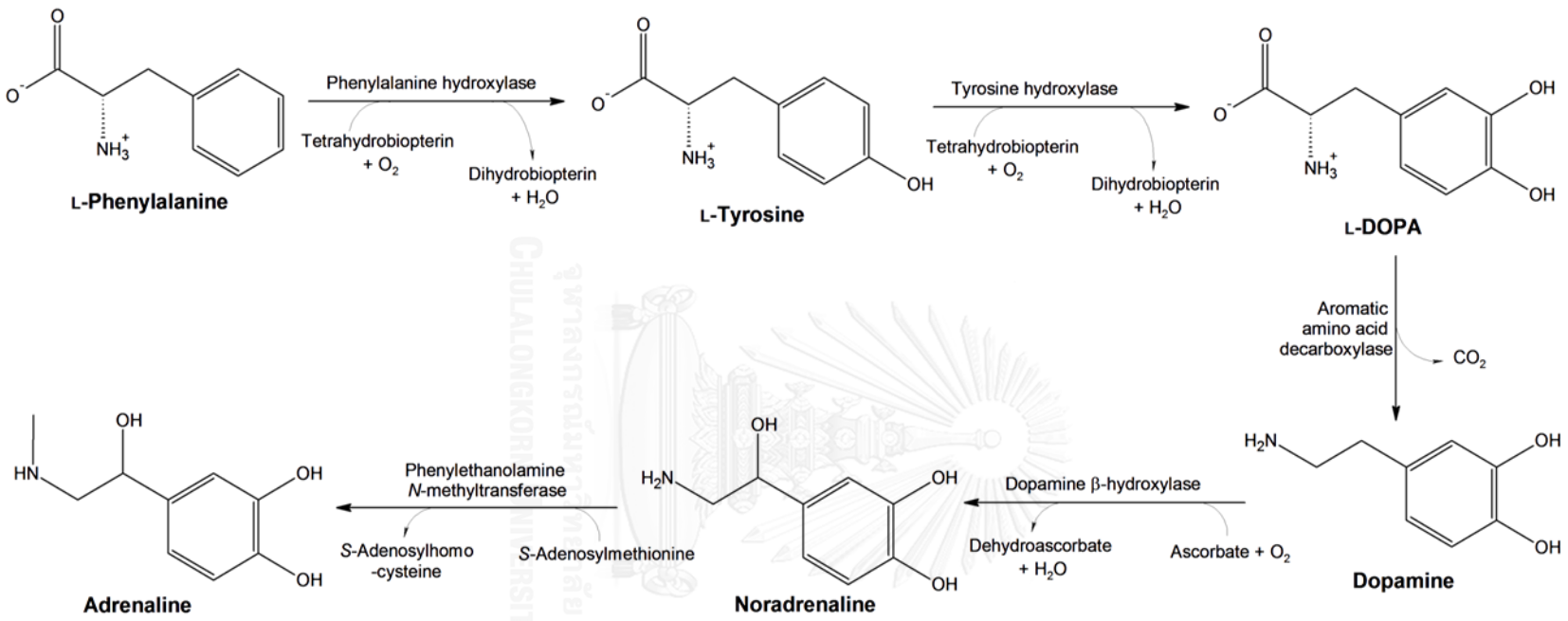

Figure 1.1 Conversion of phenylalanine and tyrosine to its biologically important derivative
Source: Van de Rest et.ai, 2015

(Baez-Viveros et al., 2004). Therefore, aspartame is found in many products including soft drinks, gum, gelatins, dessert mixes, yogurt, and some pharmaceutical such as vitamin and sugar-free candy. It is digested like a protein by the body and is 200 times as sweet as sucrose (Southwick et al., 2011). Moreover, L-Phe is a precursor of benzaldehyde, an important aromatic compound participating in flavor in the manufacture of cheese (Smit, 2004).

1.4 L-Phenylalanine production

Various methods have been proved to achieve the production of L-Phe. Traditionally, L-Phe has been synthesized by chemical method. However, the demand for optically active form of phenylalanine induced the research on bioprocessing. Fermentative and enzymatic processes have been proposed and developed over the last three decades for L-Phe production. For examples, L-Phe synthesis by enzymatic processes either with whole cells or purified enzymes by amination of *trans*cinnamic acid catalyzed by phenylalanine ammonia-lyase (PAL) or transamination of phenylpyruvate catalyzed by aromatic amino acid aminotransferase (AAT) (Chao et al., 1999) or reductive amination of phenylpyruvate catalyzed by phenylalanine dehydrogenase (PheDH) from *Brevibacterium* sp. (Hummel et al., 1986). Microbial production involve either biotransformations of phenylpyruvate and aspartate with recombinant *Escherichia coli* cells with elevated levels of aminotransferases and phosphoenolpyruvate (PEP) carboxykinase or microbial fermentations from glucose, sucrose, or molasses. Especially, recombinant strains of *Corynebacterium glutamicum* and *E. coli* are used for fermentative production of phenylalanine in industry (Ikeda and Nakagawa, 2003 and Bongaerts et al., 2001).

1.5 Pathway of aromatic amino acid biosynthesis in *E. coli*

The Figure 1.2 shows aromatic amino acid synthesis pathway that links to glycolysis and pentose phosphate pathways in *E. coli*. Condensation of phosphoenolpyruvate (PEP) from the glycolysis pathway and erythrose 4-phosphate (E4P) from the pentose phosphate pathway catalyzed by three isoforms of 3-dehydroxy-D-arabino-heptulosonate 7-phosphate (DAHP) synthase initiates the aromatic amino acid

synthesis pathway. These DAHP synthases are encoded by three paralog genes: *aroF*, *aroG*, and *aroH*. These are subjected to allosteric control by tyrosine, phenylalanine and tryptophan, respectively. About 80% of DAHPS activity is contributed by AroG, 15% from AroF, and remaining activity corresponds to AroH (Sprenger, 2007 and Herrmann, 1999). The second step is conversion of DAHP to 3-dehydroquinate (DHQ) catalyzed by DHQ synthase (encoded by *aroB*). Subsequently, DHQ dehydratase (encoded by *aroD*) catalyzes the dehydration of DHQ to produce 3-dehydroshikimate (DHS). The next step is NADP-dependent reversible reduction of DHS to shikimate (SHIK) by shikimate dehydrogenase (encoded by *aroE*) (Michel et al., 2003). SHIK is then phosphorylated to yield shikimate 3-phosphate (S3P) by shikimate kinase I and II, encoded by *aroK* and *aroL*, respectively. The condensation of S3P and a second PEP molecule is catalyzed by 5-enolpyruvyl shikimate 3-phosphate (EPSP) synthase (encoded by *aroA*) to yield EPSP. The further step is catalyzed by chorismate synthase (encoded by *aroC*) with a trans-1,4 elimination of phosphate from EPSP to form chorismate (CHA). The rate-limiting enzymes for an aromatic amino acid pathway of *E. coli* were identified as DHQ synthase (encoded by *aroB*), shikimate kinase (encoded by *aroL* or *aroK*) by analysis of intermediate metabolite accumulation (Dell and Frost, 1993). The central pathway branches at CHA to permit the terminal pathways that are specific for relevant aromatic amino acid (L-Phe or L-Tyr or L-Trp) (Maeda and Dudareva, 2012 and Bongaerts et al., 2001).

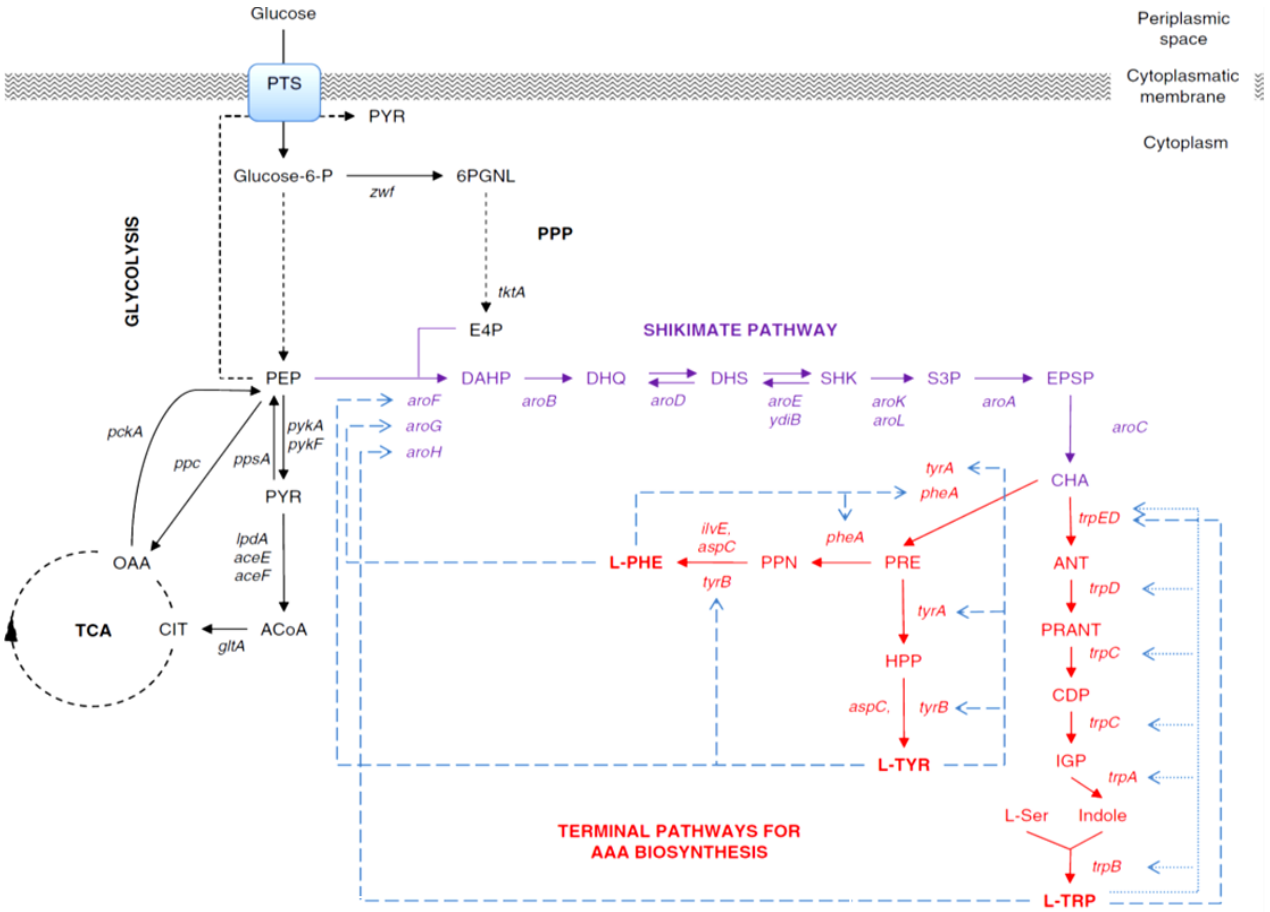

Figure 1.2 Aromatic amino acid pathway in *E. coli* (continued)

(continued)

Figure 1.2 Aromatic amino acid pathway in *E. coli*

Central carbon metabolism intermediates and genes shown: PPP (pentose phosphate pathway); TCA (tricarboxylic acid cycle); E4P(erythrose-4-P); PGNL (6-phospho D-glucono-1,5-lactone); PEP (phosphoenolpyruvate); PYR (pyruvate); ACoA (acetyl-CoA); CIT (citrate); OAA (oxaloacetate); *zwf* (glucose 6-phosphate-1 dehydrogenase); *tktA* (transketolase I); *pykA*, *pykF* (pyruvate kinase II and pyruvate kinase I, respectively) *lpdA*, *aceE*, and *aceF* (coding for PYR dehydrogenase subunits); *gltA* (citrate synthase); *pckA* (PEP carboxykinase); *ppc* (PEP carboxylase); *ppsA* (PEP synthetase).

Shikimate pathway intermediates and genes shown: DAHP (3-deoxy-D-arabino-heptulosonate-7-phosphate); DHQ (3-dehydroquinate); DHS (3-dehydroshikimate); SHK (shikimate); S3P (SHK-3-phosphate); EPSP (5-enolpyruvyl-shikimate 3-phosphate); CHA (chorismate); *aroF*, *aroG*, *aroH* (DAHP synthase AroF, AroG and AroH, respectively); *aroB* (DHQ synthase); *aroD* (DHQ dehydratase); *aroE*, *ydiB* (SHK dehydrogenase and SHK dehydrogenase/quinate dehydrogenase, respectively); *aroA* (3-phosphoshikimate-1-carboxyvinyltransferase); *aroC* (CHA synthase).

Terminal AAA biosynthetic pathways intermediates and genes shown: ANT (anthranilate); PRANT (N-(5-phosphoribosyl)-anthranilate); CDP (1-(o-carboxyphenylamino)-1'-deoxyribulose 5'-phosphate); IGP ((1S,2R)-1-C-(indol-3-yl)glycerol 3-phosphate); *trpE*, *trpD* (ANT synthase component I and II, respectively); *trpC* (indole-3-glycerol phosphate synthase/ phosphoribosylanthranilate isomerase); *trpA* (indoleglycerol phosphate aldolase); *trpB* (tryptophan synthase); PRE (prephenate); PPN (phenylpyruvate); HPP (4-hydroxyphenylpyruvate); *tyrA*, *pheA* (TyrA and PheA subunits of the CHA mutase, respectively); *ilvE* (subunit of the branched-chain amino acid aminotransferase); *aspC* (subunit of aspartate aminotransferase); *tyrB* (tyrosine aminotransferase).

Continuous arrows show single enzymatic reactions, black dashed arrows show several enzymatic reactions, long-dashed blue arrows indicate allosteric regulation and dotted blue arrows indicate transcriptional repression.

Source: Rodriguez et.at, (2014)

1.6 L-Phenylalanine biosynthesis pathway

L-Phe is synthesized in three enzymatic steps from chorismate (Figure 1.3). At first, bifunctional enzyme chorismate mutase/ prephenate dehydratase (PheA), encoded by *pheA*, catalyzes the conversion of chorismate to phenylpyruvate (PPY) via prephenate (PPA). It is the key determinant of L-Phe production (Hudson and Davidson, 1984). The PheA activity is feedback-inhibited by L-Phe. The activities of prephenate dehydratase and the chorismate mutase were inhibited by L-Phe with nearly 90% and 55%, respectively. The last step of L-Phe biosynthesis is a transamination reaction onto phenylpyruvate with amino donor glutamate to yield L-Phe, which is catalyzed by three aminotransferases encoded by *tyrB, aspC* and *ilvE* genes. Their catalytic reactions are different in detail (Rodriguez et al., 2014 and Chao et al., 1999).

1.7 Metabolic engineering for L- phenylalanine production

Metabolic engineering of aromatic amino acid pathways requires first to alleviation existing control levels (repression, attenuation and feedback inhibition), and to remove rate-limiting steps by the appropriate overproduction of enzymes of the common aromatic amino acid pathway, and then to reduce competing pathways and to improve and balance precursor supply both in the common pathway as well as in the specific branch (Sprenger, 2007). L-Phe-producing strains of *E. coli* have been constructed with the use of recombinant DNA technology. The strategies used for improved production include amplification of possible rate-limiting enzyme(s) and/or the first enzyme in the common pathway. In 1987, Sugimoto and coworkers cloned feedback-resistant *aroF* (*aroF*^{fbr}) and feedback-resistant *pheA* (*pheA*^{fbr}) genes into a temperature controllable expression vector and transformed the recombinant plasmid into an L-Tyr-auxotrophic *E. coli* strain. The maximal L-Phe titer was 16.8 g/L at the optimal temperature of 38.5 °C. Backman and coworkers (1990) engineered *E. coli* containing for *aroF*^{fbr} and *pheA*^{fbr} gene. The clone produced L-Phe with titer of 50 g/L at 36 h of fermentation. Wu and coworkers (2003) studied the effect of co-expression

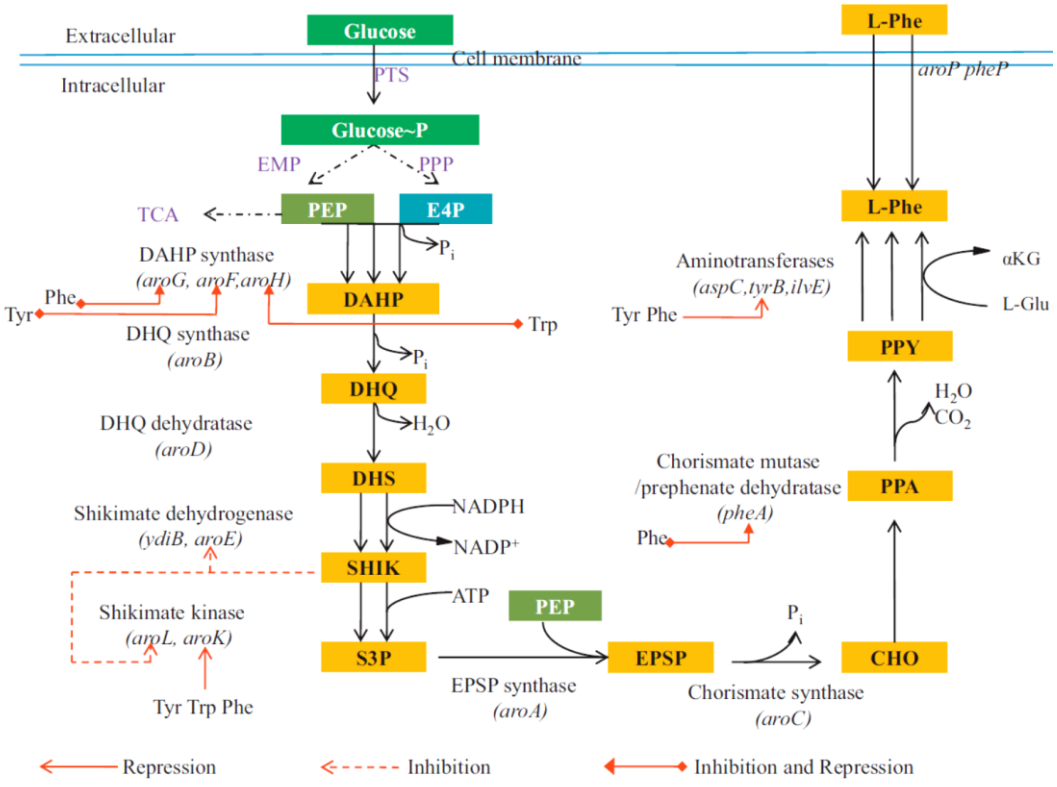

Figure 1.1 L-Phenylalanine biosynthesis pathway in *E. coli*

Metabolites abbreviations: PEP, phosphoenolpyruvate; E4P, erythrose4-phosphate; DAHP, 3-deoxy-D-arabino- heptulosonate-7-phosphate; DHQ, 5-dehydro-quinate; DHS, 5-dehydroshikimate; SHIK, shikimate; S3P, shikimate5-phosphate; ESPS, 3-enolpyruvylshimate-5-phosphate; CHO, chorismate; PPA, prephenate; PPY, phenylpyruvate; Phe, L-Phenylalanine; L-Glu, glutamate; αKG, α-ketoglutarate; Tyr, L-tyrosine; Trp, L-tryptophan.

Source: Liu et al., 2013

of *aroG*, *pheA*, PEP synthetase (*ppsA*), PEP carboxykinase (*pckA*) and prephenate dehydrogenase (*tyrB*) in pCZ vector compared with the wild-type *Brevibacterium flavum* cells, all transformants showed higher five enzyme activities, and 3.4-fold production of L-Phe. *E. coli* WSHZ06 was also constructed by recombinant plasmid that carrying $pheA^{fbr}$ gene as well as a wild-type *aroF* gene, this strain exhibited strong resistance to high-level L-Phe and over-produced of L-Phe about 35.38 g/L (Zhou et al., 2010). It was reported that L-Phe producing *E. coli* containing over-expressed *yddG* (encoding the inner membrane protein YddG) accumulated less L-Phe inside and exported the amino acid at a higher rate than wild-type (Doroshenko et al., 2007). Therefore, Thongchuang and coworkers (2012) improved L-phenylalanine production in recombinant *E. coli* BL21(DE3) by subcloning three genes including phenylalanine dehydrogenase gene (*phedh*) from *Bacillus lentus*, glycerol facilitator gene (*glpF*) to improve uptake of glycerol when *E. coli* was grown in glycerol, and aromatic amino acid exporter (*yddG*) gene as shown in Figure 1.4 into pRSFDuet. The result showed that the maximum L-Phe production was 280 mg/L in the shake flask. After that *aroB, aroL, pheA, tktA* which encode 3-dehydroquinate synthase, shikimate kinase II, chorismate mutase/prephenate dehydratase, and transketolase, respectively were co-expressed with the former three genes. The recombinant pPTFBLY clone had the highest L-Phe production rate of 3.36 mg/L/h and the L-Phe concentration of 429 mg/L was attained at 240 h after the optical density at 600 nm reached 0.6 (Thongchuang, 2011). However, morphology of recombinant *E. coli* colony on agar plate was changed. The small flat colonies were formed on agar plate with undulate margin. The altered morphology of colony occurred from basal level expression of membrane-associated protein without induction of *E. coli*-bacteriophage T7 RNA polymerase expression system (Miroux and Walker, 1996). The similar effect also found in over-production of seven membrane proteins in an *E. coli*-bacteriophage T7 RNA polymerase expression system. When expression of the target membrane was induced, most of the BL21(DE3) host cell died. Therefore protein over-production in this expression system is limited or prevented by bacterial cell death (Miroux and Walker, 1996).

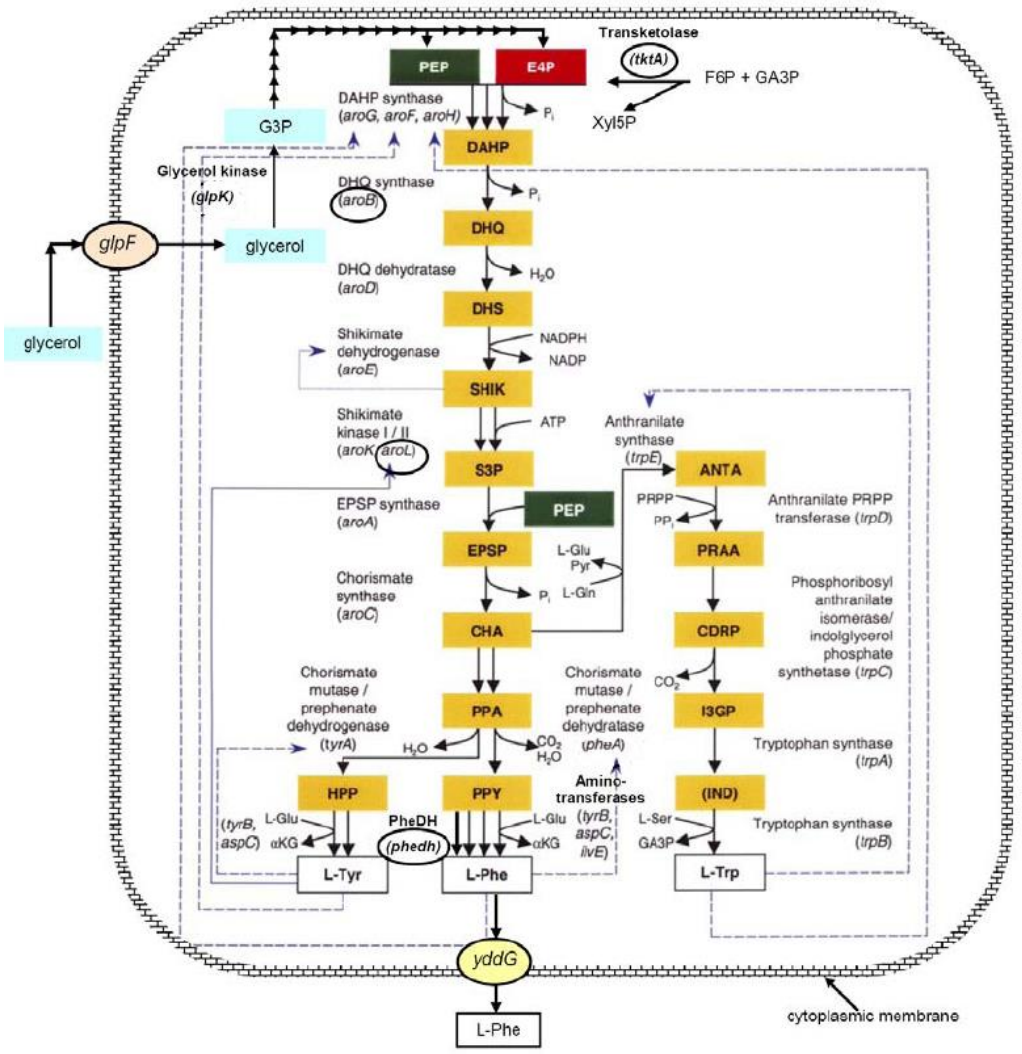

Figure 1.2 Pathway of aromatic amino acid biosynthesis and its regulation in *E. coli*

To indicate the type of regulation, different types of lines are used: – – –, transcriptional and allosteric control exerted by the aromatic amino acid end products; ……., allosteric control only; —, transcriptional control only. Abbreviations used: ANTA, anthranilate; αKG, α-ketoglutarate; CDRP, 1-(*o* carboxyphenylamino)-1-deoxyribulose 5-phosphate; CHA, chorismate; DAHP, 3-deoxy-*D arobino*-heptulosonate 7-phosphate; DHQ, 3-dehydroquinate; DHS, 3-dehydroshikimate; EPSP, 5 *enol*pyruvoylshikimate 3-phosphate; E4P, erythrose 4-phosphate; HPP, 4 hydroxyphenlypyruvate, I3GP, indole 3-glycerolphosphate; IND, indole; L-Gln, L-glutamine; L-Glu, L-glutamate; L-Phe, L-phenylalanine; L-Ser, L-serine; L-Trp, L-tryptophan; L-Tyr, L tyrosine; PEP, phospho*enol*pyruvate; PPA, prephenate; PPY, phenylpyruvate; PRAA, phosphoribosyl anthranilate; PRPP, 5-phosphoribosyl-α-pyrophosphate; Pyr, pyruvate; SHIK, shikimate; S3P, shikimate 3-phosphate **,** F6P, fructose 6-phosphate; G3P, glycerol 3-phosphate; GA3P, glyceraldehyde 3-phosphate
Source: Thongchuang, 2011

Several strategies have been described to prevent over production of toxic proteins. One of them has focused on the development of tightly regulatable expression vectors. Guzman and coworkers (1995) constructed a plasmid vector containing P_{BAD} promoter which is a part of the arabinose operon whose name derives from the genes it regulates transcription of: *araB, araA*, and a*raD* and its adjacent gene encoding the positive and negative regulator of this promoter, *araC*. *araC* encodes the AraC protein, which regulates activity of both the P_{BAD} and P_C promoters. The cyclic AMP receptor protein CAP binds between the P_{BAD} and P_C promoters, stimulating transcription of both when bound by cAMP. Transcription initiation at the P_{BAD} promoter occurs in the presence of high arabinose and low glucose concentrations. The P_{BAD} promoter allows for tight regulation and control of a target gene *in vivo*. P_{BAD} is regulated by the addition and absence of arabinose. As tested, the promoter can be further repressed with reduced levels of cAMP through the addition of glucose. Plasmid vectors have been constructed and tested with a selectable marker, origin of replication, araC and operons, multiple cloning site and P_{BAD} promoter. The pBAD system depends on catabolite repression and positive induction by tightly regulated which promoter has a minimal level of transcription, that is particularly important if the protein of interest is toxic or harmful for the host cell (Tegel et al., 2011). On the other hand, T7 polymerase system promotes a higher level of expression than pBAD. In the T7 system, recombinant protein expression is driven by promoter sequences recognized by T7 polymerase. The T7 polymerase gene is located on the bacterial chromosome under the control of a lactose-inducible bacterial promoter (Appendix B) and this promoter is leaky in the absence of inducer that may result in selective pressure from immediate and untimely expression of the toxic protein. Aaron and coworkers (2012) studied expression of transmembrane protein encoding by *ompA* gene that has an essential function in protecting the integrity of the outer membrane of *E. coli*. The vector pBAD containing the *ompA* insert was induced by arabinose control of ara promoter (Appendix C). The *ompA* expression was increased as increasing arabinose doses added to the culture medium.

1.8 Two plasmid-mediated co-expression in *E. coli*

The co-expression of two cistrons was achieved via use of a single bicistronic construct or two separate plasmids. A bicistronic construct is a single plasmid bearing two over-expressible cistrons. Ideally, for two plasmid-mediated co-expression, one needs to use compatible of replicon plasmids, defined as vectors that can co-exist in the same *E. coli* host cell to prevent exclusion and final loss of one plasmid in culture. For example, the plasmid vector pFL260 carrying the ColE1 replicon can co-exist with vector pFL261 carrying the p15A replicon in the same *E. coli* host cell. In addition, an ideal replicon-compatible overexpression system requires that each plasmid carries the gene encoding a different antibiotic resistance (Dzivenu, 2004).

Tolia and coworkers (2006) constructed two plasmids for co-expression in *E. coli*. First plasmid was prepared by subcloning GST-tagged human Ago2 (GST-hAgo2) into pGEX, pBR322 origin. Second plasmid was human heat shock protein 90 (hHSP90) inserted in pRSFDuet, RSF origin. The result showed insoluble proteins when expressed by mixing two genes in single plasmid. Indeed, they obtained soluble protein by two plasmid co-expression.

E. coli (P450pyrTM-GDH) was co-transformed with pETDuet (a pBR322 origin) containing with triple mutant I83H/M305Q/A77S (P450pyrTM) and ferredoxin reductase (*FdR*) genes and pRSFDuet (RSF origin) containing glucose dehydrogenase (GDH) and ferredoxin (*Fdx*) genes. This clone showed a high activity (12.7 Ug^{-1} cdw) for the biohydroxylation of *N*-benzylpyrrolidine and a GDH activity of 106 Ug^{-1} protein. The productivity is higher than that of the same biohydroxylation using *E. coli* (P450pyrTM) without expressing GDH (Pham et al., 2013).

Han and coworkers (2015) constructed an arabinose-inducible *O*-GlcNAc transferase (OGT) expression vector with a ColE1 origin and controlled its expression with an arabinose-inducible ara promoter (P_{BAD}). In addition, the pAT expression vector was constructed based on the pET expression system by replacing the original pBR322 with a p15A origin, which is compatible with ColE1-type plasmids. The pAT expression vector was used to express casein kinase II (CKII) which is OGT target substrates. To evaluate the expression of OGT and its target substrate, varied

concentration of IPTG was applied with constant concentration of arabinose. The results showed that CKII expression varied with IPTG concentration, while the OGT expression level was unchanged.

1.9 Use of glycerol as a carbon source

Glycerol can be produced either by microbial fermentation or chemical synthesis from petrochemical feedstock. Nowadays, biodiesel is selected to be the first alternative energy because of the abundant resources. Thailand is one of the countries that respond to this trend. Biodiesel is produced from vegetable oils and animal fats through esterification with, for instance, ethanol or methanol (alcoholysis) as shown in Figure 1.5. Generally, the reaction is catalyzed by NaOH or KOH and glycerol represents 10% of the ester production (Gonzalez-Pajuelo et al., 2004; Mu et al., 2006 and Papanikolaou et al., 2002) The availability of glycerol is increased because of the growth in the production of biodiesel worldwide (Wang et al., 2006). It was projected that the world biodiesel market will reach 37 billion gallons by 2016, which suggested that approximately 4 billion gallons of crude glycerol would be produced (Yang et al., 2012). Glycerol has been successfully used as the carbon source for various microbial productions by fermentation such as production of succinic acid by an anaerobic bacterium, *Anaerobiospirillum succiniciproducens* (Lee et al., 2001), β-hydroxypropionaldehyde by *Lactobacillus reuteri* (El-Ziney et al., 1998), 2,3-butanediol and 1,3-propandiol by *Klebsiella pneumoniae* (Biebl et al., 1998). Other samples of microorganisms that can utilize glycerol as a carbon source by fermentation are *Citrobacter freundii*, *Clostridium pasteurianum*, *Enterobacter agglomerans* and *Enterobacter aerogenes* (da Silva et al., 2009).

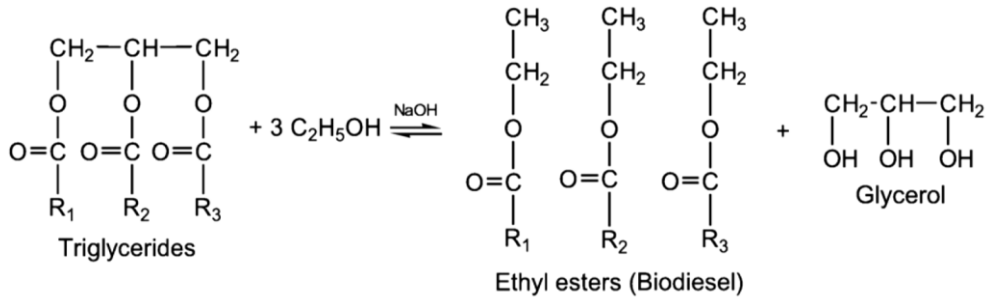

Figure 1.3 Transesterification reaction

Source: da Silva et al., 2009

Aerobic glycerol metabolism in *E. coli* is shown in Figure 1.6. The initial step of glycerol utilization is the uptake of glycerol molecule into cell by glycerol facilitator (GlpF) encoded by the *glpF* gene (Sweet et al., 1990). Intracellular glycerol can enter to the central carbon metabolism in form of the glycolytic intermediate dihydroxyacetone-phosphate (DHAP). The routes for the formation of DHAP from glycerol have been divided into two pathways as the glycerol-3-phosphate (G3P) pathway and the dihydroxyacetone pathway. In DHAP pathway, an imported glycerol is phosphorylated to G3P by ATP-dependent glycerol kinase encoded by *glpK* gene and G3P is subsequently oxidized to DHAP by G3P dehydrogenase (Gottlieb et al., 2014). Glycerol kinase catalyzes the rate-limiting step in glycerol utilization (Pettigrew et al., 1996). Intracellular glycerol can also be oxidized to dihydroxyacetone by glycerol dehydrogenase **(**GldA) (Monniot et al., 2012). DHA is converted to DHAP by the DHA kinase (DhaK) (Gonzalez et al., 2008). Both DHAP and G3P intermediates are further metabolized in glycolysis to supply phospho*enol* pyruvate, an initial precursor, for the common aromatic amino acid biosynthetic pathway. Moreover, DHAP and G3P are metabolized via gluconeogenesis to form fructose-1,6-bisphosphate (F1,6BP) which is dephosphorylated by fructose-1,6-bisphosphatase to yield fructose 6-phosphate (F6P). F6P can be shunted from glycolysis to the non-oxidative branch of the pentose phosphate pathway to supply erythrose 4-phosphate, another initial precursor of the common aromatic amino acid biosynthetic pathway.

1.10 Medium formulation

Organisms require a source of materials not only a source of energy but also for biosynthesis of cellular matter and products in cell operation, maintenance and reproduction. Some microorganisms utilize elements in the form of simple compound, other required more complex compounds, usually related to the form in which they are ultimately incorporated in the cellular material. In laboratory, bacteria can grow in the culture media which are designed to supply in solution for bacterial growth.

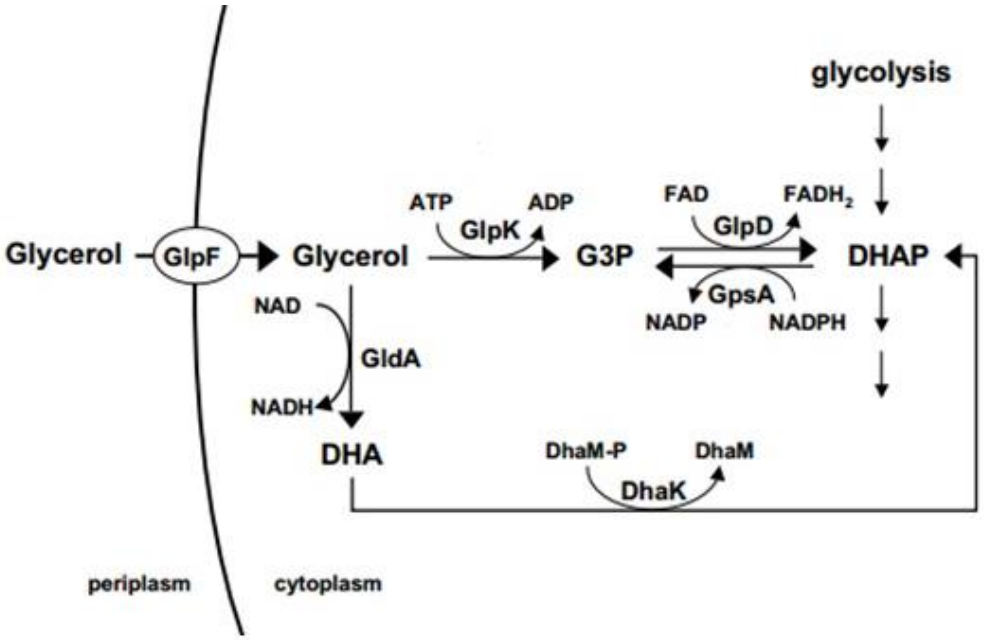

Figure 1.4 Glycerol metabolism in *E. coli*

Source: Xavier and Bassler, 2005

At an elementary level, the nutritional requirements of a bacterium such as *E. coli* consists of C, H, O, N, S. P, K, Mg, Fe, Ca, Mn, and traces of Zn, Co, Cu, and Mo (Wackett et al., 2004). These elements are found in the form of water, inorganic ions, small molecules, and macromolecules which promote either structural or functional role in the cells. The general physiological functions of the elements are outlined in Table 1.2.

Natural media such as molasses, corn steep liquor, meat extracts, etc., are not completely defined chemically (Celeste et al., 2014), however, they are the media of choice in industrial fermentations. In many cases the natural media have to be supplemented with mainly inorganic nutrients to requirements of the fermenting organism. Using pure compounds in precisely defined proportions yields a defined of synthetic medium. This is usually preferred to determine specific requirements for growth and product formation by systematically adding or eliminating chemical species from the formulation. Defined media can be easily reproduced, have low foaming tendency, show low translucency and allow easy product recovery and purification (Khamduang, 2009).

1.11 Published media for amino acid production

Shakoori and coworkers (2012) optimized fermentation media for enhanced production of amino acids by bacteria isolated from different natural sources including sewage water, fresh milk, honey, yoghurt and soil. Composition of basal media used for primary screening of amino acid producing bacteria and composition of glucose-based fermentation media used for over-production of amino acids by bacterial isolates were varied. Sixty five bacterial isolates from these natural sources were isolated and nineteen isolates were found to be producers of amino acids. Behavior of growth curves in LB medium indicated that the lag phase was very short up to 2 h and the log phase was extended upto 12 h in all organisms. After 12 h of incubation, growth of the organisms was declined and stable. Das and coworkers (1995) optimized fermentation medium for glutamic acid production from plam waste hydrolysate by *Brevibacterium lactofermentum* ATCC 13869. Among carbon

Table 1.2 Major elements, their sources and functions in bacterial cells

Element	% dry wgt	Source	Function
Carbon	50	Organic compounds or CO_2	Main constituent of cellular material
Oxygen	20	H_2O, organic compounds, CO_2, and O_2	Constituent of cell material and cell water; O2 is electron acceptor in aerobic respiration
Nitrogen	14	NH_3, NO_3, organic compounds, N_2	Constituent of amino acids, nucleic acids nucleotides, and coenzymes
Hydrogen	8	H_2O, organic compounds, H_2	Main constituent of organic compounds and cell water
Phosphorus	3	inorganic phosphates (PO_4)	Constituent of nucleic acids, nucleotides, phospholipids, LPS, teichoic acids
Sulfur	1	SO_4, H_2S, S, organic sulfur compounds	Constituent of cysteine, methionine, glutathione, several coenzymes
Potassium	1	Potassium salts	Main cellular inorganic cation and cofactor for certain enzymes
Magnesium	0.5	Magnesium salts	Inorganic cellular cation, cofactor for certain enzymatic reactions
Calcium	0.5	Calcium salts	Inorganic cellular cation, cofactor for certain enzymes and a component of endospores
Iron	0.2	Iron salts	Component of cytochromes and certain nonheme ironproteins and a cofactor for some enzymatic reactions

Soucer: Kampen, 1996

sources used (glucose, maltose, xylose, sucrose, fructose, lactose, mannitol, glycerol, ethanol, and acetic acid), glucose was the best for growth and production of glutamic acid by the bacterium. Cell growth and glutamic acid production were increased with increase in glucose concentration The glutamic acid production was 31.5 mg/mL at 48 hr. Of eight different nitrogen sources used (peptone, yeast extract, ammonium chloride, alanine, urea, ammonia, ammonium thiocynate, and ammonium sulphate), yeast extract showed the highest cell growth and the maximum production of glutamic acid was 65.5 mg/mL.

Majority of the microbes have a natural ability to convert complex organic compounds into aromatic amino acids. For phenylalanine production, four different fermentation media were selected for the study of L-Phe production in this thesis. The first media were optimized for L-Phe production in *E. coli* BL21(DE3) harboring pRSFDuet-1 with three inserted genes *phedh*, *glpF* and *yddG*. The maximum L-Phe production was 280 mg/L when the clone was cultured in shaking flask containing (g/L): glycerol 30; $(NH_4)_2SO_4$ 50; $MgCl_2 \cdot 6H_2O$ 0.81; KH_2PO_4 2.43; K_2HPO_4 2.43; yeast extract 0.085; thiamine-HCl 0.0085; $FeSO_4 \cdot 7H_2O$ 0.002; $MnSO_4 \cdot H_2O$ 0.002; $CaCl_2 \cdot 2H_2O$ 0.05; $ZnSO_4 \cdot 7H_2O$ 0.01 (Thongchuang et al., 2012). The second medium was developed by Zhou and coworkers (2011) for *E.coli* BR-42 host cell containing *aroF* and $pheA^{fbr}$ in plasmid pAP-B03. Maximum productions of phenylalanine are 57.63 g/L in a 3 L reactor. The second medium contained (g/L): glucose 20; $(NH_4)_2SO_4$ 5; KH_2PO_4 3; $MgSO_4 \cdot 7H_2O$ 3; NaCl 1; Na-citrate 1.5; $CaCl_2 \cdot 2H_2O$ 0.015, $FeSO_4 \cdot 7H_2O$ 0.1125; Thiamine-HCl 0.075; yeast extract 3 and 1.5 ml/L trace elements solution (TES). TES consisted of (g/L): $Al_2(SO_4)_3 \cdot 18H_2O$ 2.0; $CoSO_4 \cdot 7H_2O$ 0.75; $CuSO_4 \cdot 5H_2O$ 2.5; H_3BO_3 0.5; $MnSO_4 \cdot 7H_2O$ 24; $Na_2MoO_4 \cdot 2H_2O$ 3.0; $NiSO_4 \cdot 6H_2O$ 2.5 and $ZnSO_4 \cdot 7H_2O$ 15. The third medium was for *E. coli* PB12-ev2 containing *tktA*, $aroG^{fbr}$, and $pheA^{ev}$ in plasmid pACYC184 under control of *lacUV5* promoter. The production of L-Phe from glucose with $Y_{Phe/Glc}$ of 0.33 g/g corresponding to 60% of maximum theoretical yield. This medium contained glucose 10 g/L; 211 mM Na_2HPO_4; 42.8 mM NaCl; 110 mM KH_2PO_4; 74.7 mM NH_4Cl; 1 mM $MgSO_4$; 50 µM $CaCl_2$; 0.3 µM vitamin B1 and 1 ml/L of trace elements solution containing (g/l): $CaCl_2 \cdot 2H_2O$ 0.1; $CuCl_2 \cdot 5H_2O$ 0.02; $CoCl_2 \cdot 6H_2O$ 0.1; $FeSO_4 \cdot 7H_2O$ 0.2; $MnSO_4 \cdot 5H_2O$ 0.1; $ZnSO_4 \cdot 7H_2O$ 0.1 and $Na_2MoO_4 \cdot 2H_2O$ 0.01 (Baez-Viveros et

al., 2004). The last media was formulated for L-Tyr-auxotrophic *E. coli* strain with plasmid pF harboring *aroF*, *pheA*^{fbr}, *aroB* and *aroL*. This clone produced L- Phe 34 g/L when it was cultivated in the media containing (g/L): glucose 5.0; $MgSO_4 \cdot 7H_2O$ 0.3; $CaCl_2 \cdot 2H_2O$ 0.015; KH_2PO_4 3.0; K_2HPO_4 12; NaCl 1; $(NH_4)_2SO_4$ 5.0; $FeSO_4 \cdot 7H_2O$/Na-citrate 0.075/1.0; thiamine·HCl 0.0075 and trace element solution (1.5 ml/L). Trace element solution contained (g/L): $Al_2(SO_4)_3 \cdot 18H_2O$ 2.0; $CoSO_4 \cdot 7H_2O$ 0.75; $CuSO_4 \cdot 5\ H_2O$ 2.5; H_3BO_3 0.5; $MnSO_4 \cdot H_2O$ 24; $Na_2MoO_4 \cdot 2H_2O$ 3.0; $NiSO_4 \cdot 6H_2O$ 2.5 and $ZnSO_4 \cdot 7\ H_2O$ 15 (Ruffer et al., 2004).

1.12 Plasmid stability

Several alternative host cells have been proposed for plasmid DNA production, especially, a Gram-negative bacterium *E. coli* which is the most used host cell for plasmid DNA production. *E. coli* presents several advantages for rapid, high yield and economically feasible plasmid DNA production bioprocesses: fast growth with high cell densities and minimum nutrient requirements, resulting in low manufacturing costs (Sivashanmugam et al., 2009). Moreover, its well-characterized genetics; availability of a large number of cloning vectors and mutant host strains make this bacterium an attractive host for plasmid DNA bioprocess development. However, one of the most important problems for using recombinant clone is plasmid stability. Plasmid stability regularly refers to a tendency of bacterial transformed cell to lose its engineered properties due to a change in, or loss of, plasmids. The amount of plasmid DNA produced from a recombinant *E. coli* strain is strongly influenced by host cell–vector interaction, plasmid DNA instability, both structural and segregationally, and plasmid-induced metabolic stress. Host metabolic stress and plasmid stability cannot be dissociated from each other since the presence of plasmids can impose a metabolic burden on the host cell, which can lead to decreased plasmid copy number in host cells and ultimately result in higher plasmid instability. The term “metabolic burden” is defined as the amount of resources (raw material and energy) that are taken from the host cell metabolism for foreign DNA maintenance and replication (Bentley et al., 1990). Overall, the plasmid-induced metabolic burden is reflected by alterations in host cell physiology and metabolism and can also elicit several stress responses

which, in turn, can result in lower plasmid DNA yields due to the deleterious effects of these alterations on cell growth and plasmid synthesis (Silva et. al, 2012).

1.13 Response surface methodology for optimization of L-Phe

Traditionally, optimization has been carried out by monitoring the influence of one factor at a time on an experimental response. While only one parameter is changed, others are kept at a constant level. This optimization technique is called one-variable-at-a-time. Its major disadvantage is that it does not include the interactive effects among the variables studied, does not depict the complete effects of the parameter on the response and increases in the number of experiments necessary to conduct the research, which leads to an increase of time and expenses as well as an increase in the consumption of reagents and materials (Bezerra et al., 2008)

Response surface methodology (RSM) is a statistical technique for the optimization of complex processes. This technique has several advantages over optimization methods in which one variable at a time. RSM is a collection of mathematical and statistical techniques based on the fit of a polynomial equation to the experimental data, which must describe the behavior of a data set with the objective of making statistical previsions (Lundstedt et al., 1998). It can be well applied when a response or a set of responses of interest are influenced by several variables. The objective is to simultaneously optimize the levels of these variables to attain the best system performance (Enrique, 2007).

Five stages in the application of RSM are as follows: (1) the selection of independent variables of major effects on the system through screening studies and the delimitation of the experimental region; (2) the choice of the experimental design and carrying out the experiments according to the selected experimental matrix; (3) the mathematic–statistical treatment of the obtained experimental data through the fit of a polynomial function; (4) the evaluation of the model's fitness; (5) the verification of the necessity and possibility of performing a displacement in direction to the optimal region; and (6) obtaining the optimum values for each studied variable (Bezerra et al., 2008).

Central Composite Design (CCD) is one of two most frequently designs used in response surface modeling (Gilani et al., 2013). A second order prediction equation for the response is shown below.

$$y = \beta_0 + \sum_{i=1}^{k}(\beta_i x_i) + \sum_{i=1}^{k}(\beta_{ii} x^2{}_i) + \sum_{i<j}^{k}\left(\beta_{ij} x_i x_{ij}\right)$$

CCD consists of the following parts: (1) a full factorial or fractional factorial design; (2) an additional design, often a star design in which experimental points are at a distance $\alpha$from its center; and (3) a central point. Figure 1.7 (a and b) illustrates the full central composite design for optimization of two and three variables.

Full uniformly routable central composite designs present the following characteristics:

(1) The design requires an experiment number according to $N = k^2 + 2k + cp$, where k is the factor number and (cp) is the replicate number of the central point;

(2) α-values depend on the number of variables and can be calculated by $\alpha = 2^{(k-p)/4}$. For two, three, and four variables, they are, respectively, 1.41, 1.68, and 2.00;

(3) All factors are studied in five levels ($-\alpha$, −1, 0, +1, $+\alpha$).

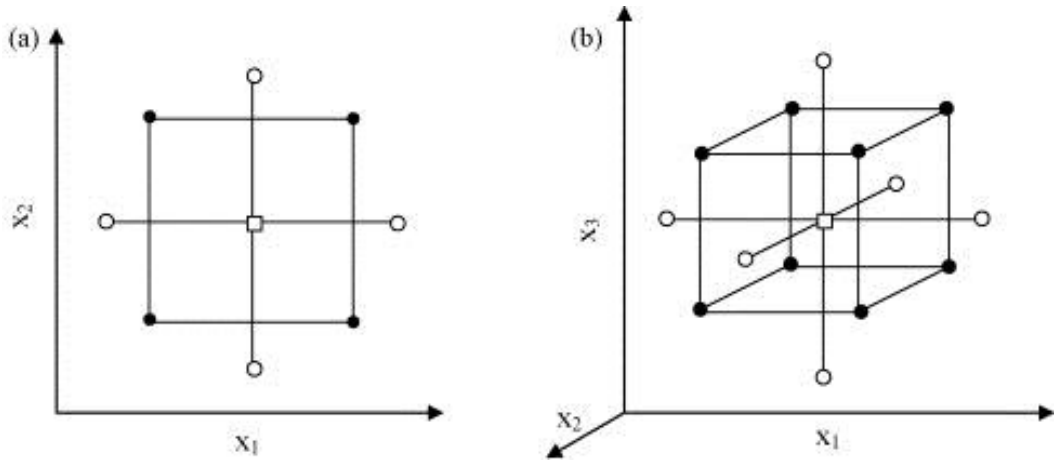

Figure 1.5 Central composite designs for the optimization of: (a) two variables (α = 1.41) and (b) three variables (α = 1.68). (●) Points of factorial design, (○) axial points and (□) central point.

Source: Bezerra et.al, (2008)

1.14 Objective of this research

1. To express the genes involving in L-Phe production in *E. coli* by dual plasmid system of pRSFDuet-1 carrying *aroB*, *aroL*, *phedh* and *tktA* genes and pBAD33 harboring *glpF* and *yddG* genes.

2. To optimize minimum medium using glycerol and $(NH_4)_2SO_4$ as carbon and nitrogen sources for L-Phe production in the recombinant clone.

CHAPTER II

MATERIALS AND METHODS

2.1 Equipments

Autoclave (MLS-3020, SANYO electric Co., Ltd., Japan)

Autopipette (Pipetman, Gilson, France)

Benchtop centrifuge (SorvallBiofuge Primo, Kendro Laboratory Products L.P., USA)

Bioreactor (BioFloIIc, New Brunswick Scientific, USA)

Dry bath incubator (MD-01N, Major Science, USA)

Electrophoresis unit (Gelmate 2000, TOYOBO Co., Ltd., Japan)

Electroporator (MicroPulserTMelectroporator, Bio-Rad Laboratories, Inc., USA)

Gel Doc (BioDoc-It® Imaging System with M-20 UV Transilluminator, UVP®, Inc., USA)

High Performance Liquid Chromatography (1100, Agilent, Germany)

Magnetic hotplate stirrer (CH-1E, Nickel Electro-Clifton, UK)

Microfuge centrifuge (22R, Beckman coulter, USA)

pH meter (S20-K SevenEasyTM, Mettler-Toledo, Switzerland)

Refrigerated centrifuge (Avanti J-30I High-Performance Centrifuge, Beckman Coulter, Inc., USA)

Chirex 3126 (D)-penicillamine size 150 mm dimension 4.6 mm (Phenomenex, USA)

Shaking incubator (Excella E24R, New Brunswick Scientific, USA)

Spectrophotometer (Beckman DU 530, Beckman Coulter, Inc., USA)

Thermo cycler (Mastercycler® Family, Eppendorf, Germany)

UV Transilluminator (MacroVueTM UV-25, Hoefer Inc., USA)

Vacuum/pressure pump (Model number. WP6111560, Millipore Inc., USA)

Vortex shaker (Topmix FB15024, Thermo Fisher Scientific Inc., USA)

2.2 Disposable materials

Membrane filter (Midisart 2000, 0.22µm, 64 mm, PTFE, sterile, Sartorius Stedim Biotech S.A., Germany)

Membrane filter (NYLON membrane filters, 0.45 µm, 47 mm, Vertical Chromatography Co., Ltd., Thailand)

Microcentrifuge tube (1.5 mL microcentrifuge tube, MCT-150, Axygen Inc., USA)

PCR tube (0.2 mL thin-wall domed-cap PCR tube, PCR-02D-C, Axygen Inc., USA)

Pipette tip (10 µL, 200 µL and 1000 µL pipette tip, Axygen Inc., USA)

Syringe (3 mL, 5 mL and 20 mL disposable syringe, Nissho Nipro Co., Ltd., Japan)

Syringe filter (0.2 µm, 13 mm, VertiPure^{TM} PTFE, Vertical Chromatography Co., Ltd., Thailand)

2.3 Markers

λDNA/*Hin*dIII Marker (#SM0103, Fermentas Inc., USA)

100 bp DNA marker (#SM0334, Fermentas Inc., USA)

2.4 Kits

Gel/PCR DNA fragment extraction kit (DF300, Geneaid, Biotech Ltd, Taiwan)

High-speed plasmid mini kit (PD300, Geneaid, Biotech Ltd, Taiwan)

2.5 Chemicals

Agar, Bacteriological grade (Criterion, USA)

Agarose (FMC Bioproducts, USA)

Ammonium sulphate (Carlo Erba, Italy)

Arabinose (Acros Organics, USA)

Bovine serum albumin (Sigma, USA)

Bromphenol blue (Merck, Germany)

Calcium chloride (Scharlau, Spain)

Chloramphenicol (Nacalaitesque, Japan)

Chloroform (Lab Scan, Thailand)

Copper sulfate (Carlo Erba, Italy)

Ethidium bromide (Sigma, USA)

Ethyl alcohol absolute (Carlo Erba, Italy)

Ethylenediaminetetraacetic acid disodium salt, EDTA (Merck, Germany)

Ferrous sulfate (Fluka, Switzerland)

Glacial acetic acid (Carlo Erba, Italy)

Glucose (Carlo Erba, Italy)

Glycerol (Ajax Finechem, Australia)

Isopropyl-β-D-thiogalactopyranoside (IPTG), Dioxane Free (US Biological, UK)

Kanamycin (Sigma, Switzerland)

Magnesium chloride (Carlo Erba, Italy)

Manganese (II) sulphate monohydrate (Carlo Erba, Italy)

Methanol, HPLC grade (Merck, Germany and LAB SCAN, Thailand)

Pancreatic digest of casein (Criterion, USA)

Phenol (BDH, UK)

L-Phenylalanine (Sigma, USA)

Potassium dihydrogen phosphate (Carlo Erba, Italy)

Potassium hydroxide (Ajax Finechem, Australia)

Sodium chloride (Carlo Erba, Italy)

Sodium citrate (Carlo Erba, Italy)

Sodium hydroxide (Carlo Erba, Italy)

Thiamine-HCl (Sigma, USA)

Tri-sodium citrate dehydrate (Scharlau, Spain)

Yeast extract (Scharlau, Spain)

Zine sulfate (BDH, England)

Other common chemicals were products obtained from Sigma, USA; BDH, UK;

Fluka, Switzerland; Merck, Germany; Ajax Finechem, Australia; Carlo Erba, Italy; and Lab Scan, Thailand.

2.6 Enzymes and restriction enzymes

Lysozyme (Sigma, USA)

Pfu DNA polymerase (Promega, USA)

Proteinase K (Sigma, USA)

Restriction enzymes (New England BioLabs, Inc., USA)

RNase A (Sigma, USA)

T4 DNA ligase (New England BioLabs, Inc., USA)

2.7 Bacterial strains and plasmids

Escherichia coli BL21(DE3), genotype: F^- *ompT* *hsdS*$_B$ ($r_B^- m_B^-$) *gal* *dcm*(DE3), was used as host for cloning and expression of recombinant plasmid of pRSFDuet-1 vector (The restriction map of pRSFDue-1 is shown in Appendix D). All plasmids are listed in Table 2.1.

Table 2.3 Plasmids used in this work

Plasmids	Relevant characteristics	Reference
pAroB	*aroB* gene inserted under T7*lac* promoter of pRSFDuet-1	Thongchuang, 2011
pBAD33	Expression vector with ara promoter (The restriction map of pBAD33 is shown in Appendix E).	Creative Biogene
pBLPT	Each *phedh*, *tktA*, *aroB* and *aroL* preceded by T7*lac* promoter inserted into pRSFDuet-1	This study
pGlpF	*glpF* gene under araBAD promoter in pBAD33	This study
pPTFBL	Each *phedh*, *tktA*, *glpF*, *aroB* and *aroL* preceded by T7*lac* inserted into pRSFDuet-1	Thongchuang, 2011
pPTFBLY	Each *phedh*, *tktA*, *glpF*, *aroB*, *aroL* and *yddG* preceded by T7*lac* promoter inserted into pRSFDuet-1	Thongchuang, 2011
pYF	*yddG* and *glpF* genes, both under ara promoter in pBAD33	This study

2.8 Media

2.8.1 Luria-Bertani broth

Luria-Bertani (LB) medium consisted of 1% peptone from casein agar, 0.5% yeast extract and 0.5% NaCl. For agar plate, 1% agar was added. 10 μg/mL chloramphenicol or 30 μg/mL kanamycin was supplemented as selective anitibiotic depending on plasmid.

2.8.2 Minimum medium

Formulas of all minimum media used in this thesis are shown in Table 2.2. The pH of media were adjusted to 7.0 and 7.4 by NaOH. Chloramphenicol (10 μg/mL) or kanamycin (30 μg/mL) were used as selective antibiotics.

2.9 Plasmid extraction

Five milliliters LB medium containing selective antibiotic was inoculated with a single colony. The culture was then incubated at 37 °C overnight with shaking at 250 rpm. After that, cell pellet was cultivated by centrifugation at 5,000 x g for 2 min at room temperature. Then, plasmid was isolated using High-Speed Plasmid Mini kit (Geneaid Biotech).

2.10 Agarose gel electrophoresis

DNA samples were separated and analyzed by electrophoresis using agarose gel containing 0.8% (w/v) agarose in 1×TBE buffer (89 mM Tris-HCl, 8.9 mM boric acid and 2.5 mM EDTA, pH 8.0 (Preparation is shown in Appendix F). The DNA samples were mixed with 6x loading buffer (30% glycerol and 0.25% bromphenol blue), then loaded into the gel. Electrophoresis was performed at 100 volt. The gel was stained with 2.5 μg/mL ethidium bromide for 1-2 min and destained by distilled water. The DNA bands were detected by exposing the gel to UV light.

Table 2.4 Minimum medium used in this thesis

Component	Concentration (g/L)			
	Formula 1	Formula 2	Formula 3	Formula 4
pH	7.4	7	7	7
glycerol	30.0	40	20	10.0
$(NH_4)_2SO_4$	50.0	5.0		5.0
NH_4Cl			4.0	
K_2HPO_4	2.4			12.0
KH_2PO_4	2.4	3.0	15.0	3.0
$MgCl_2$	0.8			
$MgSO_4 \cdot 7H_2O$		3.0	0.5	0.3
Na_2HPO_4			30.0	
Na-Citrate		1.5		1.0
NaCl		1.0	2.5	1.0
Thiamine	8.5×10^{-3}	7.5×10^{-2}	9.0×10^{-5}	7.5×10^{-3}
yeast extract	8.5×10^{-2}	3.0		
$Al_2(SO_4)_3 \cdot 18H_2O$		3.0×10^{-6}		3.0×10^{-6}
$CaCl_2$	5×10^{-2}	2.0×10^{-2}	5.6×10^{-3}	1.5×10^{-2}
$CoCl_2 \cdot 6H_2O$			1.0×10^{-7}	
$CoSO_4 \cdot 7H_2O$		1.1×10^{-6}		1.5×10^{-6}
$CuCl_2 \cdot 5H_2O$			2.0×10^{-8}	
$CuSO_4 \cdot 5H_2O$		3.8×10^{-6}		3.8×10^{-6}
$FeSO_4 \cdot 7H_2O$	3.7×10^{-2}	1.0×10^{-1}	2.0×10^{-7}	7.5×10^{-2}
H_3BO_3		7.5×10^{-7}		7.5×10^{-7}
$MnSO_4 \cdot 7H_2O$	3.7×10^{-2}	3.6×10^{-5}	1.0×10^{-7}	3.6×10^{-5}
$Na_2MoO_4 \cdot 2H_2O$		4.5×10^{-6}	1.0×10^{-8}	4.5×10^{-6}
$NiSO_4 \cdot 6H_2O$		3.8×10^{-6}		3.8×10^{-6}
$ZnSO_4 \cdot 7H_2O$	1.8×10^{-2}	2.3×10^{-5}	1.0×10^{-7}	2.3×10^{-5}

2.11 Extraction of DNA fragment from agarose gel

Extraction of DNA fragment from agarose gel was performed using Gel/PCR DNA fragment extraction kit (Geneaid Biotech).

2.12 PCR amplification

Fifty microliter of PCR reaction mixture contained 50 ng of DNA template, 0.2 mM each dNTPs, 10 pmole of each primer, 1xbuffer with $MgSO_4$ *Pfu* DNA polymerase and *Pfu* DNA polymerase. Condition for amplified gene was predenature (95 °C, 7 min), 30 cycles of denaturation (95 °C, 1 min), annealing (49 °C, 35 sec), and extension (72 °C, 2 min), and the last final extention (72 °C, 8 min). The sequence of primers are shown in Table 2.3.

2.13 PCR product cleaning

PCR product was purified using Gel/PCR DNA fragment extraction kit (Geneaid Biotech) according to the protocol.

2.14 Ligation

Ligation mixture (20 µL) contained 2 µL of 60 ng/µL of plasmid vector, 10 µL of 70 ng/µL of PCR product, 2 µL of 10x T4 DNA ligase buffer, 1 µL of T4 DNA ligase and 5 µL ultrapure water. Ligation mixture was mixed and incubated at 16 °C for 16 h.

2.15 Transformation of plasmid

2.15.1 Preparation of competent cell

A single colony of *E. coli* BL21(DE3) or *E. coli* BL21(DE3)/pBLPT from LB agar plate was grown in 100 mL of LB medium at 37 °C with shaking speed 250 rpm for 24 h. The 50 mL of starter was then inoculated to 1 liter of LB medium.

Table 2.5 Sequence and Tm of primers

Primer	Sequence (5’ to 3’)	Tm (°C)
F_yddG_*Xba*I	GCTCTAGAATGACACGACAAAAAGCAAC GCTCATA	67.5
R_yddG_*Sal*I	ACGCGTCGACTTAACCACGACGTGTCGCCAG	74.3
F_glpF__*Xba*I	GCTCTAGAATGAGTCAAACATCAACCTTGAAAGG	65.3
R_glpF_*Sal*I	ACGCGTCGACTTACAGCGAAGCTTTTTGTTCTGAAGGA	71.2
F_Ara_glpF_ *Sal*I	ACGCGTCGACCTGACGCTTTTTATCGCAACTCTCTACTG	71.6
R_Ara_glpF_ *Pst*I	AACTGCAGTTACAGCGAAGCTTTTTGTTCTGAAGGA	68.7
F_pro_glpF	CGCTGTCGTTCTCGTTCTG	56.0

After the optical density at 600 nm of cell culture reached 0.3-0.4, the culture was chilled on ice for 30 min and centrifuged at 8,000xg for 15 min at 4 °C. The cell pellets were washed with 1.5-2 medium volume of cold autoclaved distilled water. Finally, the cells were washed with 10 mL of cold 10% glycerol, centrifuged at 8,000xg for 10 min at 4 °C and resuspended with cold 10% glycerol to a final volume of 2-3 mL. Then 40 µL of cell suspension was aliquoted to 1.5 mL microcentrifuge tube and stored at -80 °C.

2.15.2 Electroporation

In the electroporation step, 0.1 cm cuvette and holder were chilled on ice. Competent cells were thawed on ice. After that, 3 µL of recombinant plasmids were mixed with 40 µL competent cells and replaced on ice for 1 min. This mixture was transferred to a cold cuvette. After the cuvette was placed into electroporation chamber and one pulse for electroporation was applied, 1 mL of LB medium was added and the cells were quickly resuspended with pipette. Then cell suspension was transferred to new tube and incubated at 37 °C for 1 h with shaking. Finally, 0.2 mL cell suspension was spread on LB agar plate containing antibiotic drug depending on the selective marker on plasmid and incubated at 37 °C for 18 h.

2.16 Nucleotide sequencing

The plasmids were sent to Macrogen, Korean for sequencing. The obtained nucleotide sequences were compared with Database in Genbank by BLAST online program.

2.17 Construction of recombinant plasmid

2.17.1 Construction of pBLPT

The recombinant plasmid pBLPT containing *aroB*, *aroL*, *phedh* and *tktA* genes was constructed using the genes from pAroB and pPTFBL. pAroB and pPTFBL were digested with restriction enzyme *Bam*HI and *Xho*I. The 20 µL of mixture for double digestion contained 1 µg of plasmid DNA , 1X of NEBuffer 4, 100 µg/mL of BSA, 10 U of *Bam*HI, and 10 U of *Xho*I. The restriction mixture was

incubated at 37 °C for 3 h. DNA fragments were separated by agarose gel electrophoresis. The 4,635 bp fragment from pAroB and 4,036 bp fragment containing *aroL, phedh* and *tktA* and their own T7 promoter as shown in Figure 2.1 were cut from gel and purified by Gel/PCR DNA fragment extraction kit. Then both purified fragment were ligated together to form pBLPT. After that pBLPT was transformed into *E. coli* BL21(DE3).

2.17.2 Construction of pYF

The complete *yddG* gene (882 bp) was amplified from pPTFBLY using forward and reverse primers: F_yddG_*Xba*I and R_yddG_*Sal*I, respectively. The gene fragment was digested and ligated into pBAD33 at *Xba*I and *Sal*I sites as shown in Figure 2.2. The sequence of *yddG* was confirmed by DNA sequencing. The pYddG was ready to use as a vector for insertion of *glp*F gene under ara promoter.

The *glpF* gene (846 bp) was amplified using pPTFBLY as a template and F_glpF_*Xba*I and R_glpF_*Sal*I as forward and reverse primers, respectively. The gene fragment was concentrated using PCR clean up protocol of gel/PCR DNA fragment extraction kit. Then DNA fragment and pBAD33 vector were digested with *Xba*I and *Sal*I and ligated together as shown in Figure 2.3. The correct sequence of *glpF* was confirmed by DNA sequencing.

The pGlpF plasmid was used as a template to amplify the DNA fragment consisting the *glpF* gene under ara promoter (937 bp). The forward and reverse primers were F_Ara_glpF_ *Sal*I and R_Ara_glpF_ *Pst*I. The PCR fragment was cleaned up, digested with *Sal*I and *Pst*I and then cloned into pYddG at *Sal*I and *Pst*I sites as shown in Figure 2.4. The sequence of *glpF* gene and its ara promoter were confirmed by DNA sequencing.

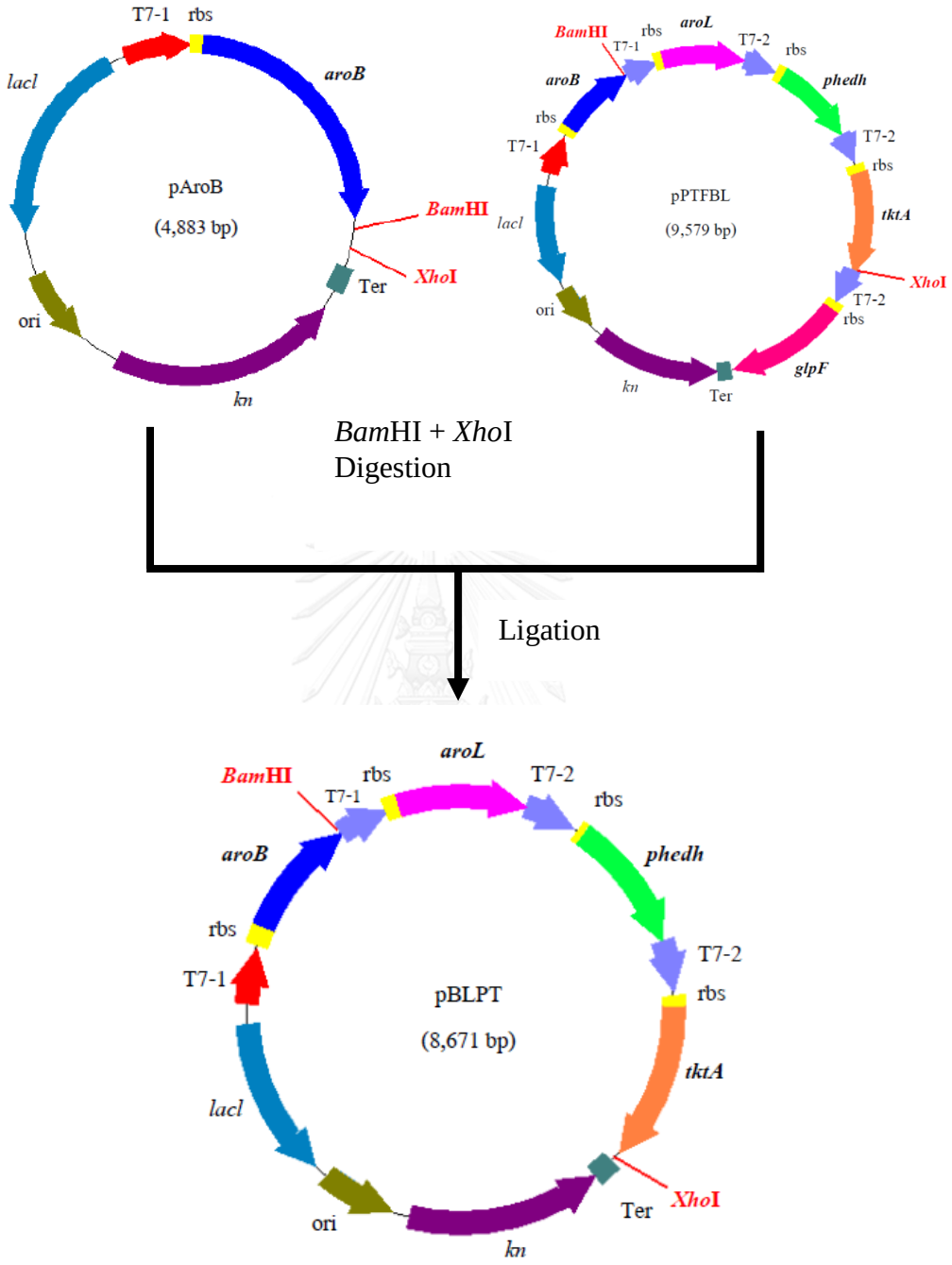

Figure 2.6 The construction of pBLPT

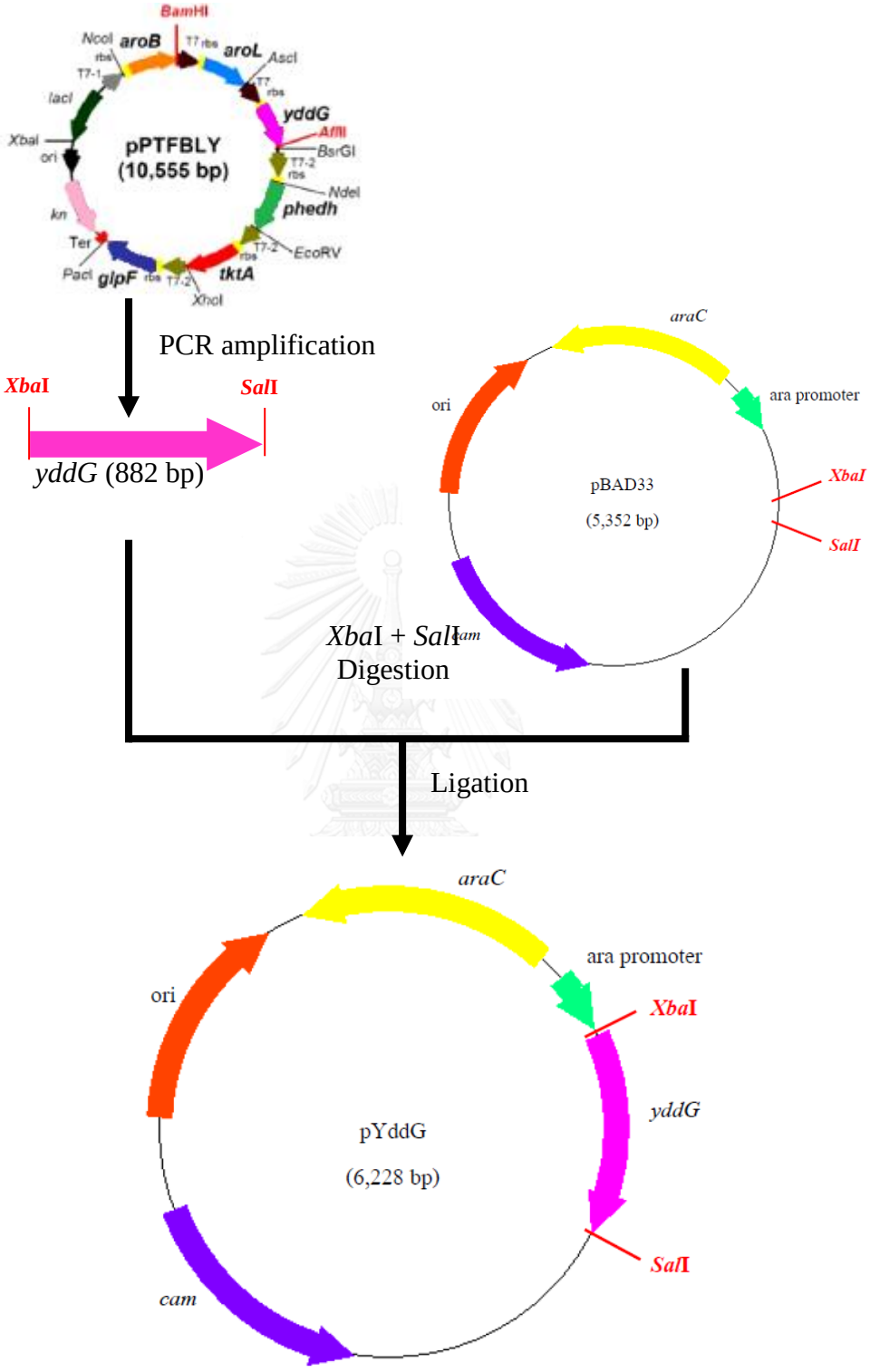

Figure 7.2 The construction of pYddG

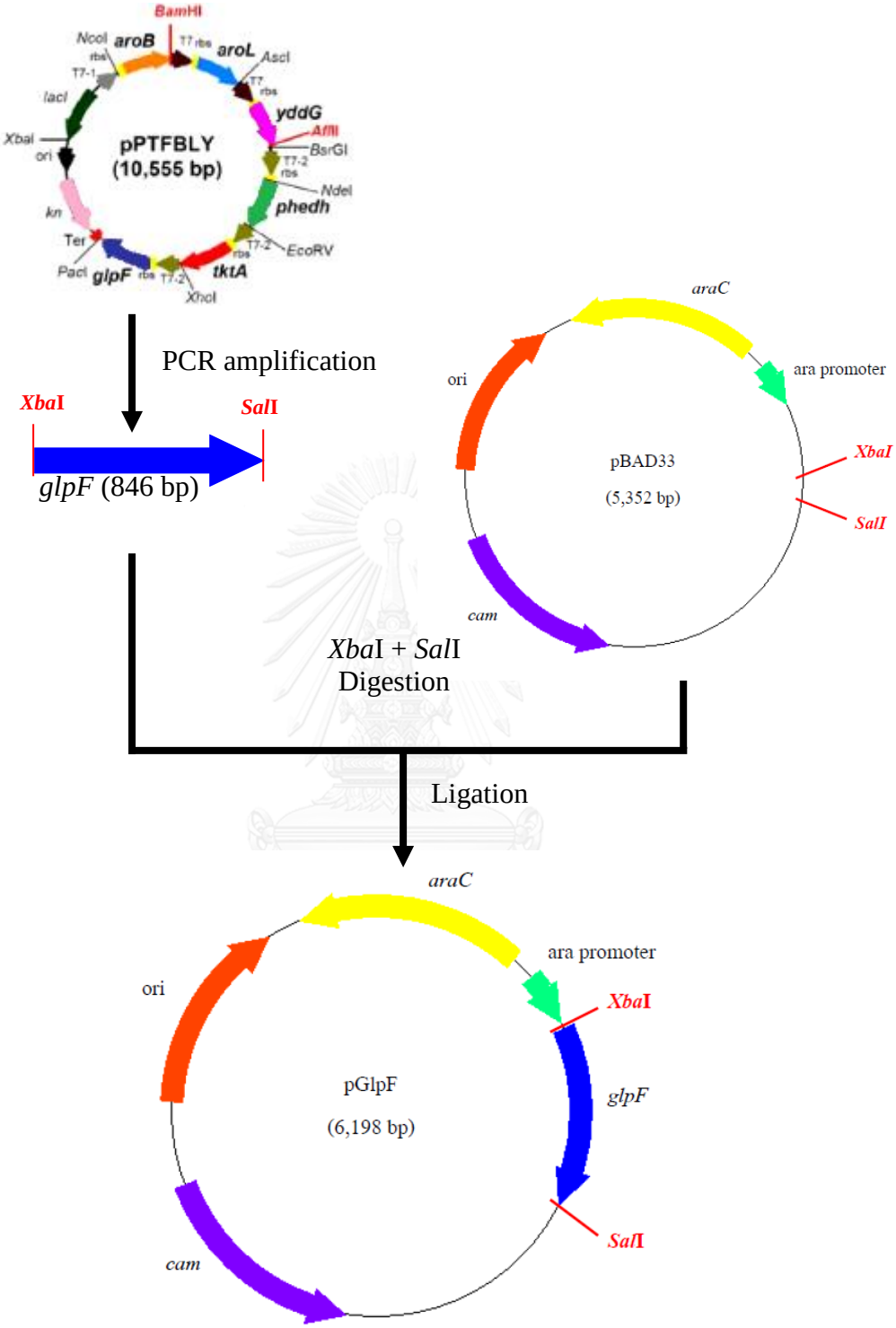

Figure 2.8 The construction of pGlpF

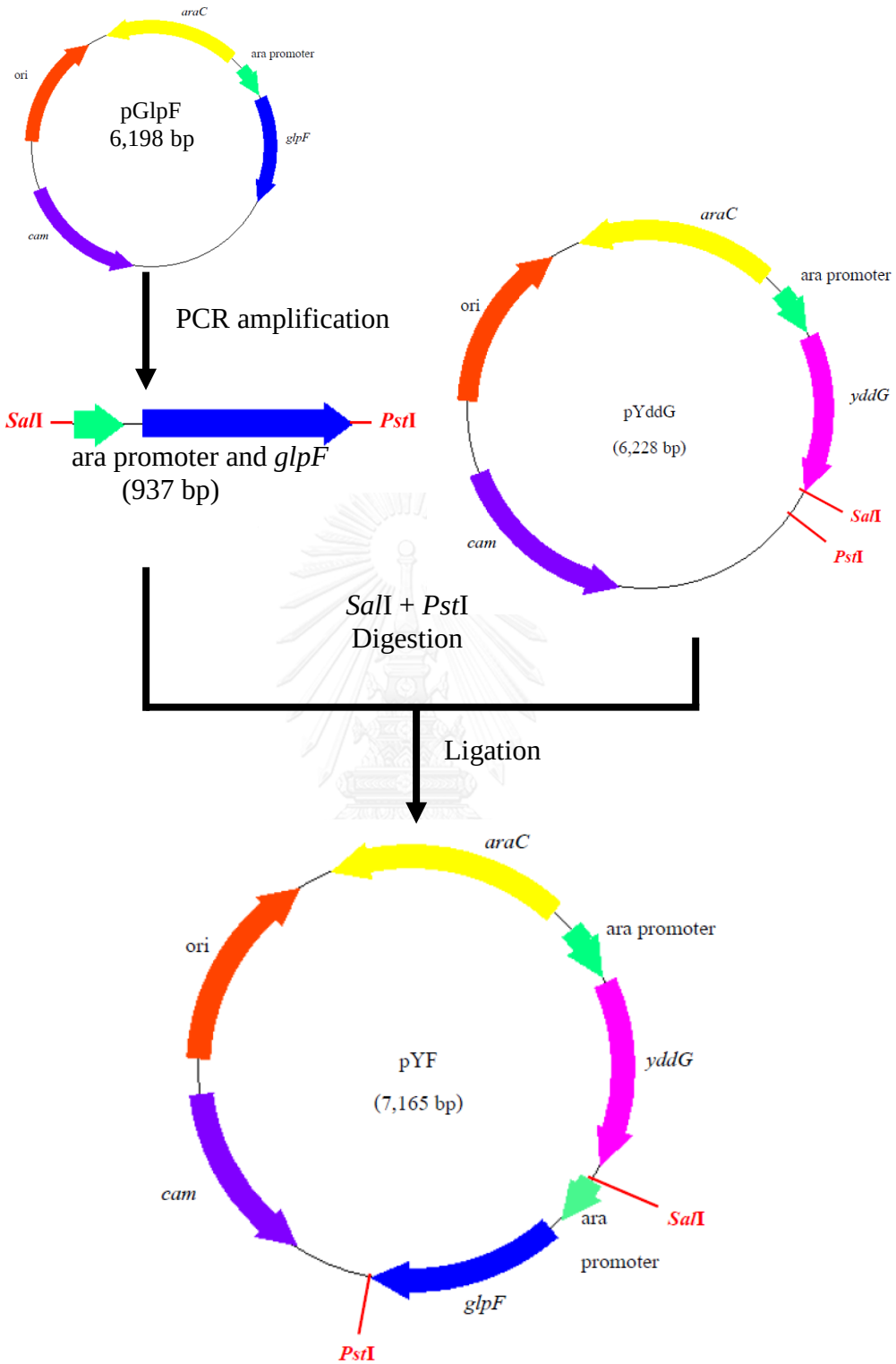

Figure 2.9 The construction of pYF

2.18 SDS-polyacrylamide gel electrophoresis

In order to determine the expression of each recombinant gene, SDS-PAGE was performed *E. coli* BL21(DE3) cells containing the recombinant plasmids were cultured in 5 mL of LB medium supplemented with 30 μg/mL of kanamycin and/or 10 μg/mL chloramphenicol at 37 °C for 18 h. The cell culture was inoculated (5% v/v) to LB medium 100 mL and incubation was continued until OD600 was about 0.6. IPTG and/or arabinose were added to a final concentration of 1 mM and 0.02%, respectively and the cultivation was continued for 3 h. The cells were harvested by centrifugation at 5,000xg for 10 min and stored at -20 °C for further analysis.

SDS-PAGE was done according to Bollag et al., 1996. The slab gel system consisted of 0.1% SDS (w/v) in 12% separating gel and 5% stacking gel. The cell pellets were resuspended in 100 μL of the 5x sample buffer (312.5 mM Tris-HCl pH 6.8, 50% (v/v) glycerol, 1% (w/v) bromophenol blue) and boiled for 15 min. After centrifugation at 12,000xg for 5 min, eight μL of each sample was loaded to the gel. The cell extract of recombinant *E. coli* BL21(DE3) clones containing pRSFDuet-1 or pBAD33 under induction with 1 mM IPTG and 0.02% arabinose were also loaded to the gel. The protein molecular weight markers were β-galactosidase (116 kDa), bovine serum albumin (66.2 kDa), ovalbumin (45 kDa), lactate dehydrogenase (35 kDa), restriction endonuclease Bsp98I (25 kDa), β-lactoglobulin (18.4 kDa) and lysozyme (14.4 kDa). After electrophoresis, the gel was stained with Coomassie blue solution and then destained by destaining solution. The standard curve for protein determination is shown in Appendix H.

2.19 Plasmid stability of pBLPT & pYF clone

pYF plasmid (pBAD33 containing *glpF* and *yddG*) was transformed into *E. coli* BL21 (DE3) containing pBLPT to construct pBLPT & pYF clone. The simple approach to the determination of plasmid stability is to look for the loss of a plasmid. Since both plasmids carried their selective antibiotic marker, the percentage of cell in culture that lost the plasmid markers was determined by using plating technique. The stability experiment was performed in duplicate, starting from inoculation of single

colony of pBLPT & pYF on LB plates inoculated into 5mL of LB medium and cultured at 37 °C with shaking at 250 rpm. Every 24 h, 10 µL of cell culture was transferred to 5 mL of new LB medium, the 24 h cell culture was diluted at 10^{-4}, 10^{-5} and 10^{-6} and then spreaded on non-antibiotic plate (LB medium) and selective plates (LB medium containing 30 µg/mL of kanamycin or 10 µg/mL of chloramphenicol). The number of colonies on plate (CFU) were counted. The percentage of cell containing plasmid can be calculated as

$$\% \text{ plasmid containing cell} = \frac{\text{number of colonies on selective plates}}{\text{number of colonies on non selective plate}} \times 100$$

2.20 L-Phenylalanine production by pBLPT & pYF clone

L-Phe production of pBLPT & pYF clone in minimum medium were studied in comparison with those of pPTFBLY clone.

2.20.1 Optimization of media for L-phenylalanine production

The single colony of pBLPT & pYF clone was cultured in 5 mL LB medium containing 30 µg/mL of kanamycin and 10 µg/mL chloramphenicol at 37 °C with shaking at 250 rpm for overnight while pPTFBLY clone was cultured in LB medium containing 30 µg/mL of kanamycin. After that 5 mL of each starter was inoculated in 200 mL LB medium containing selective antibiotic(s) and cultured in the same condition as starter. Then 5% of each cell suspension was inoculated in 100 mL minimum medium (shown in Table 2.2). One mL of cell suspension was taken for measuring the optical density at 600 nm (using medium as a blank). After OD600 reached 0.6, pBLPT & pYF was induced by addition of 0.2% arabinose. Every 24 h, 1 mL of all suspension was taken for measuring OD600 and supernatant was harvested by centrifugation at 5,000xg for 2 min and stored at -20 °C for L-Phe determination.

2.20.2 HPLC analysis for determination of L-phenylalanine

Supernatant from 2.19.1 was passed through 0.2 μm syringe filter set. The sample were analyzed by HPLC technique using Chirex 3126 (D) - penicillamine column and 2 mM copper sulfate (Preparation is shown in Appendix F) and methanol ratio 70:30 as a mobile phase. The column was operated at flow rate 1 mL/min and peaks were detected at 254 nm. The injected sample volume was 20 μL. L-Phe was quantified by comparison with the calibration curve (Appendix G).

2.20.3 Experiment design for L-phenylalanine production using response surface methodology (RSM)

Response Surface Methods use specific experimental design combinations to develop mathematical models with linear, quadratic, and interaction terms to find optimum performance from a given set of factors and response variables. The major medium components for L-Phe production were optimized using a RSM which is useful statistic method to design experiment and analysis the data. Three medium components: glycerol (carbon source), ammonium sulfate (nitrogen source), and arabinose (inducer) were used as independent variables and the maximum of L-Phe yield was used as criteria.

Statistica program was used for Central Composite Design (CCD). CCD consists of cube points for the estimation of linear and interaction effects, center points to check for curvature, and axial points to estimate quadratic terms. Alpha (α) for axial points is the distance of each axial point from the center. A central composite design with five center points (α=1.732) was used to conduct the experiments (Table 2.4). The zero level of independent variable: glycerol, ammonium sulfate and inducer were set at (w/v) of 3%, 7% and 0.15%, respectively. Three factors had 5 levels (+α, +1, 0, -1, -α) in CCD are shown in Table 2.4. The conditions for the 3 independent variables on the production of L-Phe yield were formed within the quadratic model. Levels of different process variables for percentage are shown in Table 2.5. The obtained L-Phe concentrations were used for analysis by MINITAB 17 statistical software.

Table 2.6 Level of different process variables in coded form for L-Phe production

Variables	Coded levels				
	-1.732	-1	0	+1	+1.732
Arabinose (% w/v)	0.024	0.050	0.150	0.200	0.276
Glycerol (% w/v)	1.318	2	3	4	4.682
Ammonium sulfate (% w/v)	3.636	5	7	9	10.363

Table 2.7 Experimental design obtained by CCD matrix

Run	Variables coded			Arabinose (%w/v)	Glycerol (%w/v)	Ammonium sulfate (%w/v)
	X_1	X_2	X_3			
1	-1	-1	-1	0.05	2.00	5.00
2	-1	-1	1	0.05	2.00	9.00
3	-1	1	-1	0.05	4.00	5.00
4	-1	1	1	0.05	4.00	9.00
5	1	-1	-1	0.20	2.00	5.00
6	1	-1	1	0.20	2.00	9.00
7	1	1	-1	0.20	4.00	5.00
8	1	1	1	0.20	4.00	9.00
9	-1.732	0	0	0.02	3.00	7.00
10	1.732	0	0	0.27	3.00	7.00
11	0	-1.732	0	0.15	1.31	7.00
12	0	1.732	0	0.15	4.68	7.00
13	0	0	-1.732	0.15	3.00	3.60
14	0	0	1.732	0.15	3.00	10.36
15	0	0	0	0.15	3.00	7.00
16	0	0	0	0.15	3.00	7.00

CHAPTER III

RESULTS AND DISCUSSIONS

3.1 Subcloning of *aroL, phedh* and *tktA* into pAroB

To express the genes involving in L-Phe production in *E. coli* by dual plasmid system, *aroB* (encoding 3-dehydroquinate synthase), *aroL* (encoding shikimate kinase II), *phedh* (encoding phenylalanine dehydrogenase), *tktA* (encoding transketolase) preceded by their own T7*lac* promoter were cloned into pRSFDuet-1 and co-expressed with *glpF* (encoding glycerol facilitator) and *yddG* (encoding aromatic amino acid exporter) ara promoter of pBAD33 in *E.coli* BL21 (DE3) as shown by the following results. pAroB (4,883 bp) and pPTFBL (9,579 bp) were extracted from *E. coli* BL21 (DE3) host cell as described in section 2.17.1. The plasmid pattern of pAroB and pPTFBL were examined on agarose gel electrophoresis. Three forms (relax, linear and supercoiled) were obtained as shown in Figure 3.1, lane 1 and 4, respectively. Both plasmids were cut by *Bam*HI and *Xho*I. Digestion of pAroB gave two DNA fragments of 4,635 and 248 bp (Figure 3.1, lane 2) while DNA fragments of 5,543 and 4,036 bp were obtained from pPTFBL (Figure 3.1, lane 5). Then DNA fragments of 4,635 and 4,036 bp were eluted from agarose gel, checked for their purity by agarose gel electrophoresis (Figure 3.1, lane 3 and 6, respectively), ligated together to form pBLPT and finally transformed into *E. coli* BL21 (DE3) by electroporation. The recombinant pBLPT was extracted (Figure 3.1, lane 7) and checked by double digestion with *Bam*HI and *Xho*I. Two DNA fragments of 4,635 and 4,036 bp were found in lane 8 of Figure 3.1. That means pBLPT was successfully constructed. This plasmid has *aroB, aroL*, *phedh* and *tktA* under T7*lac* promoter and ribosome binding site. The expression of gene in plasmid depends on the distance between the gene and its promoter. A gene located close to the promoter is expressed with a much higher rate compared to a gene that is located far from the promoter (Weckbecker and Hummel, 2005). Therefore, to control the expression of each gene at similar level, each gene was required to be preceded by its own T7*lac*

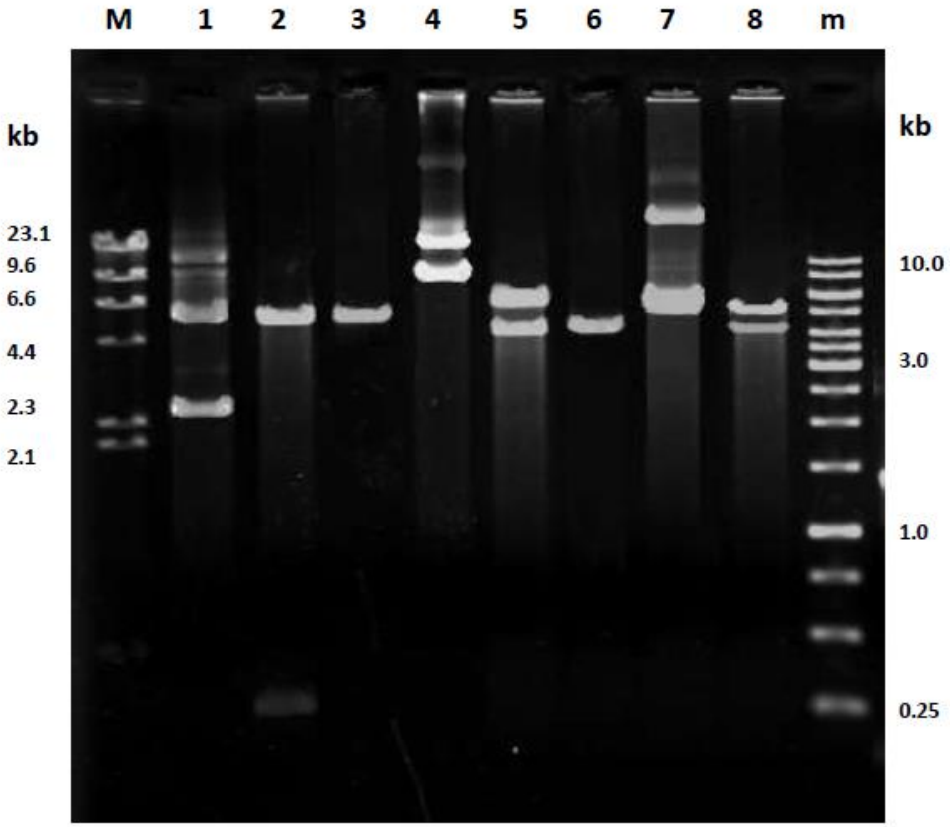

Figure 3.10 Restriction patterns of pAroB, pPTFBL and pBLPT

Lane M= λ/*Hin*dIII DNA marker
Lane 1 = undigested pAroB
Lane 2 = *Bam*HI and *Xho*I digested pAroB
Lane 3 = eluted 4,635 bp fragment
Lane 4 = undigested pPTFBL
Lane 5 = *Bam*HI and *Xho*I digested pPTFBL
Lane 6 = eluted 4,036 bp fragment
Lane 7 = undigested pBLPT
Lane 8 = *Bam*HI and *Xho*I digested pBLPT
Lane m = 100 bp DNA ladder

promoter. Figure 2.1 showed the position of four genes located on the single pRSFduet-1 vector that used in this study.

3.2 Construction of recombinant plasmid pYF

3.2.1 Cloning of *yddG* and *glpF* into pBAD33

yddG and *glpF* were amplified from pPTFBLY and cloned into pBAD33 as described in section 2.17.2. Firstly, *yddG* was amplified using primers: F_yddG_*Xba*I and R_yddG_*Sal*I while amplification of *glpF* was performed using F_glpF_*Xba*I and R_glpF_*Sal*I. Annealing temperatures were varied from 39-51 °C for suitable temperature of *yddG* and *glpF* PCR productions. The results in Figure 3.2 and Figure 3.3 showed that DNA band of *yddG* (846 bp) and *glpF* (882 bp) were thickest at annealing temperature of 42 and 45 °C, respectively. The PCR products were purified using gel/PCR DNA fragment extraction kit. The *Xba*I and *Sal*I sites in PCR product of *yddG* and *glpF* as well as plasmid vector pBAD33 were digested. After that the purified *yddG* and *glpF* ORF were separately ligated with the 5,346 bp fragment of pBAD33 to form pYddg and pGlpF. These recombinant plasmids were transformed into *E. coli* BL21 (DE3). The recombinant plasmids, pYddG and pGlpF, were extracted and digested with *Xba*I and *Sal*I as shown in Figure 3.4 and Figure 3.5, respectively. *Xba*I and *Sal*I digestion analysis showed that *yddG* was correctly inserted into pBAD33 since digested fragment in Figure 3.4, lane 5 had similar size with *Xba*I and *Sal*I digested pBAD33 (Figure 3.4, lane 2) and PCR product of *yddG* (Figure 3.4, lane 3). pGlpF digested with *Xba*I and *Sal*I (Figure 3.5, lane 5) also composed of *Xba*I and *Sal*I digested fragment of pBAD33 (Figure 3.5, lane 2) and *glpF* (Figure 3.5, lane 3).

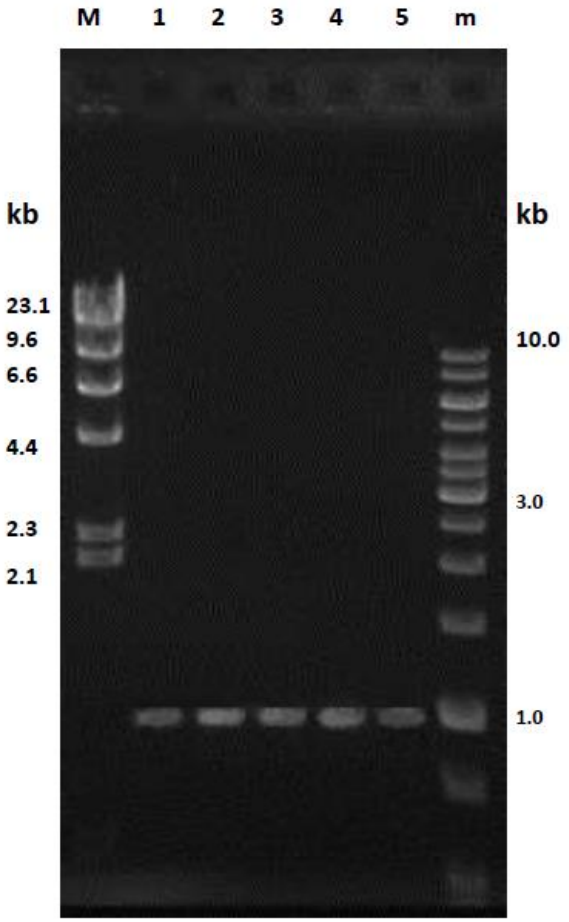

Figure 3.11 Optimization of annealing temperature for amplification of *yddG*

Lane M = λ/*Hin*dIII DNA marker
Lane 1 = annealing temperature of 39 °C
Lane 2 = annealing temperature of 42 °C
Lane 3 = annealing temperature of 45 °C
Lane 4 = annealing temperature of 48 °C
Lane 5 = annealing temperature of 51 °C
Lane m = 100 bp DNA ladder

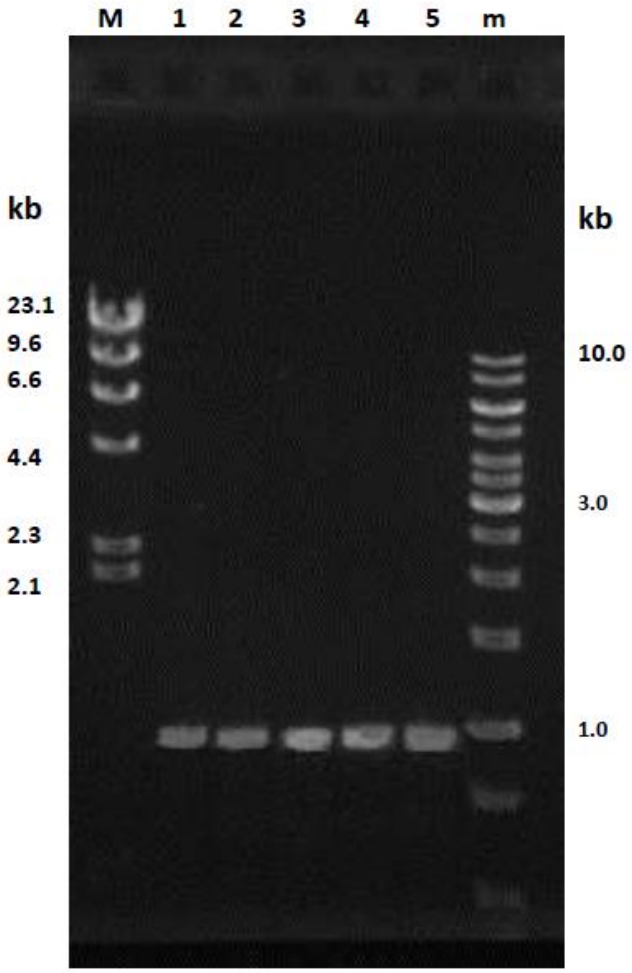

Figure 12.3 Optimization of annealing temperature for amplification of *glpF*

Lane M = λ/*Hin*dIII DNA marker
Lane 1 = annealing temperature of 39 °C
Lane 2 = annealing temperature of 42 °C
Lane 3 = annealing temperature of 45 °C
Lane 4 = annealing temperature of 48 °C
Lane 5 = annealing temperature of 51 °C
Lane m = 100 bp DNA ladder

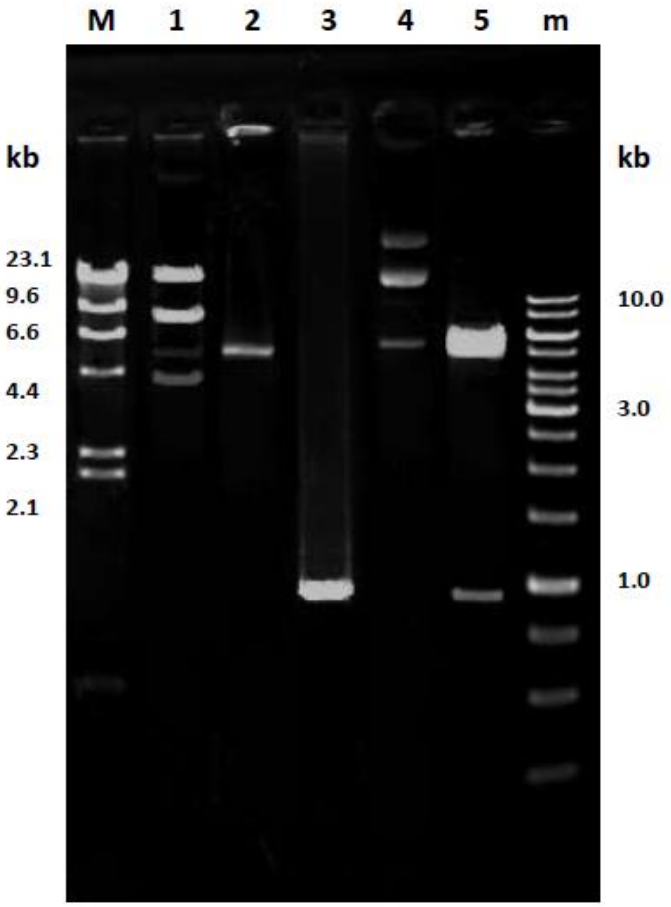

Figure 3.13 Agarose gel electrophoresis of pYddG

Lane M = λ/*Hin*dIII DNA marker
Lane 1 = undigested pBAD33 (5,352 bp)
Lane 2 = pBAD33 digested with *Xba*I and *Sal*I
Lane 3 = PCR product of *yddG*
Lane 4 = undigested pYddG
Lane 5 = pYddG digested with *Xba*I and *Sal*I
Lane m = 100 bp DNA ladder

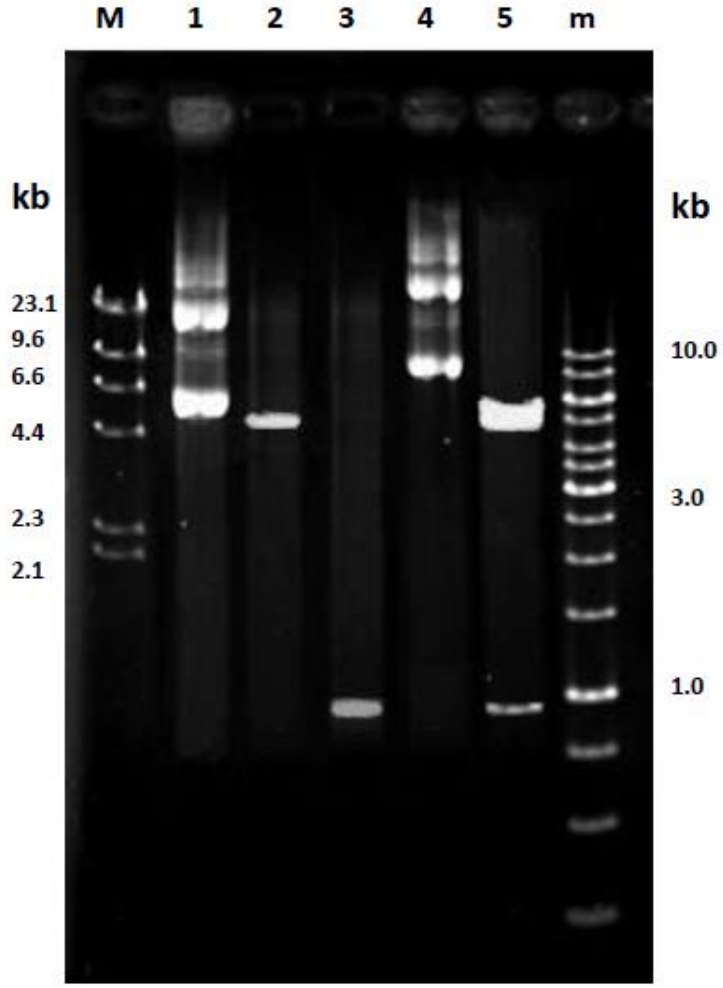

Figure 3.14 Agarose gel electrophoresis of pGlpF

Lane M = λ/*Hin*dIII DNA marker
Lane 1 = undigested pBAD33 (5,352 bp)
Lane 2 = pBAD33 digested with *Xba*I and *Sal*I
Lane 3 = PCR product of *glpF*
Lane 4 = undigested pGlpF
Lane 5 = pGlpF digested with *Xba*I and *Sal*I
Lane m = 100 bp DNA ladder

It is important to verify the sequence of the cloned genes before use in further experiments. Therefore, pYddG and pGlpF were sent to Macrogen, Korean for sequencing of *yddG* and *glpF* ORFs. Using pBAD_fwd_primer and pBAD_rev_primer which complementary to each strand of pBAD33, ORF of inserted *yddg* gene (846 bp) with 104 bp of upstream sequence and 90 bp of downstream sequence were obtained. The inserted *yddG* showed 100% identity with *yddG* from *E. coli* str. K-12 substr. DH10B (Gene ID.6062375) as shown in Figure 3.6. In parallel, the alignment of inserted *glpF* (950 bp) and *glpF* from *E. coli* str. K-12 substr. DH10B (Gene ID.6062231) also showed 100% identity (Figure 3.7). Moreover, alignments also proved that both *yddG* and *glpF* were inserted in frame.

3.2.2 Subcloning of *glpF* into pYddG

To construct recombinant plasmid pYF containing *glpF* and *yddG* under ara promoter as shown in Figure 2.4, ara promoter and *glpF* of pGlpF were amplified using F_Ara_glpF_*Sal*I and R_Ara_glpF_*Pst*I (Table 2.4). As shown in Figure 3.8, the amount of 937 bp PCR product gained from varying annealing temperature ranged from 47 °C to 51 °C were not significantly difference. Therefore, annealing at 49 °C was used. The PCR product and pYddG were cleaved with the same restriction enzymes, *Sal*I and *Pst*I and then ligated to form pYF. pYF was further transformed into *E. coli* BL21 (DE3).

The recombinant plasmid pYF was extracted from *E. coli* host cell and digested with *Sal*I and *Pst*I as shown in Figure 3.9, lane 5. This digestion resulted in fragments of 6,228 bp and 937 bp. *Sal*I and *Pst*I digestion analysis showed that ara promoter and *glpF* were correctly inserted into pYddG since digested fragment had similar size with *Sal*I and *Pst*I digested pYddG (Figure 3.9, lane 2) and PCR product of *glpF* (Figure 3.9, lane 3).

(continued)

Figure 3.15 Nucleotide sequence alignment of *yddG* gene from pYddG

The sequence of *yddG* (846 bp) from pYddG was aligned with *glpF* from *E. coli* str. K-12 substr. DH10B (GeneID: 6062375) and the sequences at upstream and downstream of *yddG* were aligned with the sequences of pBAD33 obtained from Addgene Vector Database. The start codon of *yddG* is shown in green. *Xba*I site is shown in yellow. *Sal*I site is shown in red. ⋆ shows nucleotide identity between pYddG and GI.6062375. ◦ shows nucleotide identity between pBAD33 and pYddG.

(continued)

```
pBAD33          ------------------------------------------------------------
pYddG           CTGACAATTCTCTTTGCCATTCTGTTTAATGGTCAGAAAACCAACTGGTTGATTGTACCT 480
GI.6062375      CTGACAATTCTCTTTGCCATTCTGTTTAATGGTCAGAAAACCAACTGGTTGATTGTACCT 372
                ************************************************************

pBAD33          ------------------------------------------------------------
pYddG           GGATTATTATTAGCCCTCGTCGGCGTCTGTTGGGTGTTAGGCGGTGACAATGGGTTACAT 540
GI.6062375      GGATTATTATTAGCCCTCGTCGGCGTCTGTTGGGTGTTAGGCGGTGACAATGGGTTACAT 432
                ************************************************************

pBAD33          ------------------------------------------------------------
pYddG           TATGATGAAATCATCAATAATATCACCACCAGCCCATTGAGTTATTTCCTGGCGTTCATT 600
GI.6062375      TATGATGAAATCATCAATAATATCACCACCAGCCCATTGAGTTATTTCCTGGCGTTCATT 492
                ************************************************************

pBAD33          ------------------------------------------------------------
pYddG           GGTGCGTTTATCTGGGCAGCCTATTGCACAGTAACGAATAAATACGCACGCGGATTTAAT 660
GI.6062375      GGTGCGTTTATCTGGGCAGCCTATTGCACAGTAACGAATAAATACGCACGCGGATTTAAT 552
                ************************************************************

pBAD33          ------------------------------------------------------------
pYddG           GGAATTACCGTTTTTGTCCTGCTAACGGGAGCAAGTCTGTGGGTTTACTATTTTCTTACG 720
GI.6062375      GGAATTACCGTTTTTGTCCTGCTAACGGGAGCAAGTCTGTGGGTTTACTATTTTCTTACG 612
                ************************************************************

pBAD33          ------------------------------------------------------------
pYddG           CCACAACCAGAAATGATATTTAGCACGCCCGTCATGATTAAACTCATCTCTGCGGCATTT 780
GI.6062375      CCACAACCAGAAATGATATTTAGCACGCCCGTCATGATTAAACTCATCTCTGCGGCATTT 672
                ************************************************************
```

(continued)

Figure 3.6 Nucleotide sequence alignment of *yddG* gene from pYddG

The sequence of *yddG* (846 bp) from pYddG was aligned with *glpF* from *E. coli* str. K-12 substr. DH10B (GeneID: 6062375) and the sequences at upstream and downstream of *yddG* were aligned with the sequences of pBAD33 obtained from Addgene Vector Database. The start codon of *yddG* is shown in green. *Xba*I site is shown in yellow. *Sal*I site is shown in red. ⋆ shows nucleotide identity between pYddG and GI.6062375. ◦ shows nucleotide identity between pBAD33 and pYddG.

(continued)

```
pBAD33          ------------------------------------------------------------
pYddG           ACCTTAGGATTTGCTTATGCTGCATGGAATGTCGGTATATTGCATGGCAATGTCACCATT 840
GI.6062375      ACCTTAGGATTTGCTTATGCTGCATGGAATGTCGGTATATTGCATGGCAATGTCACCATT 732
                ************************************************************

pBAD33          ------------------------------------------------------------
pYddG           ATGGCGGTAGGTTCGTATTTTACGCCTGTACTTTCCTCAGCGCTTGCAGCCGTGCTGCTC 900
GI.6062375      ATGGCGGTAGGTTCGTATTTTACGCCTGTACTTTCCTCAGCGCTTGCAGCCGTGCTGCTC 792
                ************************************************************

pBAD33          ------------------------------------------------------------
pYddG           AGCGCCCCGCTGTCGTTCTCGTTCTGGCAAGGCGCGCTGATGGTCTGCGGCGGTTCCCTG 960
GI.6062375      AGCGCCCCGCTGTCGTTCTCGTTCTGGCAAGGCGCGCTGATGGTCTGCGGCGGTTCCCTG 852
                ************************************************************

                                                °°°°°°°°°°°°°°°°°°°°°°°°°°°°°°°°
pBAD33          -------------------------------GTCGACCTGCAGGCATGCAAGCTTGGCTGT 119
pYddG           CTCTGCTGGCTGGCGACACGTCGTGGTTAAGTCGACCTGCAGGCATGCAAGCTTGGCTGT 1020
GI.6062375      CTCTGCTGGCTGGCGACACGTCGTGGTTAA------------------------------ 882
                ******************************

                °°°°°°°°°°°°°°°°°°°°°°°°°°°°°°°°°°°°°°°°°°°°°°°°°°°°°°°°°°°°
pBAD33          TTTGGCGGATGAGAGAAGATTTTCAGCCTGATACAGATTAAATCAGAACGCAGAAGCGGT 179
pYddG           TTTGGCGGATGAGAGAAGATTTTCAGCCTGATACAGATTAAATCAGAACGCAGAAGCGGT 1080
GI.6062375      ------------------------------------------------------------
```

Figure 3.6 Nucleotide sequence alignment of *yddG* gene from pYddG

The sequence of *yddG* (846 bp) from pYddG was aligned with *glpF* from *E. coli* str. K-12 substr. DH10B (GeneID: 6062375) and the sequences at upstream and downstream of *yddG* were aligned with the sequences of pBAD33 obtained from Addgene Vector Database. The start codon of *yddG* is shown in green. *Xba*I site is shown in yellow. *Sal*I site is shown in red. ⋆ shows nucleotide identity between pYddG and GI.6062375. ◦ shows nucleotide identity between pBAD33 and pYddG.

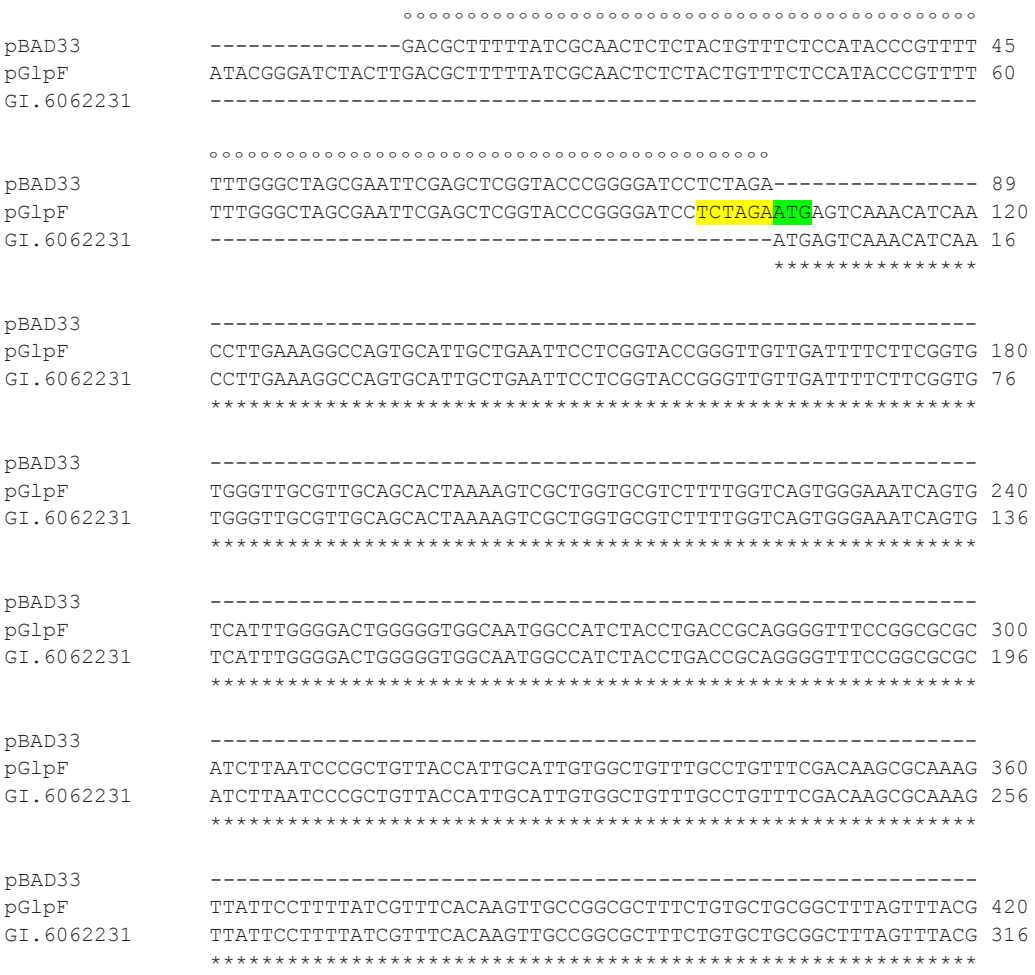

(continued)

Figure 3.16 Nucleotide sequence alignment of *glpF* from pGlpF.

The sequence of *glpF* (882 bp) from pGlpF was aligned with *glpF* from *E. coli* str. K-12 substr. DH10B (GeneID: 6062231) and the sequences at upstream and downstream of *glpF* were aligned with the sequences of pBAD33 obtained from Addgene Vector Database. The start codon of *glpF* is shown in green. *Xba*I site is shown in yellow. *Sal*I site is shown in red. ⋆ shows nucleotide identity between pGlpF and GI.6062231. ◦ shows nucleotide identity between pBAD33 and pGlpF.

(continued)

```
pBAD33          ------------------------------------------------------------
pGlpF           GGCTTTACTACAATTTATTTTTCGACTTCGAGCAGACTCATCACATTGTTCGCGGCAGCG 480
GI.6062231      GGCTTTACTACAATTTATTTTTCGACTTCGAGCAGACTCATCACATTGTTCGCGGCAGCG 376
                ************************************************************

pBAD33          ------------------------------------------------------------
pGlpF           TTGAAAGTGTTGATCTGGCTGGCACTTTCTCTACTTACCCTAATCCTCATATCAATTTTG 540
GI.6062231      TTGAAAGTGTTGATCTGGCTGGCACTTTCTCTACTTACCCTAATCCTCATATCAATTTTG 436
                ************************************************************

pBAD33          ------------------------------------------------------------
pGlpF           TGCAGGCTTTCGCAGTTGAGATGGTGATTACCGCTATTCTGATGGGGCTGATCCTGGCGT 600
GI.6062231      TGCAGGCTTTCGCAGTTGAGATGGTGATTACCGCTATTCTGATGGGGCTGATCCTGGCGT 496
                ************************************************************

pBAD33          ------------------------------------------------------------
pGlpF           TAACGGACGATGGCAACGGTGTACCACGCGGCCCTTTGGCTCCCTTGCTGATTGGTCTAC 660
GI.6062231      TAACGGACGATGGCAACGGTGTACCACGCGGCCCTTTGGCTCCCTTGCTGATTGGTCTAC 556
                ************************************************************

pBAD33          ------------------------------------------------------------
pGlpF           TGATTGCGGTCATTGGCGCATCTATGGGCCCATTGACAGGTTTTGCCATGAACCCAGCGC 720
GI.6062231      TGATTGCGGTCATTGGCGCATCTATGGGCCCATTGACAGGTTTTGCCATGAACCCAGCGC 616
                ************************************************************

pBAD33          ------------------------------------------------------------
pGlpF           GTGACTTCGGTCCGAAAGTCTTTGCCTGGCTGGCGGGCTGGGGCAATGTCGCCTTTACCG 780
GI.6062231      GTGACTTCGGTCCGAAAGTCTTTGCCTGGCTGGCGGGCTGGGGCAATGTCGCCTTTACCG 676
                ************************************************************

pBAD33          ------------------------------------------------------------
pGlpF           GCGGCAGAGACATTCCTTACTTCCTGGTGCCGCTTTTCGGCCCTATCGTTGGCGCGATTG 840
GI.6062231      GCGGCAGAGACATTCCTTACTTCCTGGTGCCGCTTTTCGGCCCTATCGTTGGCGCGATTG 736
                ************************************************************
```

(continued)

Figure 3.7 Nucleotide sequence alignment of *glpF* from pGlpF

The sequence of *glpF* (882 bp) from pGlpF was aligned with *glpF* from *E. coli* str. K-12 substr. DH10B (GeneID: 6062231) and the sequences at upstream and downstream of *glpF* were aligned with the sequences of pBAD33 obtained from Addgene Vector Database. The start codon of *glpF* is shown in green. *Xba*I site is shown in yellow. *Sal*I site is shown in red. ⋆ shows nucleotide identity between pGlpF and GI.6062231. ◦ shows nucleotide identity between pBAD33 and pGlpF.

(continued)

```
pBAD33          ------------------------------------------------------------
pGlpF           TAGGTGCATTTGCCTACCGCAAACTGATTGGTCGCCATTTGCCTTGCGATATCTGTGTTG 900
GI.6062231      TAGGTGCATTTGCCTACCGCAAACTGATTGGTCGCCATTTGCCTTGCGATATCTGTGTTG 796
                ************************************************************

                                                           °°°°°°°°°°
pBAD33          ----------------------------------------------------GTCGACCTGC 99
pGlpF           TGGAAGAAAAGGAAACCACAACTCCTTCAGAACAAAAAGCTTCGCTGTAAGTCGACCTGC 960
GI.6062231      TGGAAGAAAAGGAAACCACAACTCCTTCAGAACAAAAAGCTTCGCTGTAA---------- 846
                ********************************************

                °°°°°°°°°°°°°°°°°°°°°°°°°°°°°°°°°°°°°°°°°°°°°°°°°°°°°°°°°°°
pBAD33          AGGCATGCAAGCTTGGCTGTTTTGGCGGATGAGAGAAGATTTTCAGCCTGATACAGATTA 159
pGlpF           AGGCATGCAAGCTTGGCTGTTTTGGCGGATGAGAGAAGATTTTCAGCCTGATACAGATTA 1020
GI.6062231      ------------------------------------------------------------

                °°°°°°°°°°°°°°°°°°°°°°°°°°°°°°°°°°°°°°°°°°°°°°°°°°°°°°°°°°°
pBAD33          AATCAGAACGCAGAAGCGGTCTGATAAAACAGAATTTGCCTGGCGGCAGTAGCGCGGTGG 219
pGlpF           AATCAGAACGCAGAAGCGGTCTGATAAAACAGAATTTGCCTGGCGGCAGTAGCGCGGTGG 1080
GI.6062231      ------------------------------------------------------------

                °°°°°°°°°°°°°°°°°°°°°°°°°°°°°°°°°°°°
pBAD33          TCCCACCTGACCCCATGCCGAACTCAGAAGTGAAACGCC---------------------- 258
pGlpF           TCCCACCTGACCCCATGCCGAACTCAGAAGTGAAACGCCTACCCCCAAAGGTAATTTGGG 1140
GI.6062231      ------------------------------------------------------------
```

Figure 3.7 Nucleotide sequence alignment of *glpF* from pGlpF

The sequence of *glpF* (882 bp) from pGlpF was aligned with *glpF* from *E. coli* str. K-12 substr. DH10B (GeneID: 6062231) and the sequences at upstream and downstream of *glpF* were aligned with the sequences of pBAD33 obtained from Addgene Vector Database. The start codon of *glpF* is shown in green. *Xba*I site is shown in yellow. *Sal*I site is shown in red. ⋆ shows nucleotide identity between pGlpF and GI.6062231. ◦ shows nucleotide identity between pBAD33 and pGlpF.

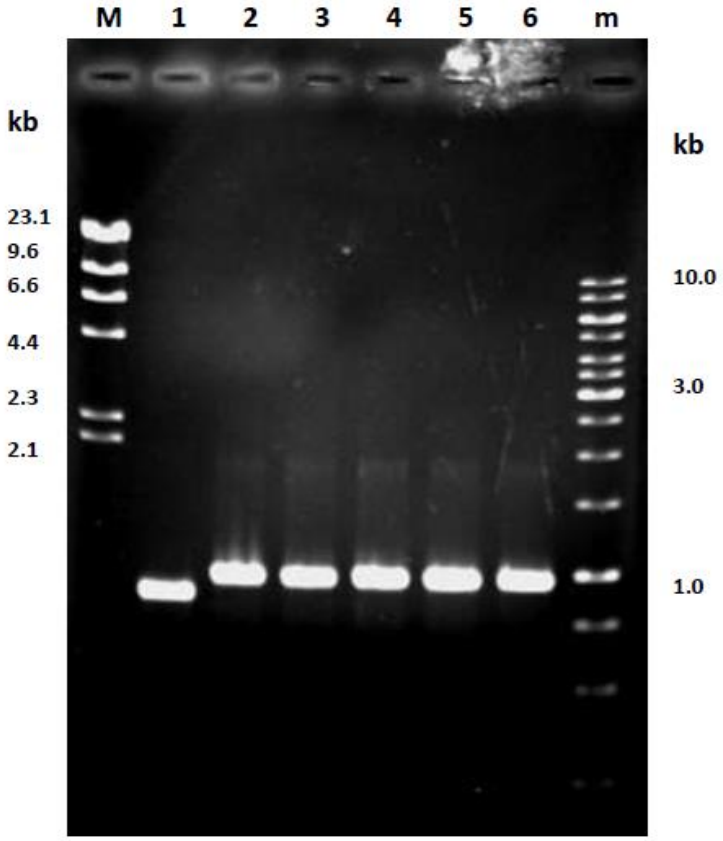

Figure 3.8 Optimization of annealing temperature for amplification of *glpF* and its ara promoter

Lane M= λ/*Hin*dIII DNA marker

Lane 1 = PCR product of *glpF* (846 bp)

Lane 2 = PCR product of *glpF* and ara promoter at annealing temperature of 47 °C (937 bp)

Lane 3 = PCR product of *glpF* and ara promoter at annealing temperature of 48 °C

Lane 4 = PCR product of *glpF* and ara promoter at annealing temperature of 49 °C

Lane 5 = PCR product of *glpF* and ara promoter at annealing temperature of 50 °C

Lane 6 = PCR product of *glpF* and ara promoter at annealing temperature of 51 °C

Lane m= 100 bp DNA ladder

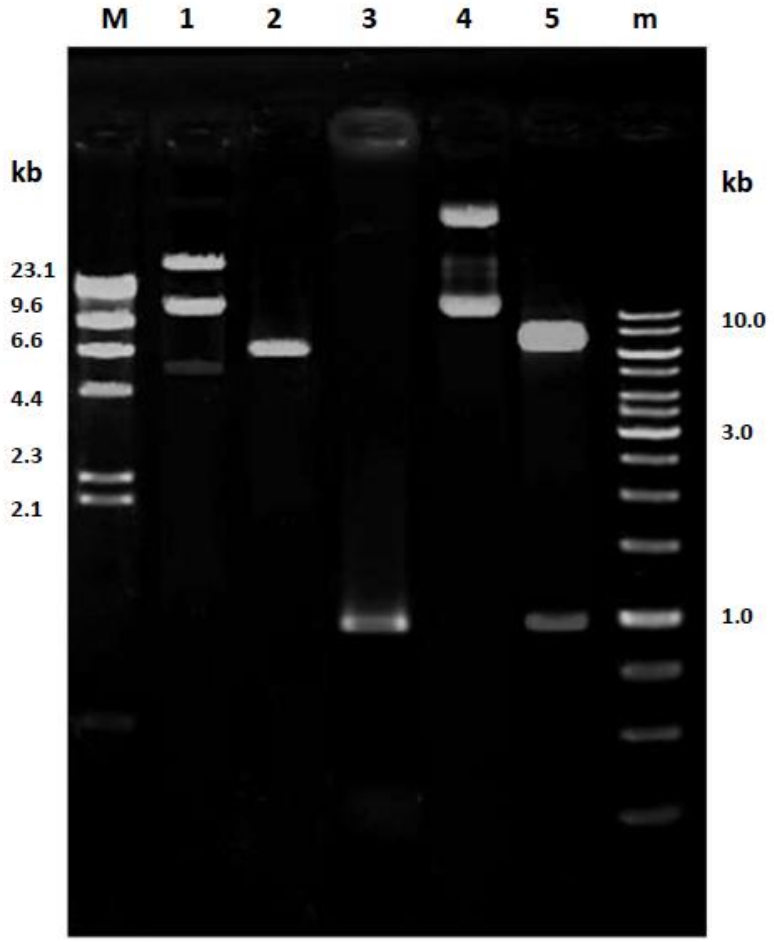

Figure 3.9 Agarose gel electrophoresis of recombinant plasmid pYF

Lane M = λ/*Hin*dIII DNA marker
Lane 1 = undigested pYddG (6,228 bp)
Lane 2 = pYddG digested with *Sal*I and *Pst*I
Lane 3 = PCR product of *ara* promoter and *glpF*
Lane 4 = undigested pYF
Lane 5 = pYF digested with *Sal*I and *Pst*I
Lane m = 100 bp DNA ladder

pYF was sent to Macrogen, Korean for sequencing of ara promoter and *glpF* ORFs (Figure 3.10). Using F_pro_glpF and pBAD_REV_primer, ORF of *glpF* and its ara promoter (937 bp) and 91 bp of its upstream as well as 18 bp of its downstream were obtained. The in frame inserted ara promoter and *glpF* showed 100% identity with pBAD33 from Addgene Vector Database and *glpF* of *E. coli* str. K-12 substr. DH10B (Gene ID. 6062231), respectively.

3.2.3 Restriction patterns of recombinant plasmids pBLPT & pYF

The pYF containing *glpF* and *yddG* under ara promoter (Figure 3.11, lane 3) was co-transformed into competent *E. coli* BL21(DE3) containing *aroB, aroL, phedh* and *tktA* under T7*lac* promoter (Figure 3.11, lane 1) then plated onto agar plates supplemented with 30 μg/mL of kanamycin and 10 μg/mL chloramphenicol. Morphology of colonies were normal. Transformants containing both plasmids were grown in LB broth in the presence of kanamycin and chloramphenicol. The plasmid were extracted from pBLPT and pYF clone (Figure 3.11, lane 5) and cut with *Bam*HI (Figure 3.11, lane 6). The digestion resulted in three DNA fragments with 8,671 bp (same size with pBLPT digested by *Bam*HI in Figure 3.11, lane 2) 6,195 and 970 bp (same sizes with pYF digested by *Bam*HI in Figure 3.11, lane 4). The results indicated that *E. coli* BL21(DE3) harboring *aroB, aroL, phedh* and *tktA* genes with their T7*lac* promoter in pRSFDuet-1 as well as *yddG* and *glpF* gene under ara promoter in pBAD33 was successfully constructed. The main reason of this success is plasmid compatibility. pRSFDuet-1 contains RSF 1030 replicon (Novagen uses Protocol no 340, 2011; (Appendix I) which is compatible with p15A replicon of pBAD33. Therefore, they do not compete for replication factors. However, plasmid stability of pBLPT and pYF in the recombinant bacteria should be concerned.

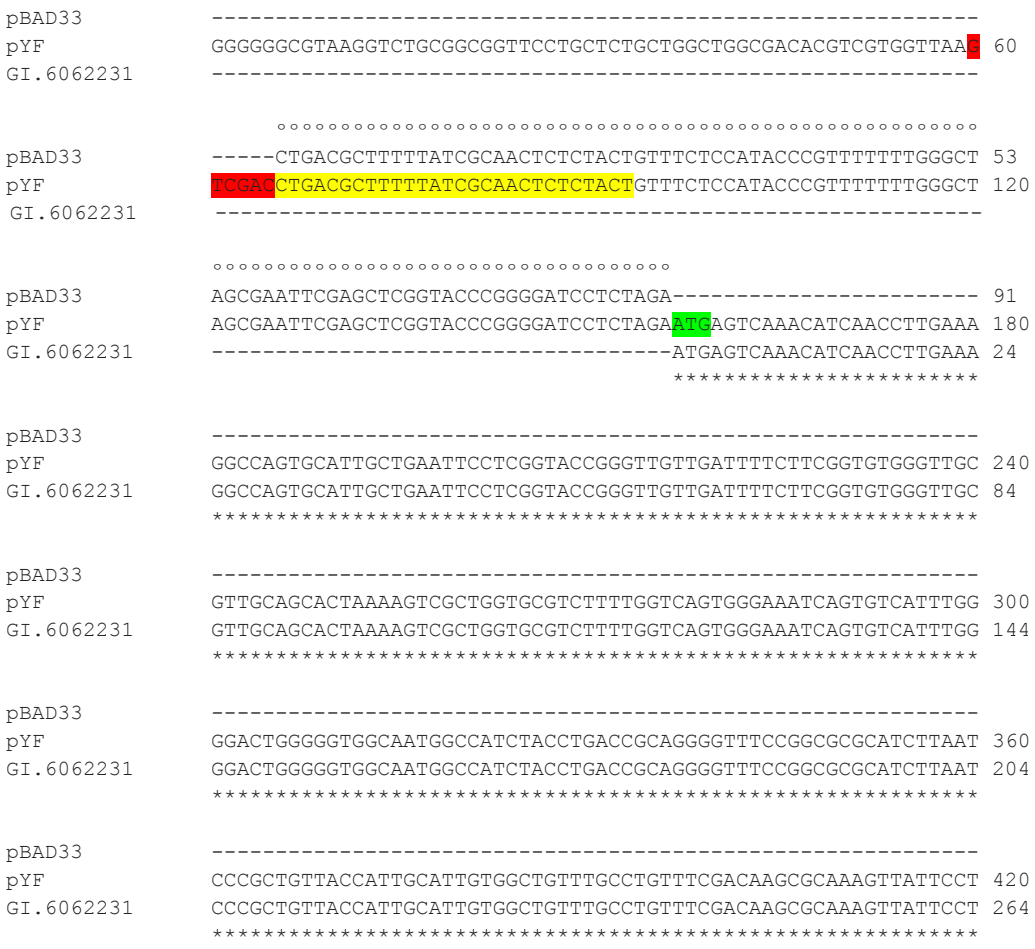

(continued)

Figure 3.10 Nucleotide sequence alignment of *glpF* and its ara promoter from pYF

The sequence of *glpF* (882 bp) from pYF was aligned with *glpF* from *E. coli* str. K-12 substr. DH10B **(**GeneID: 6062231) and the sequences at upstream and downstream of pYF were aligned with the sequences of pBAD33 obtained from Addgene Vector Database. The start codon of *glpF* is shown in green. The ara promoter is shown by yellow. The restriction of *Sal*I enzyme is shown in red. *Pst*I site is shown in blue. ⋆ shows nucleotide identity between pYF and GI.6062231. ◦ shows nucleotide identity between pBAD33 and pYF.

(continued)

```
pBAD33          ------------------------------------------------------------
pYF             TTTATCGTTTCACAAGTTGCCGGCGCTTTCTGTGCTGCGGCTTTAGTTTACGGGCTTTAC 480
GI.6062231      TTTATCGTTTCACAAGTTGCCGGCGCTTTCTGTGCTGCGGCTTTAGTTTACGGGCTTTAC 324
                ************************************************************

pBAD33          ------------------------------------------------------------
pYF             TACAATTTATTTTTCGACTTCGAGCAGACTCATCACATTGTTCGCGGCAGCGTTGAAAGT 540
GI.6062231      TACAATTTATTTTTCGACTTCGAGCAGACTCATCACATTGTTCGCGGCAGCGTTGAAAGT 384
                ************************************************************

pBAD33          ------------------------------------------------------------
pYF             GTTGATCTGGCTGGCACTTTCTCTACTTACCCTAATCCTCATATCAATTTTGTGCAGGCT 600
GI.6062231      GTTGATCTGGCTGGCACTTTCTCTACTTACCCTAATCCTCATATCAATTTTGTGCAGGCT 444
                ************************************************************

pBAD33          ------------------------------------------------------------
pYF             TTCGCAGTTGAGATGGTGATTACCGCTATTCTGATGGGGCTGATCCTGGCGTTAACGGAC 660
GI.6062231      TTCGCAGTTGAGATGGTGATTACCGCTATTCTGATGGGGCTGATCCTGGCGTTAACGGAC 504
                ************************************************************

pBAD33          ------------------------------------------------------------
pYF             GATGGCAACGGTGTACCACGCGGCCCTTTGGCTCCCTTGCTGATTGGTCTACTGATTGCG 720
GI.6062231      GATGGCAACGGTGTACCACGCGGCCCTTTGGCTCCCTTGCTGATTGGTCTACTGATTGCG 564
                ************************************************************

pBAD33          ------------------------------------------------------------
pYF             GTCATTGGCGCATCTATGGGCCCATTGACAGGTTTTGCCATGAACCCAGCGCGTGACTTC 780
GI.6062231      GTCATTGGCGCATCTATGGGCCCATTGACAGGTTTTGCCATGAACCCAGCGCGTGACTTC 624
                ************************************************************
```

(continued)

Figure 3.10 Nucleotide sequence alignment of *glpF* and its ara promoter from pYF

The sequence of *glpF* (882 bp) from pYF was aligned with *glpF* from *E. coli* str. K-12 substr. DH10B **(**GeneID: 6062231) and the sequences at upstream and downstream of pYF were aligned with the sequences of pBAD33 obtained from Addgene Vector Database. The start codon of *glpF* is shown in green. The ara promoter is shown by yellow. The restriction of *Sal*I enzyme is shown in red. *Pst*I site is shown in blue. ⋆ shows nucleotide identity between pYF and GI.6062231. ◦ shows nucleotide identity between pBAD33 and pYF.

(continued)

```
pBAD33          ------------------------------------------------------------
pYF             GGTCCGAAAGTCTTTGCCTGGCTGGCGGGCTGGGGCAATGTCGCCTTTACCGGCGGCAGA 840
GI.6062231      GGTCCGAAAGTCTTTGCCTGGCTGGCGGGCTGGGGCAATGTCGCCTTTACCGGCGGCAGA 684
                ************************************************************

pBAD33          ------------------------------------------------------------
pYF             GACATTCCTTACTTCCTGGTGCCGCTTTTCGGCCCTATCGTTGGCGCGATTGTAGGTGCA 900
GI.6062231      GACATTCCTTACTTCCTGGTGCCGCTTTTCGGCCCTATCGTTGGCGCGATTGTAGGTGCA 744
                ************************************************************

pBAD33          ------------------------------------------------------------
pYF             TTTGCCTACCGCAAACTGATTGGTCGCCATTTGCCTTGCGATATCTGTGTTGTGGAAGAA 960
GI.6062231      TTTGCCTACCGCAAACTGATTGGTCGCCATTTGCCTTGCGATATCTGTGTTGTGGAAGAA 804
                ************************************************************

                                                    °°°°°°°°°°°°°°°°°°
pBAD33          -------------------------------------------CTGCAGGCATGCAAGCTT 113
pYF             AAGGAAACCACAACTCCTTCAGAACAAAAAGCTTCGCTGTAACTGCAGGCATGCAAGCTT 1020
GI.6062231      AAGGAAACCACAACTCCTTCAGAACAAAAAGCTTCGCTGTAA------------------- 846
                ******************************************
```

Figure 3.10 Nucleotide sequence alignment of *glpF* and its ara promoter from pYF

The sequence of *glpF* (882 bp) from pYF was aligned with *glpF* from *E. coli* str. K-12 substr. DH10B **(**GeneID: 6062231) and the sequences at upstream and downstream of pYF were aligned with the sequences of pBAD33 obtained from Addgene Vector Database. The start codon of *glpF* is shown in green. The ara promoter is shown by yellow. The restriction of *Sal*I enzyme is shown in red. *Pst*I site is shown in blue. ⋆ shows nucleotide identity between pYF and GI.6062231. ◦ shows nucleotide identity between pBAD33 and pYF.

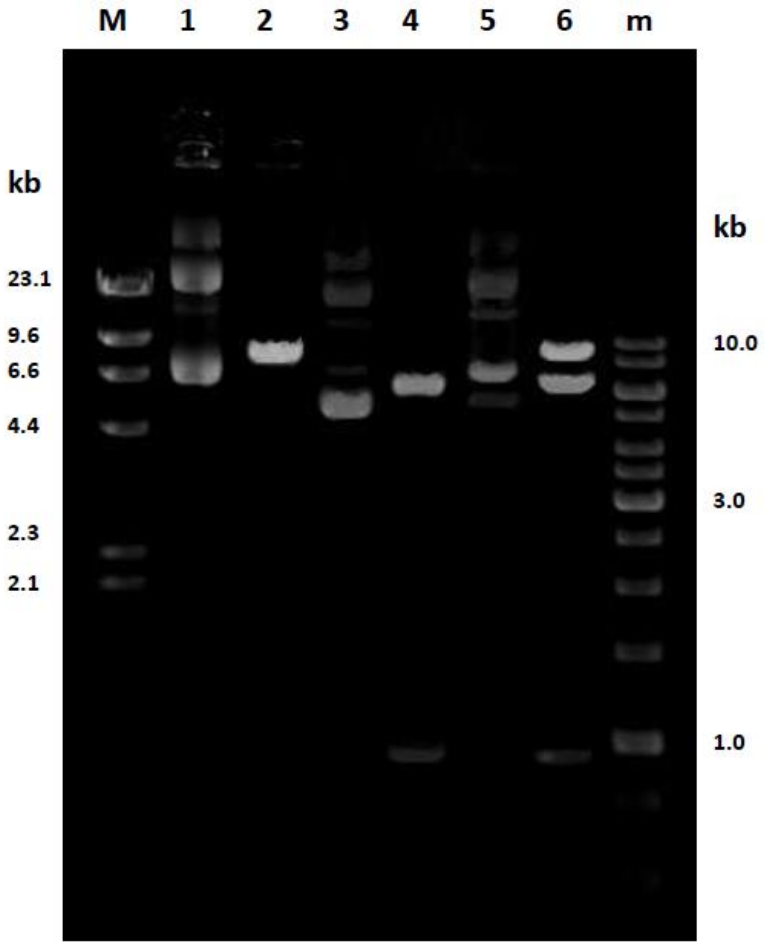

Figure 3.17 Analysis of pBLPT & pYF from recombinant clone

Lane M = λ/*Hin*dIII DNA marker
Lane 1 = undigested pBLPT (8,671 bp)
Lane 2 = pBLPT digested with *Bam*HI
Lane 3 = undigested pYF (7,165 bp)
Lane 4 = pYF digested with *Bam*HI
Lane 5 = undigested pBLPT & pYF
Lane 6 = pBLPT & pYF digested with *Bam*HI
Lane m = 100 bp DNA ladder

3.3 Expression of recombinant plasmid pPTFBLY, pBLPT, pYF, and pBLPT & pYF in *E. coli* BL21(DE3)

The expression of *aroB*, *aroL*, *glpF*, *pheDH*, *tktA* and *yddG* in each recombinant *E. coli* clone was determined in protein level by SDS-PAGE. The recombinant clones were grown in LB broth containing selective antibiotic(s) until OD600 reach 0.6, then recombinant protein synthesis was induced by addition of IPTG and/or arabinose for 3 h.

Protein pattern of whole cell and crude extract of each clone were shown in Figure 3.12. *E. coli* BL21(DE3) wild type and *E. coli* BL21(DE3) harboring plasmid vector pRSFDuet-1 and pBAD33 were used as controls (Figure 3.12, lane 1-3). It was disclosed that AroB, AroL, PheDH and TktA were highly produced in *E. coli* clone harboring pBLPT & pYF under the induction condition since the intense protein bands at molecular weight of approximately 39, 19, 42, and 73 kDa, respectively, were detected. All of these four proteins presented mainly in soluble form (Figure 3.12 B, lane 7). Protein bands of GlpF (39 kDa) and YddG (19 kDa) could not be detected in whole cell of *E. coli* harboring pYF or pBLPT & pYF (Figure 3.12 A, lane 6 and 7). The similar results were also found by Thongchuang (2011). That we cannot detect band of membrane protein from whole cell by Coomassie blue staining. When compared with protein patterns of pPTFBLY clone (Figure 3.12 B, lane 4), the expression of *aroB*, *aroL*, *phedh* and *tktA* of pBLPT & pYF clone in crude extract were higher. Therefore, dual plasmid system should be suitable for production of L-Phe.

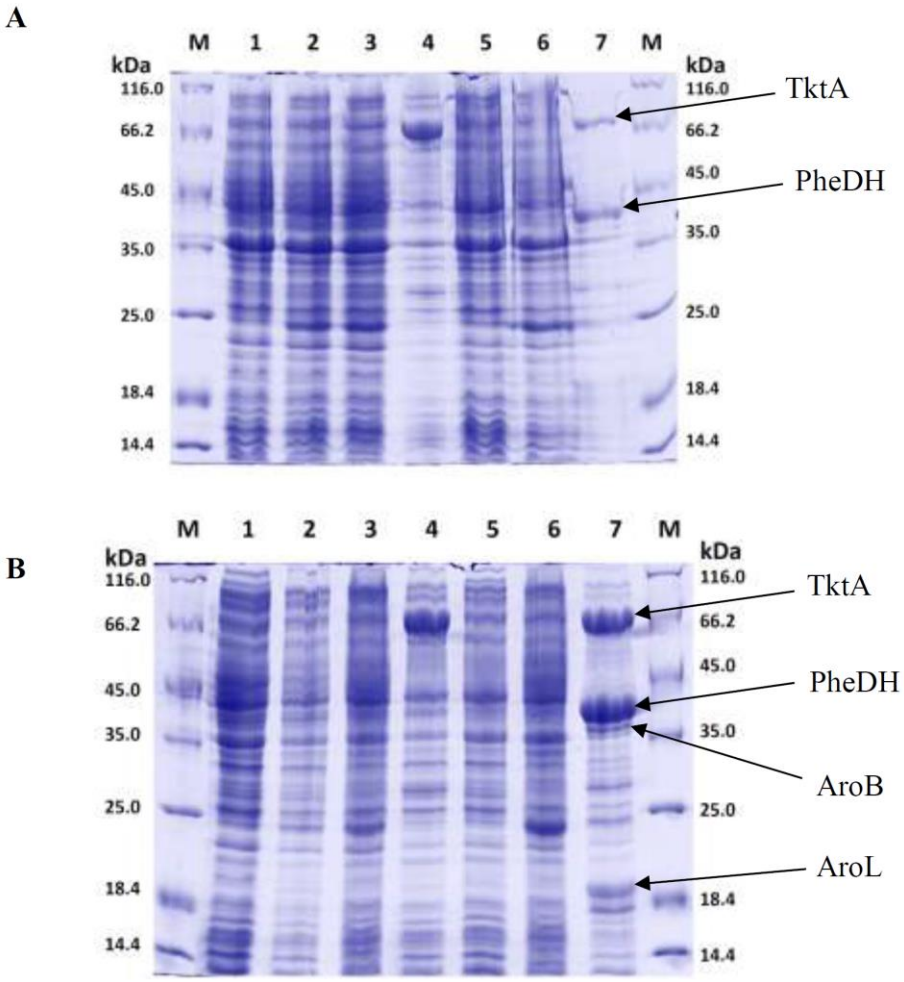

Figure 3.12 SDS-PAGE of recombinant *E.coli* BL21(DE3) harboring different plasmid(s) after induction with 1mM IPTG and/or 0.02% arabinose for 3 h

A: whole cell

B: crude extract

Lane M = protein molecular weight marker

Lane 1 = *E. coli* BL21(DE3) wildtype

Lane 2 = *E. coli* BL21(DE3)/ pRSFDuet-1

Lane 3 = *E. coli* BL21(DE3)/pBAD33

Lane 4 = *E. coli* BL21(DE3)/pPTFBLY

Lane 5 = *E. coli* BL21(DE3)/pBLPT

Lane 6 = *E. coli* BL21(DE3)/pYF

Lane 7 = *E. coli* BL21(DE3)/pBLPT & pYF

3.4 Plasmid stability of pBLPT & pYF clone

To apply pBLPT & pYF clone for production of L-phenylalanine, plasmid stability test was performed as described in section 2.19 and generation time was calculated as shown in Appendix J. pBLPT harboring cell fraction of the recombinant clone was calculated from number of colonies on LB plate containing kanamycin in comparison with number of colonies on LB plate. The resulted showed that when the clone was subcultured in LB broth without a selective antibiotic, numbers of colonies containing pBLPT were continuously decreased. About 50% of pBLPT harboring cell were remained after 45 generations and pBLPT was completely lost at 74 generations. For pYF, the loss of plasmid was more rapaid than pBLPT. About 50% and 100% loss of pYF was found at 30 and 67 generations, repectively (Figure 3.13). Thus plasmid stability of pBLPT & pYF clone was adequate for L-phenylalanine production by fermentation process.

De Gelder and coworkers (2007) was studied stability of pB10 plasmid in different hosts. The goal of this study was to examine whether the stability characteristics of pB10 could be variable within hosts. Their experiment differed from ours that they subcultured in medium containing selective antibiotic. In 10 strains, pB10 was considered stable that were detected during 210 generations of growth. Two strains, *P. putida* S37 and *E. coli* K-12, showed a few segregants, but no clear sweeps within 210 and 330 generations, respectively (call as sporadic loss). Three strains, *Pseudomonas koreensis* R28, *P. putida* H2 and *Stenotrophomonas maltophilia* P21, showed very high plasmid loss as the fraction of plasmid-containing cells dropped below 2 % after about 80 generations (call as high instability).

Summers and Sherratt (1985) demonstrated that low copy plasmid is lost from a growing cell population faster than high copy plasmid. This work supports the result from pBLPT & pYF clone since pBLPT derived from pRSFDuet-1 which is high copy number plasmid (>100) and compatible with P15A, which in pBAD33 was classified as low copy number (10-12) while pYF originated from pBAD33, low copy number (10-12).

Plasmid instability is generally originated from either structural instability caused by changes in the plasmid itself, such as point mutation, deletion, insertion or rearrangement in the plasmid DNA; or segregational instability caused by defective partitioning of plasmids between the daughter cells during cell division (Kumar et al., 1991). Studies have shown that plasmid stability is determined by many factors such as plasmid load, plasmid copy number, replication patterns, substrate type, medium composition, host background (Summers, 1991), culture conditions and culture temperature (Silva et al., 2009).

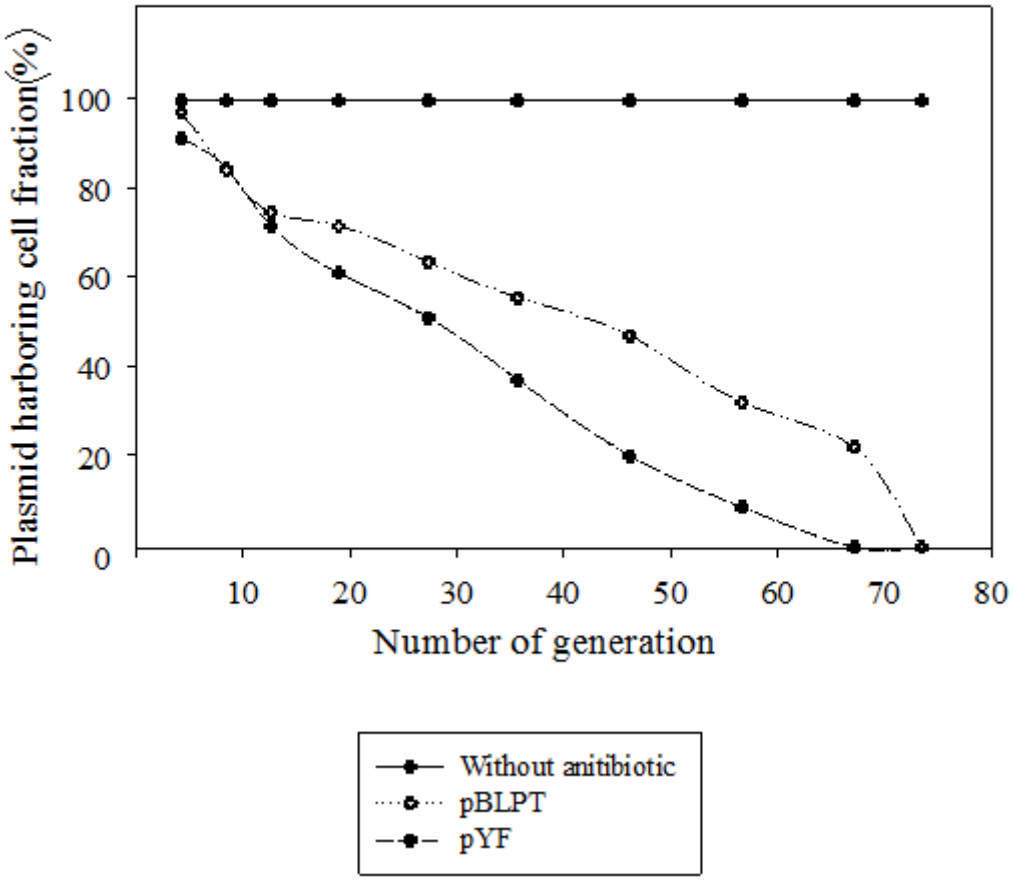

Figure 3.18 Plasmids stability of pBLPT and pYF. Results are average of two independent experiments

3.5 Preliminary experiments for optimization of medium for L-phenylalanine production

To compare L-Phe production of *E.coli* Bl21(DE3) harboring pBLPT & pYF and pPTFBLY in various minimum medium, three different minimum media from published L-Phe production by *E.coli* were used in comparison with the best L-Phe production medium from Thongchuang (2011) as described in section 2.20.

Growths of the recombinant clones were detected by measuring OD at 600 nm. pBLPT & pYF clone grew fastest in medium formula 4 following by 2, 3 and 1, respectively (Figure 3.14). Peak areas were used for calculation of L-phenylalanine concentration as shown in Figure 3.15, L-Phe production at 240 h were 495, 115, 56 and 47 mg/L when the clone was cultured in medium formula 1, 4, 3 and 2, respectively (Figure 3.15).

pPTFBLY clone showed different patterns when compared with pBLPT & pYF clone. It grew well in medium formula 2, 1, 3 and 4, respectively (Figure 3.14) while L-Phe production was highest in medium formula 1 (449 mg/L) following by formula 4 (93 mg/L), formula 3 (78 mg/L), respectively. No L-Phe product was detected in medium formula 2. Growth patterns in 4 different fermentation media for pBLPT & pYF and pPTFBLY clones were similar to growth patterns of pPTFBLY studied by Thongchuang (2011). Log phase of all cultures were formed during 0-100 h and then after 100 h they became stationary phase. L-Phe production could be detected since 50 h and increased rapidly in late log phase to stationary phase. Zhang and colleagues (1998) studied glutamic acid fermentation by time-dependent kinetic model and found that product formation was separated into three stages: the lag stage (in early log phase of cell growth), positive acceleration stage (in late log phase to early stationary of cell growth) and negative acceleration stage (in stationary of cell growth).

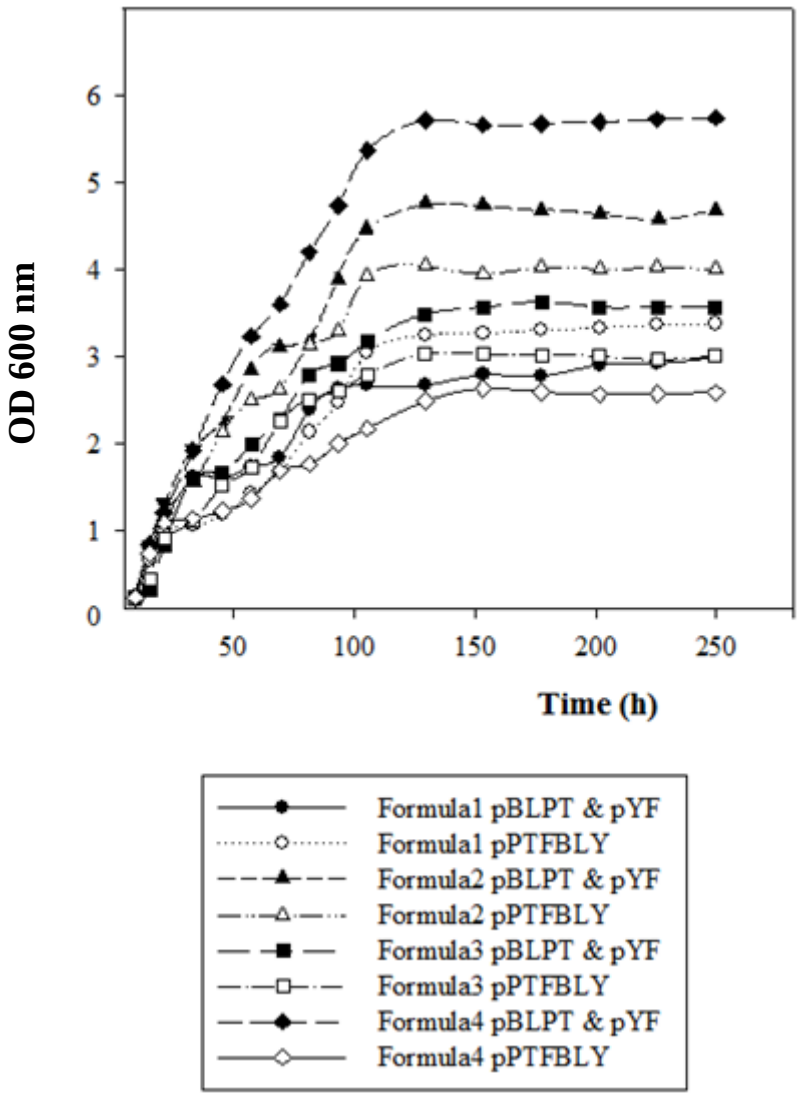

Figure 3.19 Growth curve of recombinant clones in various minimum media Data were representative of three independent experiments

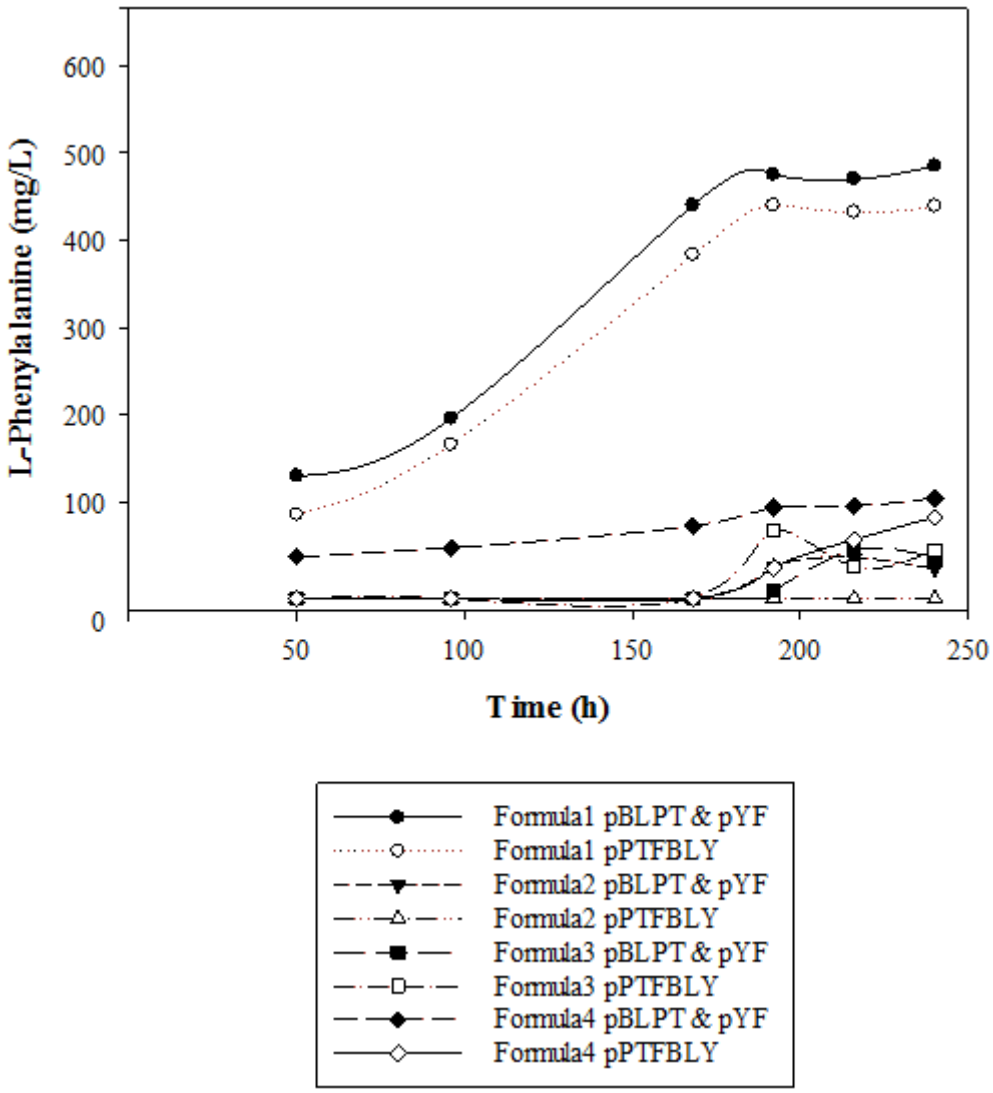

Figure 3.20 L-Phenylalanine production of recombinant clones in various minimum media

Data were representative of three independent experiments.

A) Standard L-phenylalanine

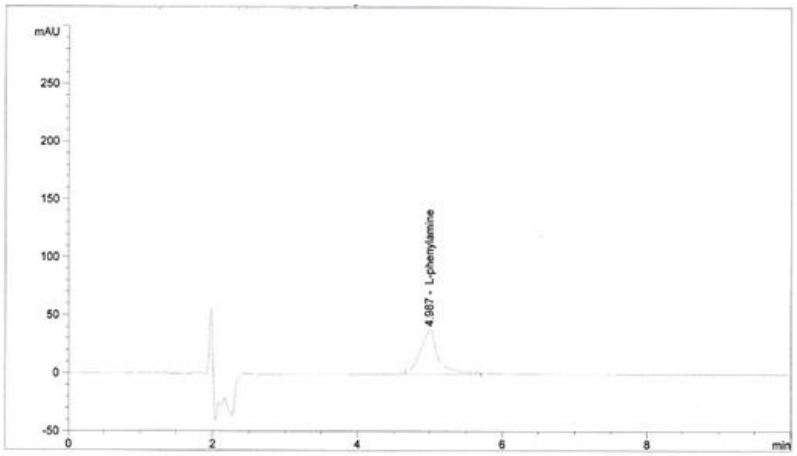

B) Sample

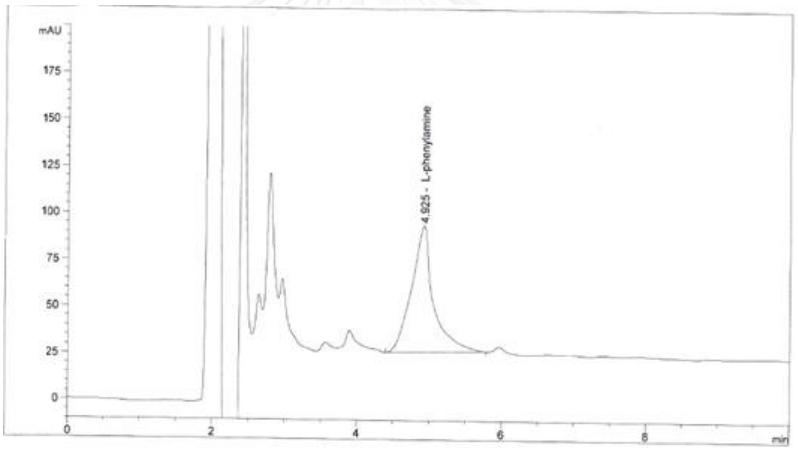

Figure 3.21 Chromatograms of L-phenylalanine

From the result in Figure 3.14 and 3.15, the production of L-Phe was not proportional to growth of *E. coli* clones. For example, pPBLT & pYF clone grew in medium formula 4 faster than formula 1 but L-Phe production was less than that of formula 1. It is important to optimize culture conditions that affected to growth and amino acid production such as carbon and nitrogen sources, C/N ration of the medium (Kumar and Shimizu, 2010).

Therefore, source and amount of carbon and nitrogen in medium formula 2, 3 and 4 were adjusted as same as that used in medium formula 1. Those adjusted media were name as formula 1.1, 2.1, 3.1 and 4.1, respectively. The growth curve and L-Phe production was shown in Figure 3.17 and 3.18 respectively.

Recombinant pBLPT & pYF clone showed the high growth in medium formula 4.1 following by formula 2.1, 3.1 and 1.1, respectively (Figure 3.17). L-Phe peoduction were 737, 608, 495 and 230 mg/L in medium formula 4.1, 2.1, 1.1 and 3.1 respectively (Figure 3.18). Growth and L-Phe production of recombinant pPTFBLY the reference clone, were significantly lower than those of pBLPT & pYF clone in medium formula 2.1 and 4.1. In medium formula 1.1, growth and L-Phe productin in both clones were similar. On the other hand, pPTFBLY clone could grow faster and produced higher amount of L-Phe than pBLPT & pYF clone when they were cultured in medium formula 3.1.

Changing in concentration of glycerol (to 30 g/L) and $(NH_4)_2SO_4$ (to 50 g/L) in most of media did not effect on cell growth and L-Phe concentration of pBLPT & pYF clone and pPTFBLY clone. pBLPT & pYF clone cultured in formula 3 showed higher growth than that formula 3.1 medium. Chloride ions existed within the media might effect on *E.coli* growth. pPTFBLY clone in formula 4 grew better than in formula 4.1. pBLPT & pYF clone in formula 4.1 and 2.1 produced L-Phe about 6 and 12 fold of those in formula 4 and 2.

Consequently, medium formula 4.1 was further studied for optimization of L-Phe production by pBLPT & pYF clone.

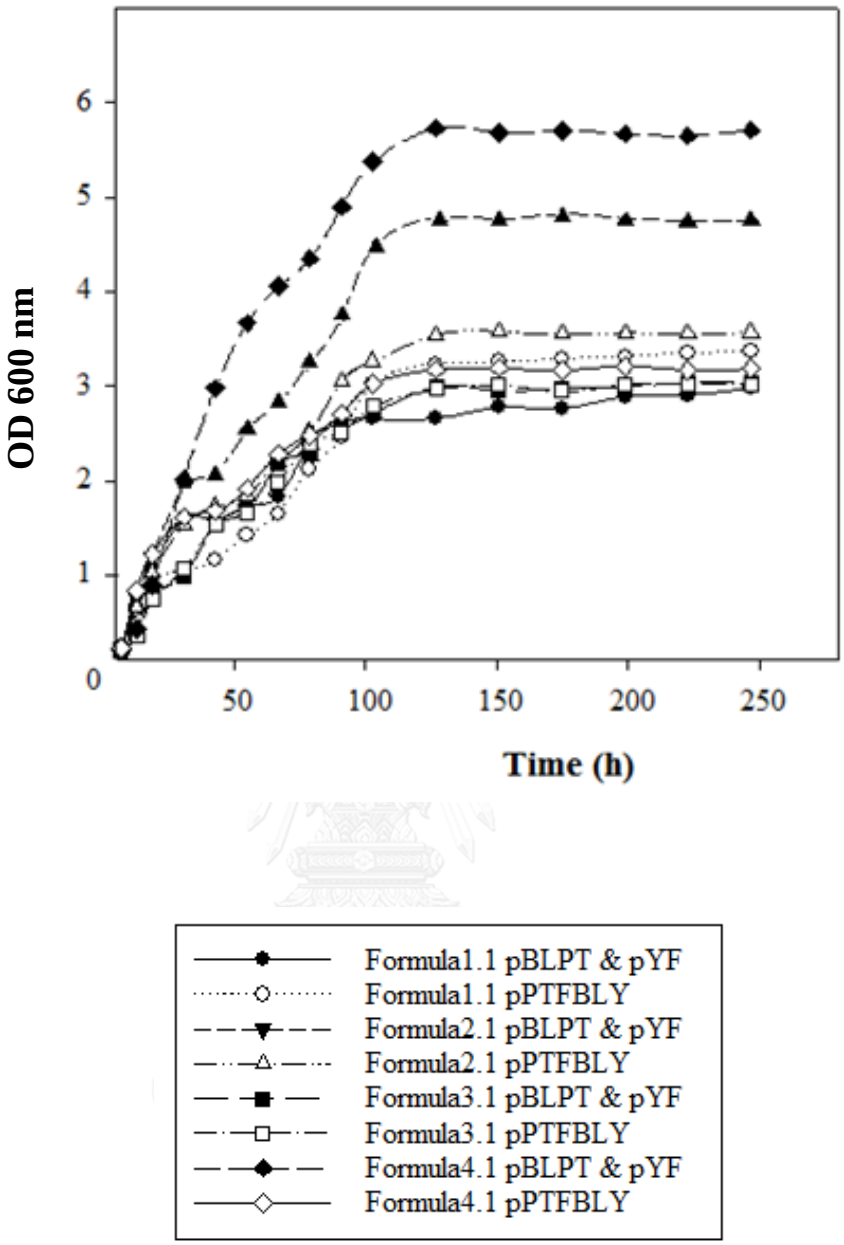

Figure 3.17 Growth curve of recombinant clones in various minimum media containing 30 g/L of glycerol and 50 g/L of $(NH_4)_2SO_4$. Data were representative of three independent experiments.

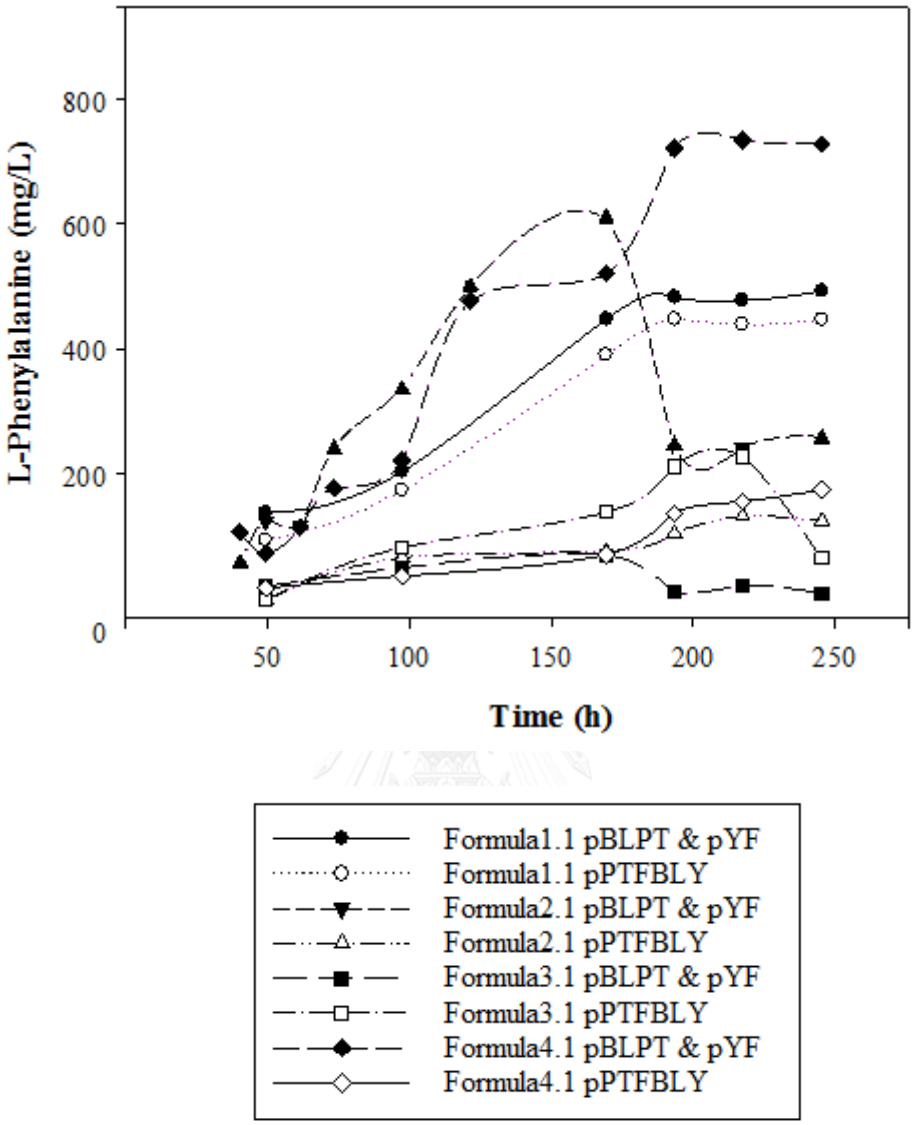

Figure 3.18 L-Phenylalanine production of recombinant clones in various minimum media containing 30 g/L of glycerol and 50 g/L of $(NH_4)_2SO_4$

Data were representative of three independent experiments.

3.5 Optimization of medium component using a responses surface methodology (RSM)

The regression equation can be expressed graphically in the form of surface plot and contour plot which depict the interaction among the independent variables and their influence on L-Phe production. The plot of glycerol concentration versus $(NH_4)_2SO_4$ concentration is elliptical in contour plot (Figure 3.19) and maximum in surface plot indicating significant interaction between the two variables. The surface plot between arabinose concentration and glycerol concentration (Figure 3.20) as well as arabinose concentration and $(NH_4)_2SO_4$ concentration (Figure 3.21) are saddle points, indicating that there are fewer interactions between them.

The maximum predicted of L-Phe by the program was 792 mg/L at medium component concentration of 3.1 % (w/v) of glycerol and 6.3 % (w/v) of $(NH_4)_2SO_4$. At maximum predict condition, the observed of L-Phe was 746 g/L at 240 h.

In this study, four genes in L-Phe biosynthesis pathway including *aroB* (encoding 3-dehydroquinate synthase), *aroL* (encoding shikimate kinase II), *phedh* (encoding phenylalanine dehydrogenase), *tktA* (encoding transketolase) under T7*lac* promoter were co-expressed with *glpF* (encoding glycerol facilitator) and *yddG* (encoding aromatic amino acid exporter) under tight regulated ara promoter in *E.coli* BL21 (DE3). The culture mediums for L-Phe product in the recombinant clone were optimized. The highest production of L-Phe at 746 mg/L was obtained when the clone was cultured in minimum medium containing (g/L): glycerol 31, $(NH_4)_2SO_4$ 63, $MgSO_4 \cdot 7H_2O$ 0.3; $CaCl_2 \cdot 2H_2O$ 0.015; KH_2PO_4 3.0; K_2HPO_4 12; NaCl 1; $(NH_4)_2SO_4$ 5.0; $FeSO_4 \cdot 7H_2O$/Na-citrate 0.075 /1.0; thiamine·HCl 0.0075 and trace element solution 1.5 ml/L, (contained (g/L)): $Al_2(SO_4)_3 \cdot 18H_2O$ 2.0; $CoSO_4 \cdot 7H_2O$ 0.75; $CuSO_4 \cdot 5\ H_2O$ 2.5; H_3BO_3 0.5; $MnSO_4 \cdot H_2O$ 24; $Na_2MoO_4 \cdot 2H_2O$ 3.0; $NiSO_4 \cdot 6H_2O$ 2.5 and $ZnSO_4 \cdot 7\ H_2O$ 15) at 37 °C after induction with 0.02% arabinose for 240 h. L-Phe was about 1.7 fold of the reference strain *E.coli* harboring pPTFBLY reported by Thongchuang (2011).

Table 3.8 Experimental design obtained by applying the CCD matrix for three factors and responses for L-Phe production

Run	Variables coded			Arabinose (%w/v)	Glycerol (%w/v)	Ammonium sulfate (%w/v)	L-Phe (mg/L)
	X_1	X_2	X_3				
1	-1	-1	-1	0.05	2.00	5.00	311
2	-1	-1	1	0.05	2.00	9.00	206
3	-1	1	-1	0.05	4.00	5.00	553
4	-1	1	1	0.05	4.00	9.00	125
5	1	-1	-1	0.20	2.00	5.00	338
6	1	-1	1	0.20	2.00	9.00	275
7	1	1	-1	0.20	4.00	5.00	259
8	1	1	1	0.20	4.00	9.00	93
9	-1.732	0	0	0.02	3.00	7.00	730
10	1.732	0	0	0.27	3.00	7.00	626
11	0	-1.732	0	0.15	1.31	7.00	139
12	0	1.732	0	0.15	4.68	7.00	149
13	0	0	-1.732	0.15	3.00	3.60	294
14	0	0	1.732	0.15	3.00	10.36	130
15	0	0	0	0.15	3.00	7.00	266
16	0	0	0	0.15	3.00	7.00	271

A.

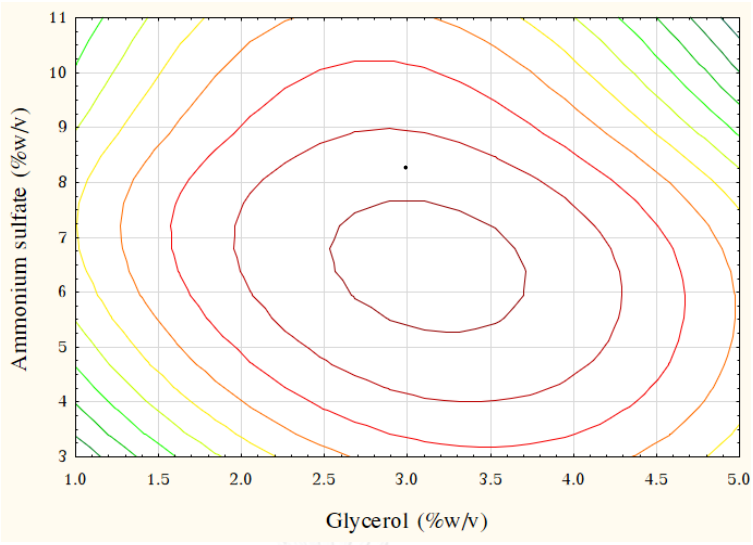

B.

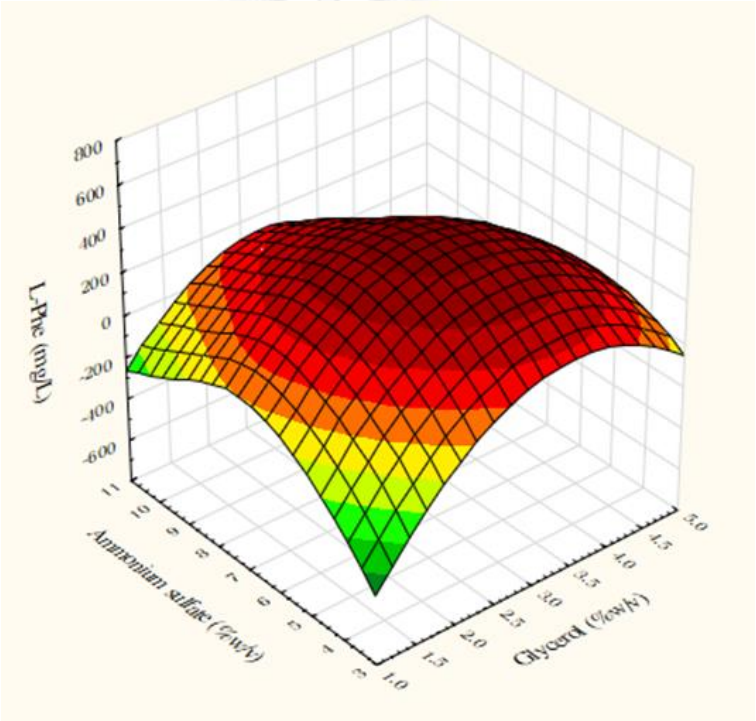

Figure 3.19 Plots describing the effect of glycerol and $(NH_4)_2SO_4$ on L-Phe production (A) Contour plot (B) Surface plot

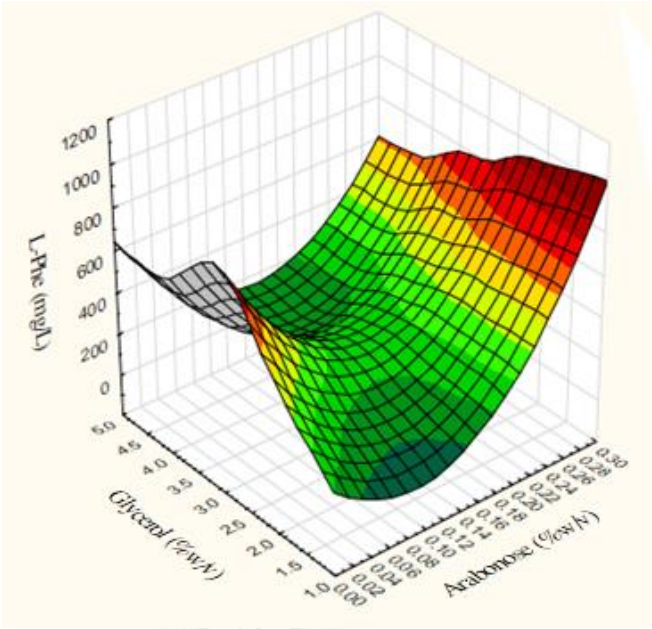

Figure 3.20 Surface plots describing the effect of arabinose and glycerol on L-Phe production

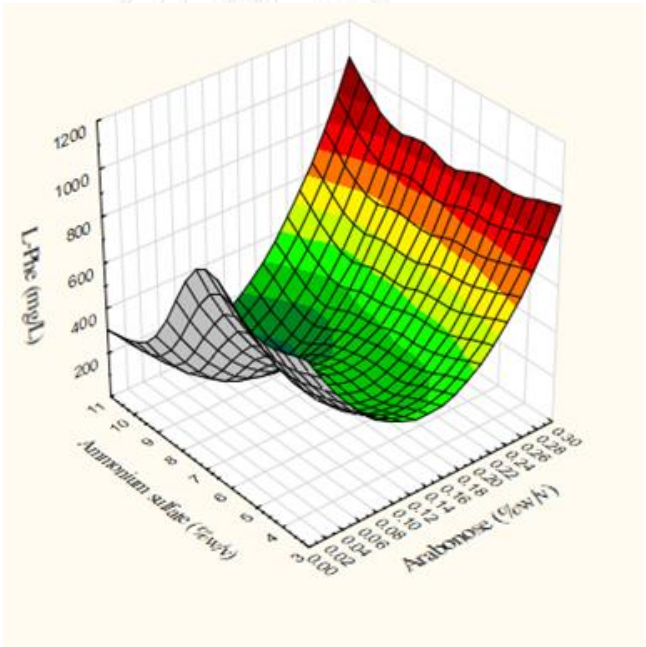

Figure 3.21 Surface plots describing the effect of arabinose and $(NH_4)_2SO_4$ on L-Phe production

CHAPTER IV

CONCLUSIONS

1. Dual plasmids system of the six genes (*aroB* encoding 3-dehydroquinate synthase, *aroL* encoding shikimate kinase II, *glpF* encoding glycerol facilitator *phedh* encoding phenylalanine dehydrogenase, *tktA* encoding transketolase and *yddG* encoding aromatic amino acid exporter) was constructed in *E. coli* BL21(DE3). *aroB*, *aroL*, *phedh* and *tktA* preceded by T7*lac* promoter were inserted into pRSFDuet-1 to create pBLPT. In parallel, *glpF* and *yddG* were inserted under ara promoter of pBAD33 leading to recombinant pYF. Both recombinant plasmids were co-transformed into *E. coli* BL21 (DE3).
2. Without selective antibiotic, pBLPT and pYF showed their moderate stability. Fifty percent of plasmid harboring cells was found in pBLPT and pYF clones after 45 and 30 generation, respectively.
3. When recombinant clones were cultured in minimum medium containing (g/L): glycerol 30, $(NH_4)_2SO_4$ 50, $MgSO_4 \cdot 7H_2O$ 0.3; $CaCl_2 \cdot 2H_2O$ 0.015; KH_2PO_4 3.0; K_2HPO_4 12; NaCl 1; $(NH_4)_2SO_4$ 5.0; $FeSO_4 \cdot 7H_2O$/Na-citrate 0.075/1.0; thiamine·HCl 0.0075 and trace element solution (1.5 ml/L). Trace element solution contained (g/L): $Al_2(SO_4)_3 \cdot 18H_2O$ 2.0; $CoSO_4 \cdot 7H_2O$ 0.75; $CuSO_4 \cdot 5\ H_2O$ 2.5; H_3BO_3 0.5; $MnSO_4 \cdot H_2O$ 24; $Na_2MoO_4 \cdot 2H_2O$ 3.0; $NiSO_4 \cdot 6H_2O$ 2.5 and $ZnSO_4 \cdot 7\ H_2O$ 15 at 37 °C for 240 h, the *E.coli* clone harboring pBLPT & pYF produced L-phe about 1.6 fold of that from pPTFBLY clone.
4. The highest L-Phe production at 746 mg/L was obtained when the *E.coli* harboring pBLPT & pYF was cultured in minimum medium containing (g/L): glycerol 31, $(NH_4)_2SO_4$ 63, $MgSO_4 \cdot 7H_2O$ 0.3; $CaCl_2 \cdot 2H_2O$ 0.015; KH_2PO_4 3.0; K_2HPO_4 12; NaCl 1; $(NH_4)_2SO_4$ 5.0; $FeSO_4 \cdot 7H_2O$/Na-citrate 0.075/1.0; thiamine·HCl 0.0075 and trace element solution (1.5 ml/L). Trace element solution contained (g/L): $Al_2(SO_4)_3 \cdot 18H_2O$ 2.0; $CoSO_4 \cdot 7H_2O$ 0.75; $CuSO_4 \cdot 5$

H_2O 2.5; H_3BO_3 0.5; $MnSO_4 \cdot H_2O$ 24; $Na_2MoO_4 \cdot 2H_2O$ 3.0; $NiSO_4 \cdot 6H_2O$ 2.5 and $ZnSO_4 \cdot 7\ H_2O$ 15 at 37 °C after induction with 0.02% arabinose for 240 h.

APPENDICES

APPENDIX A

List of drug containing phenylalanine

PRODUCT	Phe CONTENT
OVER THE COUNTER DRUGS	
Cold and Allergy Non-prescription Products	
Alka-Seltzer Plus sparkling original flavor	8.4mg/tablet
Alka-Seltzer Plus Cold and Cough medicine	11mg/tablet
Alka-Seltzer Plus Cold and Sinus	4mg/tablet
Alka-Seltzer Plus Cold medicine cherry flavor	5.6mg/tablet
Alka-Seltzer Plus Cold medicine orange zest flavor	4.2mg/tablet
Alka-Seltzer Plus Flu w/Max-Strength Pain Reliever, honey orange	6.7mg/tablet
Alka-Seltzer Plus Nose and Throat Cold Medicine, citrus blend	5.6mg/tablet
Alka-Seltzer Plus Night-Time Cold Medicine	7.8mg/tablet
Augmentin 200mg	2.1mg/tablet
Augmentin 400mg	4.2mg/tablet
Benadryl allergy and sinus fastmelt	4.6mg/tablet
Benadryl allergy chewables	4.2mg/tablet
Benadryl, Childrens allergy and cold fast melt tablets	4.6mg/tablet
Childrens PediaCare Multi-Symptom Cold Chewables, Cherry flavor	8.4mg/tablet
Diabetic Tussin Maximum strength DM	8.4mg/teaspoon
Diabetic Tussin Regular strength DM	8.4mg/teaspoon
Halls sugar free menthol cough supressant drops	2mg/drop
Ricola Sugar free herb throat drops	1mg/drop
Robitussin sugar free throat drops	3.37mg/drop
Sudafed childrens chewables	0.78mg/tablet
TheraFlu Maximum strength Flu and Congestion non-drowsy	24mg/packet
TheraFlu Maximum Strength Flu and Sore throat packets	22mg/packet
TheraFlu Maximum Strength Severe cold and congestion night time	17mg/packet
TheraFlu Maximum Strength Severe cold and congestion non-drowsy	17mg/packet
TheraFlu Regular Strength Cold and Sore throat packets	11mg/packet
TheraFlu Regular strength Cough and Cold packet	13mg/packet
Triaminic softchews allergy and congestion	17.6mg/tablet
Triaminic softchews allergy, runny nose and congestion	17.5mg/tablet
Triaminic softchews cough	22.5mg/tablet
Triaminic softchews cough and sore throat	28.1mg/tablet
Walgreens Effervescent Cold Relief Plus, original flavor	8.4mg/tablet
Wal-Tussin DM Clear (Walgreens brand)	14mg/teaspoon
Valu-Rite Expectorant DM clear cough syrup	14mg/teaspoon

Analgesic Non-prescription Products	
Advil, Childrens 50mg chewable tablets grape	2.1mg/tablet
Advil, Junior strength 100mg fruit	4.2mg/tablet
Alka-Seltzer PM	4.04mg/tablet
Excedrin Quick Tabs	Free
Motrin, Junior Strength chewable tablets 100mg grape	2.8mg/tablet
Motrin. Childrens chewable tablets 50mg orange/grape flavor	1.4mg/tablet
Non-Aspirin, Childrens soft chewable tablets all flavors (Walgreens brand)	6mg/tablet
Non-Aspirin, Junior strength all flavors (Walgreens brand)	12mg/tablet
Tempra quicklets childrens or junior stengths	21mg/tablet
Antacids	
Alka-Seltzer antacid and pain relief medicine lemon-lime	9mg/tablet
Alka-Seltzer Heartburn Relief lemon lime	11mg/2 tablets
Alka-Seltzer Morning Relief	9mg/tablet
Chooz antacid/calcium supplement	2.4mg/tablet
Surpass antacid chewable gum extra Strength wintergreen flavor	3.9mg/piece
Surpass antacid chewable gum Regular strength fruit flavor	3.9mg/piece
Laxatives	
Citrucel sugar free fiber therapy	52mg/adult dose(10.2gm)
Maalox Quick dissolve Max Stength assorted flavor or lemon flavor	0.9mg/tablet
Maalox Quick dissolve Max Stength wild berry flavor	0.5mg/tablet
Metamucil sugar free fiber Orange flavor	25mg/teaspoon
Reguloid sugar free regular flavor	6mg/rounded teaspoon
Reguloid sugar free orange flavor	30mg/rounded teaspoon
NVP sugar free orange flavor (Walgreens brand)	21mg/teaspoon
Medilax chewable tablets	2mg/tablet
Vitamins and Minerals	
Citracal Liquitab Effervescent tablets	12mg/tablet
Bugs Bunny complete, plus iron or plus extra vit C chewable tablets	3mg/tablet
Bugs Bunny childrens chewable tablets	2mg/tablet
Centrum Junior chewable tablets	4mg/tablet
Flinstones vitamins complete or with calcium	2mg/tablet
Garfield complete with mineral chewable vitamins	3mg/tablet
Sunkist multivitamin complete	4mg/tablet
Sunkist multivitamins plus iron or plus extra C chewable tablets	6mg/tablet

Electrolyte Replacement	
Pedialyte freezer pops	16mg/pop
Kao Lectrolyte electrolyte replenisher unflavored or bubble gum	11mg/packet
Kao Lectrolyte electrolyte replenisher grape flavor	23mg/packet
Motion Sickness and Nausea Medicine	
Dramamine chewable formula tablets	1.5mg/tablet
Dramamine chewable tablets	1.5mg/tablet
Nauzene chewable tabs for nausea wild cherry	18mg/4 tablets
Misc	
DentiPatch	0.62mg/system
Kank-a Professional Strength oral solution	contains aspartame
Phazyne quick dissolve 125mg chewable tablets	0.4mg/tablet
PRESCRIPTION DRUGS	
Antibiotics and Antivirals	
Amoxicillin 250mg chew tabs by WarnerChilcott	2mg/tablet
Amoxil 200mg chewable tablet	1.82mg/tablet
Amoxil 400mg chewable tablet	3.64mg/tablet
Augentin 200mg/5ml suspension	7mg/5ml
Augmentin 200mg chewable tablet	2.1mg/tablet
Augmentin 400mg chewable tablet	4.2mg/tablet
Augmentin 400mg/5ml suspension	7mg/5ml
Augmentin ES 600mg/5ml	7mg/5ml
Cefzil 125mg/5ml	28mg/5ml
Cefzil 250mg/5ml	28mg/5ml
Penicillin V Potassium for Oral Susp (by Warner Chilcott)	4mg/5ml
Videx chewable tablet (all strengths)	36.5mg/tablet
Viracept powder for Oral Suspension	11.2mg/GM of powder
Zyvox 100mg/5ml suspension	20mg/5ml
Antiemetics	
Zofran ODT 4mg	<0.03mg/tablet
Zofran ODT 8mg	<0.03mg/tablet
Antilipemics (Cholesterol)	
Cholestyramine powder	14mg/packet
Colestid flavored granules	15-18mg/7.5mg dose
Prevalite powder	14mg/packet
Questran Lite powder	17 mg / 5 gm
Antipsycotics and Antidepressants	
Remeron 15ng Soltabs	2.6mg/tablet

Remeron 30mg Soltabs	5.2mg/tablet
Remeron 45mg Soltabs	7.8mg/tablet
Zyprexa Zydis 5mg ODTablet	0.34mg/tablet
Zyprexa Zydis 10mg ODTablet	0.45mg/tablet
Zyprexa Zydis 15mg ODTablet	0.67mg/tablet
Zyprexa Zydis 20mg ODTablet	0.90mg/tablet
Singulair 5mg chewable tablet	0.842mg/tablet
H-2 Antagonists (stomach)	
Pepcid 20mg RPD Tablet	1.05mg/tablet
Pepcid 40mg RPD tablet	2.10mg/tablet
Zantac efferdose tablets and granules	16.84mg/150mg
Migraine treatment	
Maxalt-MLT 5mg tablet	1.05mg/tablet
Maxalt-MLT 10mg tablet	2.1mg/tablet
Transplant medication	
CellCept Oral Suspension	0.56mg/ml

Last update: September 2007
National PKU News: www.pkunews.org
E-mail: schuett@pkunews.org

APPENDIX B

Control of the T7*lac* promoter

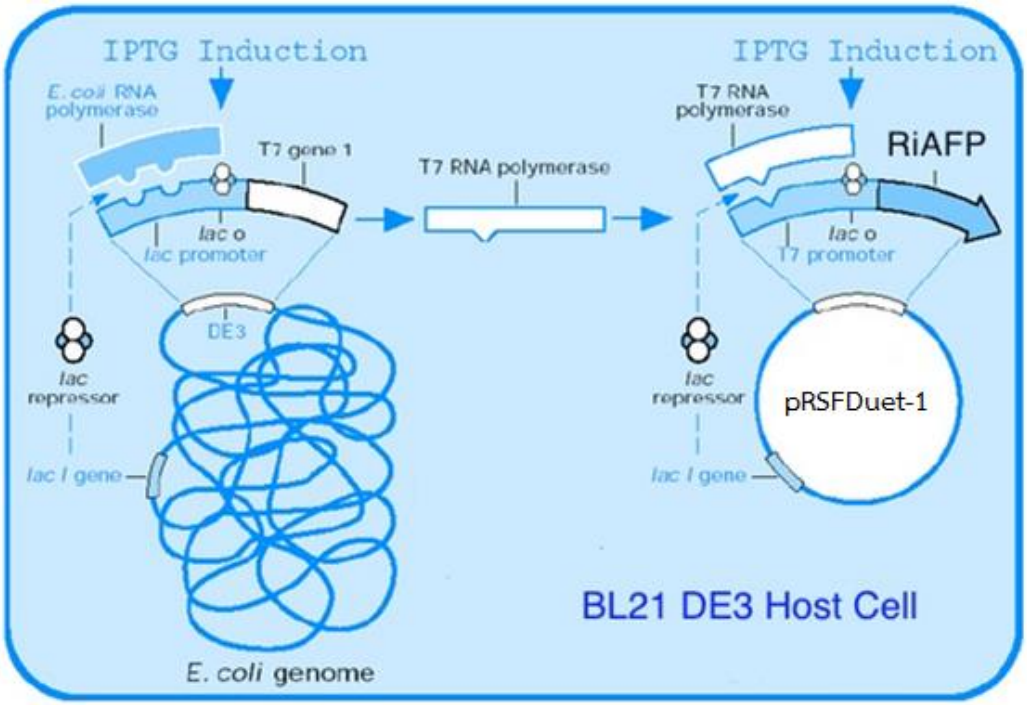

Source: http://www.quora.com/How-does-IPTG-induced-gene-expression-work-at-a-molecular-level

APPENDIX C

Control of the ara promoter

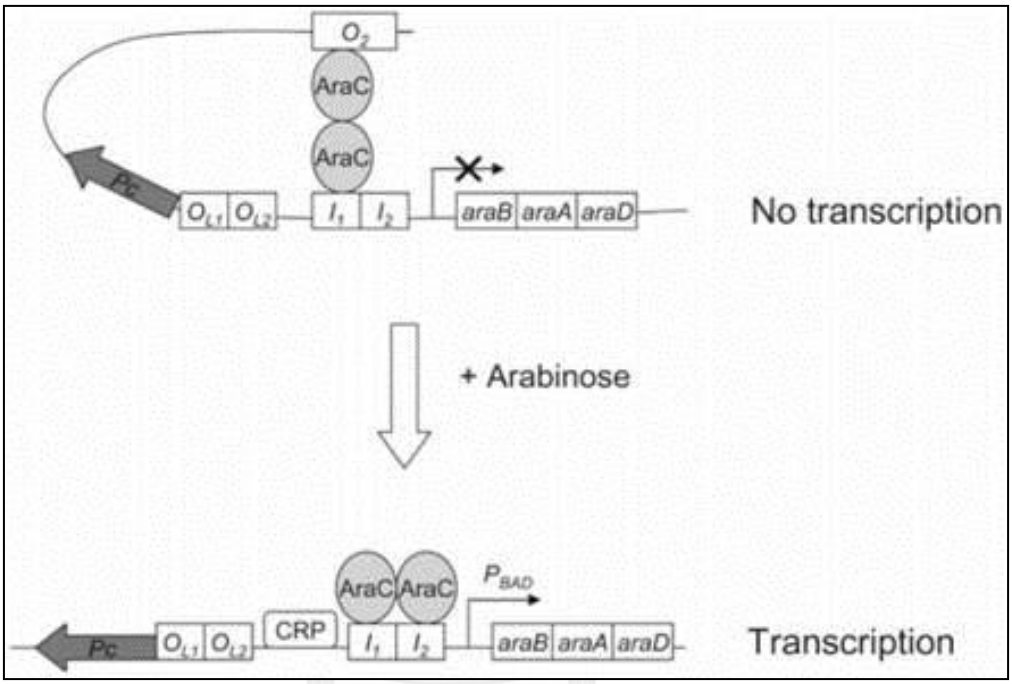

Source: http://www.mfa.od.ua/page265.htm

APPENDIX D

Restriction map of pRSFDuet-1

pRSFDuet-1 DNA	71341-3
pRSFDuet-1 sequence landmarks	
T7 promoter-1	3582–3598
T7 transcription start-1	1
His•Tag® coding sequence	83–100
Multiple cloning sites-1 (*Nco* I–*Afl* II)	60–168
T7 promoter-2	214–230
T7 transcription start-2	231
Multiple cloning sites-2 (*Nde* I–*Avr* II)	297–438
S•Tag™ coding sequence	366–410
T7 terminator	462–509
kan (Kn^R) coding sequence	742–1554
RSF origin	1662–2411
lacI coding sequence	2610–3689

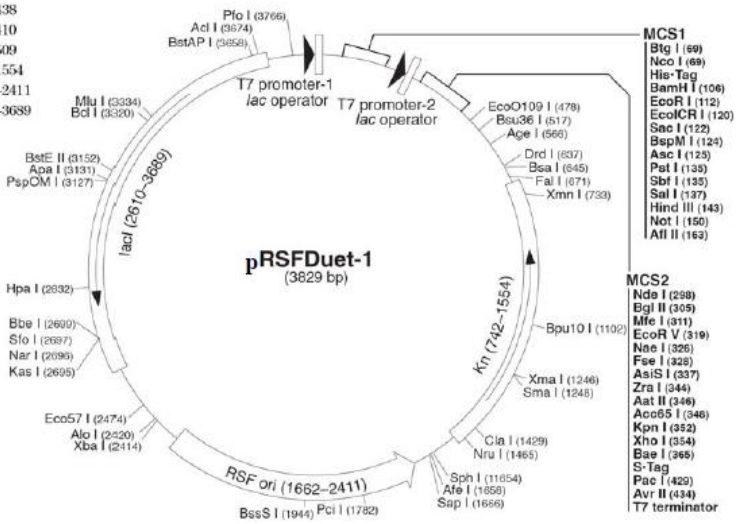

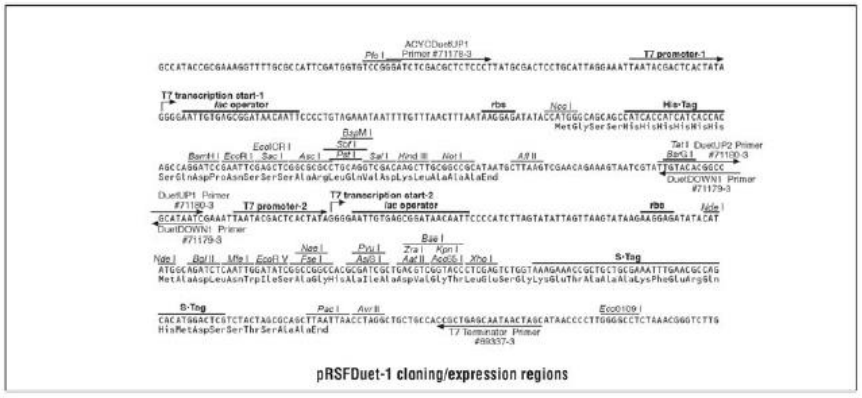

Source: http://www.helmholtz muenchen.de/fileadmin/PEPF/pRSF_vectors/ pRSFDuet-1_map.pdf

APPENDIX E

Restriction map of pBAD33

regulator: araC, <-, 3452-4330
operator: O2, 4359-4376
promoter: araC, <-, 4481-4509
operator: O1, 4517-4538
operator: I2 + I1, 4569-4607
promoter for expression: arabinose BAD, ->, 4606-4633
MCS: NheI...HindIII, ->, 4656-4718
transcription terminator: rrnB T1 + T2, ->, 4719-5144
marker(s): cmLR, <-, 1348-2007
replicon: p15A, 2369-3213

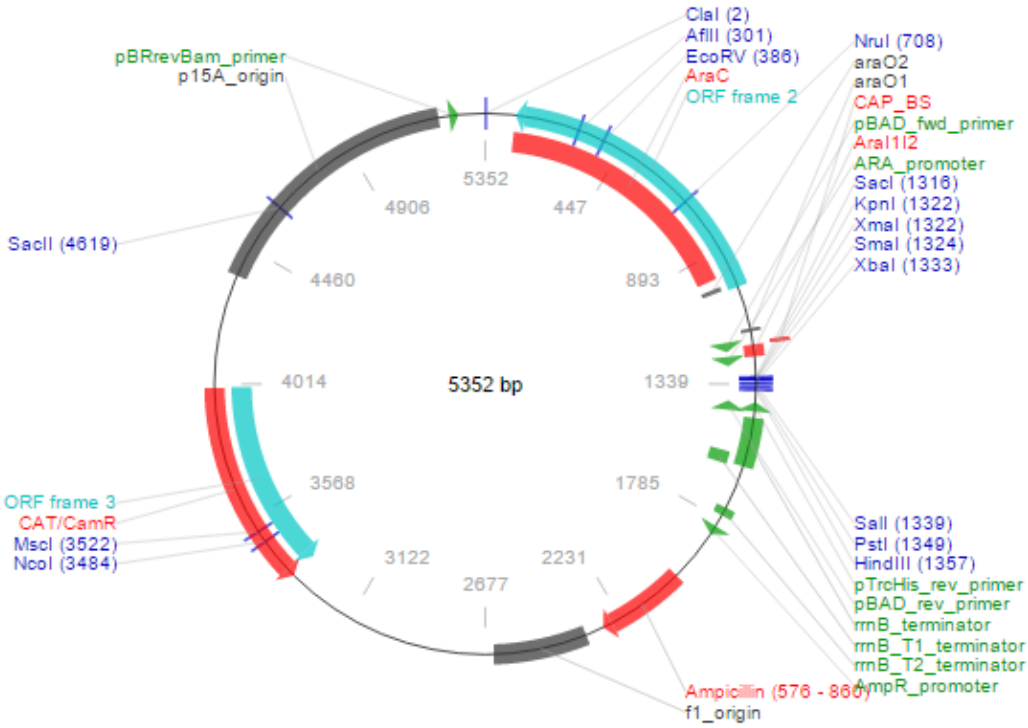

Source: http://www.biovisualtech.com/bvplasmid/pBAD33.htm

APPENDIX F

Sample preparation for agarose gel electrophoresis and HPLC mobile phase

1. **Electrophoresis buffer (10x TBE)**

Tris (hydroxymethyl)-aminmethane	54	g
Boric acid	27.5	g
Ethylenediaminetetraacetic Acid, Disodium salt	9.3	g

Adjust volume to 1 liter with deionized water and may take some time to dissolve, even with fast stirring

2. **HPLC mobile phase (2 mM Copper sulfate)**

Copper sulfate	0.5	g

Adjust volume to 1 liter with ultrapure water and filtrated for remove impurity that can block up in HPLC column.

APPENDIX G

Standard curve for determination of L-phenylalanine concentration by HPLC

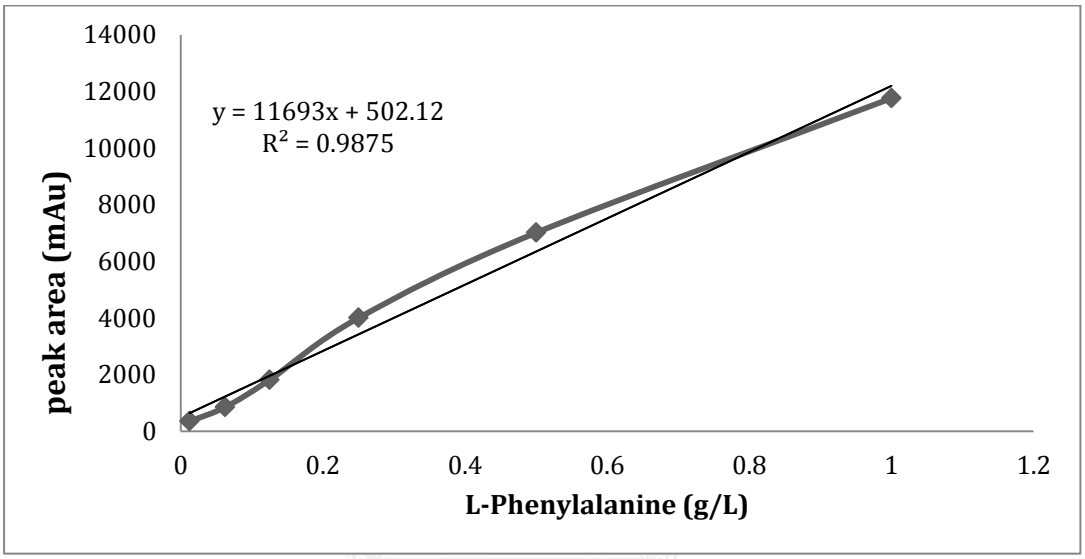

APPENDIX H

Standard curve for protein determination by Lowry's method

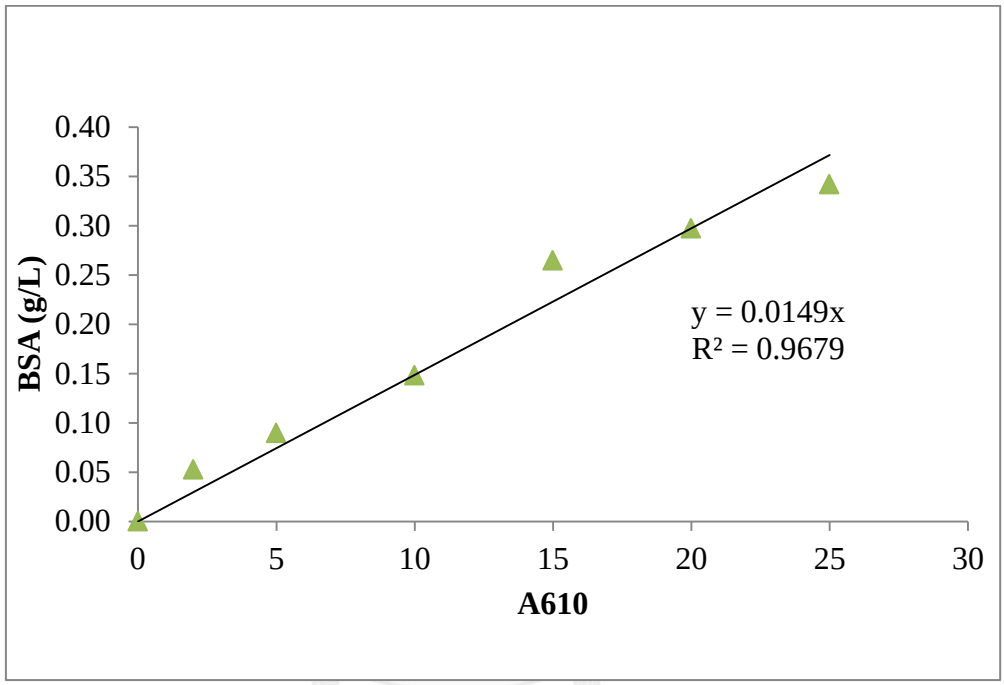

APPENDIX I

Plasmid replicon and compatibility

Plasmid(s)	Replicon (source)	Copy number*	Compatible Replicons
pET (all), pETDuet-1	ColE1 (pBR322)	~40	P15A, Mini-F/RK2, CloDF13, RSF1030, ColA
pACYCDuet-1, pLysS, pLysE, pLacI, pRARE, pRARE-2	P15A (pACYC184)	10–12	ColE1, Mini-F/RK2, CloDF13, RSF1030, ColA
pCDFDuet™-1, pCDF	CloDF13	20–40	ColE1, P15A, RSF1030, ColA
pRSFDuet-1, pRSF	RSF1030	> 100	ColE1, P15A, CloDF13
pCOLADuet™-1	ColA	20–40	ColE1, P15A, CloDF13, Mini-F/RK2
pETcoco™ (all)	Mini-F/RK2 (pBeloBAC11, RK2)	amplifiable to ~40	ColE1, P15A , ColA

* Copy number was estimated based on gel analysis (9, 16)

Source: User Protocol TB340 Rev. D 0304, Novagen

Host strain compatibility

For protein production, the Duet recombinants are transferred to an *E. coli* expression host (DE3) containing a chromosomal copy of the gene for T7 RNA polymerase. The choice of expression host strain is based on strain characteristics and expression vector compatibility. Review the Competent Cells Protocol (User Protocol TB009) for complete descriptions of the host strain characteristics. Use the following tables to determine compatibility. Compatible vectors and host strains are listed in Table 3 below. For expression host strain group, see Table 4 (page 6). For compatible combinations with pETcoco™ plasmid, please consult User Protocol TB333.

Note: The pETcoco vectors are not compatible with pCDFDuet-1 or pRSFDuet-1.

Table 3 Vector and host strain compatibility

Compatible Vector Combinations				Number of coexpressed target proteins	Compatible expression host strains
Vector 1	Vector 2	Vector 3	Vector 4*		
pETDuet™-1 (Amp^R)	pACYCDuet™-1 (Cam^R)	pRSFDuet™-1 or pCOLADuet™-1 (Kan^R)	pCDFDuet™-1 (Sm^R)	8	Group A
pETDuet-1 (Amp^R)	pRSFDuet-1or pCOLADuet-1 (Kan^R)	pCDFDuet-1 (Sm^R)		6	Group C
pETDuet-1 (Amp^R)	pACYCDuet-1 (Cam^R)	pRSFDuet-1 or pCOLADuet-1 (Kan^R)		6	Group A
pETDuet-1 (Amp^R)	pACYCDuet-1 (Cam^R)	pCDFDuet-1 (Sm^R)		6	Group B
pRSFDuet-1 or pCOLADuet-1 (Kan^R)	pCDFDuet-1 (Sm^R)	pACYCDuet-1 (Cam^R)		6	Group A
pETDuet-1 (Amp^R)	pRSFDuet-1 or pCOLADuet-1 (Kan^R)			4	Group C
pETDuet-1 (Amp^R)	pCDFDuet-1 (Sm^R)			4	Group D
pETDuet-1 (Amp^R)	pACYCDuet-1 (Cam^R)			4	Group B
pRSFDuet™-1 or pCOLADuet-1 (Kan^R)	pCDFDuet-1 (Sm^R)			4	Group C
pACYCDuet-1 (Cam^R)	pRSFDuet™-1 or pCOLADuet-1 (Kan^R)			4	Group A
pACYCDuet-1 (Cam^R)	pCDFDuet-1 (Sm^R)			4	Group B

Amp; ampicillin/carbenicillin, 50 µg/ml: Kan; kanamycin, 30 µg/ml: Cam; chloramphenicol, 34 µg/ml: Sm; streptomycin/spectinomycin, 50 µg/ml

*When cotransforming four Duet plasmids, the antibiotic concentrations should be reduced by half.

Table 4 Vector and Host Strain Compatibility

Vector	Compatible expression host strains
pET Duet	Group D
pACYC Duet	Group B
pCDF Duet	Group D
pRSF Duet or pCOLA Duet	Group C

Source: User Protocol TB340 Rev. D 0304, Novagen

Table 4 Strain groups

Group A	Group B	Group C	Group D
B834(DE3)	B834(DE3)	B834(DE3)	B834(DE3)
BL21(DE3)	BL21(DE3)	B834(DE3)pLysS	B834(DE3)pLysS
BLR(DE3)	BLR(DE3)	BL21(DE3)	BL21(DE3)
HMS174(DE3)	HMS174(DE3)	BL21(DE3)pLysS	BL21(DE3)pLysS
NovaBlue(DE3)	NovaBlue(DE3)	BLR(DE3)	BLR(DE3)
Origami™ 2(DE3)*	Origami(DE3)*	BLR(DE3)pLysS	BLR(DE3)pLysS
Tuner™(DE3)	Origami 2(DE3)*	HMS174(DE3)	HMS174(DE3)
	Origami B(DE3)	HMS174(DE3)pLysS	HMS174(DE3)pLysS
	Tuner(DE3)	NovaBlue(DE3)	NovaBlue(DE3)
		Origami 2(DE3)*	Origami(DE3)*
		Origami 2(DE3)pLysS*	Origami(DE3)pLysS*
		Rosetta™(DE3)	Origami 2(DE3)*
		Rosetta(DE3)pLysS	Origami 2(DE3)pLysS*
		Rosetta 2(DE3)	Origami B(DE3)
		Rosetta 2(DE3)pLysS	Origami B(DE3)pLysS
		RosettaBlue™(DE3)	Rosetta(DE3)
		RosettaBlue(DE3)pLysS	Rosetta(DE3)pLysS
		Rosetta-gami™ 2(DE3)*	Rosetta 2(DE3)
		Rosetta-gami 2(DE3)pLysS*	Rosetta 2(DE3)pLysS
		Tuner(DE3)	RosettaBlue(DE3)
		Tuner(DE3)pLysS	RosettaBlue(DE3)pLysS
			Rosetta-gami(DE3)*
			Rosetta-gami(DE3)pLysS*
			Rosetta-gami 2(DE3)*
			Rosetta-gami 2(DE3)pLysS*
			Rosetta-gami B(DE3)
			Rosetta-gami B(DE3)pLysS
			Tuner(DE3)
			Tuner(DE3)pLysS

*These strains carry a mutation in ribosomal protein (*rpsL*) conferring resistance to streptomycin; thereforestreptomycin is not necessary to maintain strain genotype. If using pCDF vectors, spectinomycin must be used for antibiotic selection because *rpsL* mutation confers streptomycin resistance.

Source: User Protocol TB340 Rev. D 0304, Novagen

APPENDIX J

Calculate of generation time

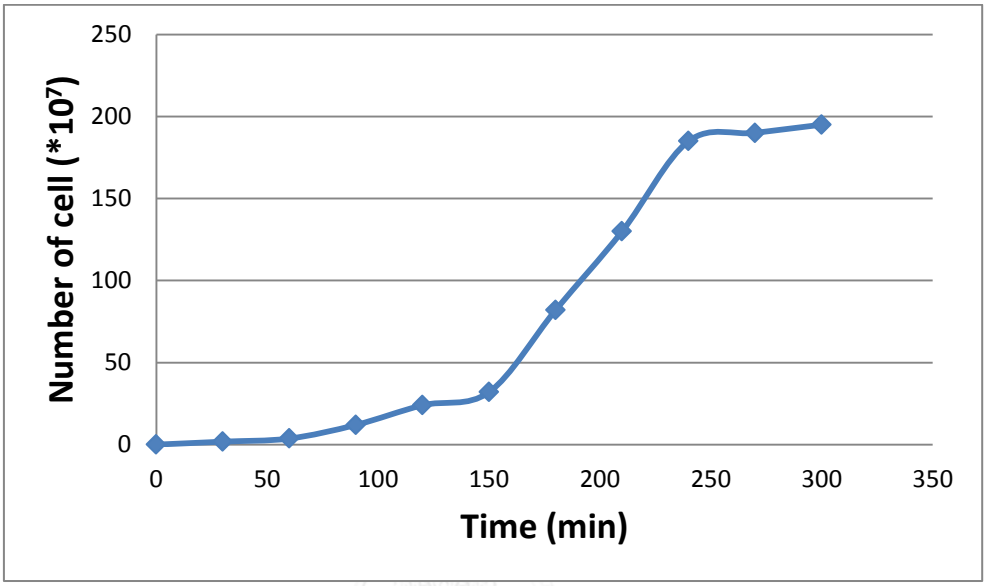

When growing exponentially by binary fission, the increase in a bacterial population is by geometric progression. If we start with one cell, when it divides, there are 2 cells in the first generation, 4 cells in the second generation. The **generation time** is the time interval required for the cells (or population) to divide.

G (generation time) = (time, in minutes or hours)/n(number of generations)

G = t/n

t = time interval in hours or minutes

B = number of bacteria at the beginning of a time interval

b = number of bacteria at the end of the time interval

n = number of generations (number of times the cell population doubles during the time interval)

$b = B \times 2^n$ (This equation is an expression of growth by binary fission)

Solve for n:

$$\log b = \log B + n \log 2$$

$$n = \frac{\log b - \log B}{\log 2}$$

$$n = \frac{\log b - \log B}{0.301}$$

$$n = 3.3 \log b/B$$

$$G = t/n$$

Solve for G:

$$G = \frac{t}{3.3 \log b/B}$$

The generation in this study:

$$G = \frac{90}{(3.3)\ 0.5 \log 10^7/10^6}$$

$$G = \frac{90}{1.84}$$

$$= 48 \text{ min}$$

Source: http://textbookofbacteriology.net/growth_3.html

REFERENCES

Aaron Lal, J. V., Justin Yee and Eric Yuan. 2012. Rescuing the *ompA* deletion mutant *Escherichia coli* JW0940 by reintroducing *ompA* in the TOPO cloning vector pBAD. *Experimental Microbiology and Immunology.* 16: 108-112.

Aermold L. Demain, C. A. D. 2007. The business of biotechnology. *Peer Review.* 3: 269-283.

Backman, K., O'Connor, M. J., Maruya, A., Rudd, E., McKay, D., Balakrishnan, R., Radjai, M., DiPasquantonio, V., Shoda, D., Hatch, R., and et al. 1990. Genetic engineering of metabolic pathways applied to the production of phenylalanine. *Annals of the New York Academy of Sciences.* 589: 16-24.

Baez-Viveros, J. L., Osuna, J., Hernandez-Chavez, G., Soberon, X., Bolivar, F., and Gosset, G. 2004. Metabolic engineering and protein directed evolution increase the yield of L-phenylalanine synthesized from glucose in *Escherichia coli*. *Biotechnology and bioengineering.* 87: 516-524.

Bentley, W. E., Mirjalili, N., Andersen, D. C., Davis, R. H., and Kompala, D. S. 1990. Plasmid-encoded protein: the principal factor in the "metabolic burden" associated with recombinant bacteria. *Biotechnology and bioengineering.* 35: 668-681.

Bezerra, M. A., Santelli, R. E., Oliveira, E. P., Villar, L. S., and Escaleira, L. A. 2008. Response surface methodology (RSM) as a tool for optimization in analytical chemistry. *Talanta.* 76: 965-977.

Biebl, H., Zeng, A. P., Menzel, K., and Deckwer, W. D. 1998. Fermentation of glycerol to 1,3-propanediol and 2,3-butanediol by *Klebsiella pneumoniae*. *Applied microbiology and biotechnology.* 50: 24-29.

Birkmayer, W., Riederer, P., Linauer, W., and Knoll, J. 1984. L-deprenyl plus L-phenylalanine in the treatment of depression. *Journal of neural transmission.* 59: 81-87.

Bongaerts, J., Krämer, M., Müller, U., Raeven, L., and Wubbolts, M. 2001. Metabolic engineering for microbial production of aromatic amino acids and derived compounds. *Metabolic Engineering.* 3: 289-300.

Celeste, M., Todaro, C., and Henry, C. 2014. *Fermentation and biochemical engineering handbook.* Principles, Process design, and Equipment. Oxford: Elsevier

Chao, Y.-P., Lai, Z. J., Chen, P., and Chern, J.-T. 1999. Enhanced conversion rate of L-phenylalanine by coupling reactions of aminotransferases and phosphoenolpyruvate carboxykinase in *Escherichiacoli* K-12. *Biotechnology Progress.* 15: 453-458.

Da Silva, G. P., Mack, M., and Contiero, J. 2009. Glycerol: A promising and abundant carbon source for industrial microbiology. *Biotechnology Advances.* 27: 30-39.

Daniel, P. M., Moorhouse, S. R., and Pratt, O. E. 1976. Amino acid precursors of monoamine neurotransmitters and some factors influencing their supply to the brain. *Psychological medicine.* 6: 277-286.

Das, K., Anis, M., Azemi, B. M., and Ismail, N. 1995. Fermentation and recovery of glutamic acid from palm waste hydrolysate by ion-exchange resin column. *Biotechnology and bioengineering.* 48: 551-555.

Doroshenko, V., Airich, L., Vitushkina, M., Kolokolova, A., Livshits, V., and Mashko, S. 2007. *YddG* from *Escherichia coli* promotes export of aromatic amino acids. *FEMS microbiology letters.* 275: 312-318.

Dzivenu, O. K., Park, H. H., and Wu, H. 2004. General co-expression vectors for the overexpression of heterodimeric protein complexes in *Escherichia coli*. *Protein expression and purification.* 38: 1-8.

El-Ziney, M. G., Arneborg, N., Uyttendaele, M., Debevere, J., and Jakobsen, M. 1998. Characterization of growth and metabolite production of *Lactobacillus reuteri* during glucose/glycerol cofermentation in batch and continuous cultures. *Biotechnol Lett.* 20: 913-916.

Enrique, C. A. 2007. *Process Optimization.* A Statistical Approach. Berlin: Springer

Farah, R. S., Afsheen, M., Butt, N., A., M., Z., M. T., and , A. R. a. A. R. S. 2012. Optimization of fermentation media for enhanced amino acids production by bacteria isolated from natural sources. *Pakistan Journal of Zoology.* 44: 1145-1157.

Fernstrom, J. D., and Fernstrom, M. H. 2007. Tyrosine, phenylalanine, and catecholamine synthesis and function in the brain. *The Journal of nutrition.* 137: 1539S-1547S; discussion 1548S.

Gilani, H. G., Samper, K. G., and Haghi, R. K. 2013. *Advanced process control and stimulation for chemical engineers.* Chemical Process Control. New Jersey: Apple Academic Press

Glushakov, A. V., Dennis, D. M., Sumners, C., Seubert, C. N., and Martynyuk, A. E. 2003. L-phenylalanine selectively depresses currents at glutamatergic excitatory synapses. *Journal of neuroscience research.* 72: 116-124.

Gonzalez-Pajuelo, M., Andrade, J. C., and Vasconcelos, I. 2004. Production of 1,3-propanediol by *Clostridium butyricum* VPI 3266 using a synthetic medium and raw glycerol. *Journal of Industrial Microbiology and Biotechnology.* 31: 442-446.

Gonzalez, R., Murarka, A., Dharmadi, Y., and Yazdani, S. S. 2008. A new model for the anaerobic fermentation of glycerol in enteric bacteria: trunk and auxiliary pathways in *Escherichia coli*. *Metabolic Engineering.* 10: 234-245.

Gottlieb, K., Albermann, C., and Sprenger, G. A. 2014. Improvement of L-phenylalanine production from glycerol by recombinant Escherichia coli

strains: the role of extra copies of *glpK*, *glpX*, and *tktA* genes. *Microbial cell factories.* 13: 96.

Guzman, L. M., Belin, D., Carson, M. J., and Beckwith, J. 1995. Tight regulation, modulation, and high-level expression by vectors containing the arabinose *pBAD* promoter. *Journal of bacteriology.* 177: 4121-4130.

Han, C., Shan, H., Bi, C., Zhang, X., Qi, J., Zhang, B., Gu, Y., and Yu, W. 2015. A highly effective and adjustable dual plasmid system for O-GlcNacylated recombinant protein production in *E. coli*. *Journal of biochemistry.*

Ikeda, M., and Nakagawa, S. 2003. The Corynebacterium glutamicum genome: features and impacts on biotechnological processes. *Applied microbiology and biotechnology.* 62: 99-109.

Kampen, W. H. 1996. *Nutritional requirements in fermentation Processes.* Process Design and Equipment. New Jersey: William Andrew Publishing

Kumar, P. K., Maschke, H. E., Friehs, K., and Schugerl, K. 1991. Strategies for improving plasmid stability in genetically modified bacteria in bioreactors. *Trends in Biotechnology.* 9: 279-284.

Kumar, R., and Shimizu, K. 2010. Metabolic regulation of *Escherichia coli* and its *gdhA*, *glnL*, *gltB*, D mutants under different carbon and nitrogen limitations in the continuous culture. *Microbial cell factories.* 9: 8.

Lee, P. C., Lee, W. G., Lee, S. Y., and Chang, H. N. 2001. Succinic acid production with reduced by-product formation in the fermentation of *Anaerobiospirillum succiniciproducens* using glycerol as a carbon source. *Biotechnology and bioengineering.* 72: 41-48.

Leuchtenberger, W., Huthmacher, K., and Drauz, K. 2005. Biotechnological production of amino acids and derivatives: current status and prospects. *Applied microbiology and biotechnology.* 69: 1-8.

Liu, S.-P., Xiao, M.-R., Zhang, L., Xu, J., Ding, Z.-Y., Gu, Z.-H., and Shi, G.-Y. 2013. Production of L-phenylalanine from glucose by metabolic engineering of wild type *Escherichia coli* W3110. *Process Biochemistry.* 48: 413-419.

London, I. M., Shemin, D., West, R., and Rittenberg, D. 1949. Heme synthesis and red blood cell dynamics in normal humans and in subjects with polycythemia vera, sickle-cell anemia, and pernicious anemia. *Journal of Biological Chemistry.* 179: 463.

Lundstedt, T., Seifert, E., Abramo, L., Thelin, B., Nyström, Å., Pettersen, J., and Bergman, R. 1998. Experimental design and optimization. *Chemometrics and Intelligent Laboratory Systems.* 42: 3-40.

Maeda, H., and Dudareva, N. 2012. The shikimate pathway and aromatic amino acid biosynthesis in plants. *Annual review of plant biology.* 63: 73-105.

Michel, G., Roszak, A. W., Sauve, V., Maclean, J., Matte, A., Coggins, J. R., Cygler, M., and Lapthorn, A. J. 2003. Structures of shikimate dehydrogenase *aroE* and its paralog *ydiB*. A common structural framework for different activities. *The Journal of biological chemistry.* 278: 19463-19472.

Miroux, B., and Walker, J. E. 1996. Over-production of proteins in *Escherichia coli*: mutant hosts that allow synthesis of some membrane proteins and globular proteins at high levels. *Journal of Molecular Biology.* 260: 289-298.

Mitchell, B. J., T.; Dwight, L. M. 2008. *Herb, nutrient and drug interaction: Clinical implications and therapeutic strategies.* Clinical Implications and Therapeutic Strategies. California: Elsevier Health Sciences

Monniot, C., Zebre, A. C., Ake, F. M., Deutscher, J., and Milohanic, E. 2012. Novel listerial glycerol dehydrogenase- and phosphoenolpyruvate-dependent dihydroxyacetone kinase system connected to the pentose phosphate pathway. *Journal of bacteriology.* 194: 4972-4982.

Mu, Y., Teng, H., Zhang, D.-J., Wang, W., and Xiu, Z.-L. 2006. Microbial production of 1,3-propanediol by *Klebsiella pneumoniae* using crude glycerol from biodiesel preparations. *Biotechnol Lett.* 28: 1755-1759.

Papanikolaou, S., Muniglia, L., Chevalot, I., Aggelis, G., and Marc, I. 2002. *Yarrowia lipolytica* as a potential producer of citric acid from raw glycerol. *Journal of applied microbiology.* 92: 737-744.

Pham, S. Q., Gao, P., and Li, Z. 2013. Engineering of recombinant *E. coli* cells co-expressing P450pyrTM monooxygenase and glucose dehydrogenase for highly regio- and stereoselective hydroxylation of alicycles with cofactor recycling. *Biotechnology and bioengineering.* 110: 363-373.

Rodriguez, A., Martinez, J., Flores, N., Escalante, A., Gosset, G., and Bolivar, F. 2014. Engineering *Escherichia coli* to overproduce aromatic amino acids and derived compounds. *Microbial cell factories.* 13: 126.

Ruffer, N., Heidersdorf, U., Kretzers, I., Sprenger, G. A., Raeven, L., and Takors, R. 2004. Fully integrated L-phenylalanine separation and concentration using reactive-extraction with liquid-liquid centrifuges in a fed-batch process with *E. coli*. *Bioprocess and biosystems engineering.* 26: 239-248.

Sakamoto, S., Terada, I., Lee, Y. C., Uehara, K., Matsuzawa, H., and Iijima, M. 1996. Efficient production of Thermus protease aqualysin I in *Escherichia coli*: effects of cloned gene structure and two-stage culture. *Applied microbiology and biotechnology.* 45: 94-101.

Silva, F., Passarinha, L., Sousa, F., Queiroz, J. A., and Domingues, F. C. 2009. Influence of growth conditions on plasmid DNA production. *Journal of microbiology and biotechnology.* 19: 1408-1414.

Sivashanmugam, A., Murray, V., Cui, C., Zhang, Y., Wang, J., and Li, Q. 2009. Practical protocols for production of very high yields of recombinant proteins using *Escherichia coli*. *Protein Science : A Publication of the Protein Society.* 18: 936-948.

Smit, B. A. 2004. *Formation of amino acid derived cheese flavor compounds.* Ph.D thesis. Program in Food Chemistry, Faculty of Science. Wageningen University.

Southwick, A. A., Nair, M. G., and Zoltai, P. T. 2011. Reduced calorie flavored milk or dairy beverage. United States patent US 20110200723 A1.

Sprenger, G. A. 2007. From scratch to value: engineering *Escherichia coli* wild type cells to the production of L-phenylalanine and other fine chemicals derived from chorismate. *Applied microbiology and biotechnology.* 75: 739-749.

Summers, D. K. 1991. The kinetics of plasmid loss. *Trends in Biotechnology.* 9: 273-278.

Summers, D. K., and Sherratt, D. J. 1985. Bacterial plasmid stability. *BioEssays.* 2: 209-211.

Sweet, G., Gandor, C., Voegele, R., Wittekindt, N., Beuerle, J., Truniger, V., Lin, E. C., and Boos, W. 1990. Glycerol facilitator of *Escherichia coli*: cloning of *glpF* and identification of the *glpF* product. *Journal of bacteriology.* 172: 424-430.

Tegel, H., Ottosson, J., and Hober, S. 2011. Enhancing the protein production levels in *Escherichia coli* with a strong promoter. *FEBS Journal.* 278: 729-739.

Thongchuang, M. 2011. *Improvement of L-phenylalnine production in Escherichia coli*

by metabolic engineering process. Ph.D thesis. Program in Biotechnology, Faculty of Science. Chulalongkorn University.

Thongchuang, M., Pongsawasdi, P., Chisti, Y., and Packdibamrung, K. 2012. Design of a recombinant *Escherichia coli* for producing L-phenylalanine from glycerol. *World Journal of Microbiology and Biotechnology.* 28: 2937-2943.

Van de Rest, O., Van der Zwaluw, N. L., and De Groot, L. C. P. G. M. 2015. *Chapter 71 - dietary protein, cognitive decline, and dementia.* Diet and nutrition in dementia and cognitive decline San Diego: Academic Press

Wackett, L. P., Dodge, A. G., and Ellis, L. B. 2004. Microbial genomics and the periodic table. *Applied and environmental microbiology.* 70: 647-655.

Wang, L., Du, W., Liu, D., Li, L., and Dai, N. 2006. Lipase-catalyzed biodiesel production from soybean oil deodorizer distillate with absorbent present in tert-butanol system. *Journal of Molecular Catalysis B: Enzymatic.* 43: 29-32.

Weckbecker, A., and Hummel, W. 2005. Glucose dehydrogenase for the regeneration of NADPH and NADH. *Microbial Enzymes and Biotransformations.* 17: 225-238.

Wendisch, V. F. 2007. *Amino acid biosynthesis -pathways, regulation and metabolic engineering.* Microbiology Monographs. Berlin: Springer

Wu, Y. Q., Jiang, P. H., Fan, C. S., Wang, J. G., Shang, L., and Huang, W. D. 2003. Co-expression of five genes in *E coli* for L-phenylalanine in *Brevibacterium flavum*. *World Journal of Gastroenterology.* 9: 342-346.

Xavier, K. B., and Bassler, B. L. 2005. Regulation of uptake and processing of the quorum-sensing autoinducer AI-2 in *Escherichia coli*. *Journal of bacteriology.* 187: 238-248.

Yang, F., Hanna, M. A., and Sun, R. 2012. Value-added uses for crude glycerol--a byproduct of biodiesel production. *Biotechnology for Biofuels.* 5: 13-13.

Zhang, X.-W., Sun, T., Sun, Z.-Y., Liu, X., and Gu, D.-X. 1998. Time-dependent kinetic models for glutamic acid fermentation. *Enzyme and Microbial Technology.* 22: 205-209.

Zhou, H., Liao, X., Liu, L., Wang, T., Du, G., and Chen, J. 2011. Enhanced L-phenylalanine production by recombinant *Escherichia coli* BR-42 (pAP-B03) resistant to bacteriophage BP-1 via a two-stage feeding approach. *Journal of Industrial Microbiology and Biotechnology.* 38: 1219-1227.

Zhou, H., Liao, X., Wang, T., Du, G., and Chen, J. 2010. Enhanced L-phenylalanine biosynthesis by co-expression of *pheA*$^{(fbr)}$ and *aroF*$^{(wt)}$. *Bioresource technology.* 101: 4151-4156.

APPENDIX

VITA

Miss Pakinee Ratchaneeladdajit was born on April 3, 1984 in Kanchanaburi province, Thailand. She finished high school from Visuttharangsi School, Kanchanaburi in 2003. After graduating with the degree of Bachelor of Science from the Department of

Chemistry, Faculty of Science, Rajamangala University of Technology Krungthep in 2008, she kept on working at the Dental Innovation Foundation under Royal Patronage until resign for study in the Master degree of Science in program of Biochemistry and Molecular Biology in 2011. In fourth year of research work, she submited some parts of her work to Veridian E-Journal Science and Technology, Silpakorn University in a topic of "L-Phenylalanine production using dual plasmid system in recombinant Escherichia coli."